QUARTERLY STATUS REPORT NO. 8

and

SUMMARY REPORT

1 January - 31 December 1964

ELECTROCHEMICAL STUDIES IN THE SYNTHESIS
OF N-F COMPOUNDS

April 7, 1965

**DDC**

APR 26 1965

DDC-IRA E

TRACOR

INC

SUMMARY REPORT
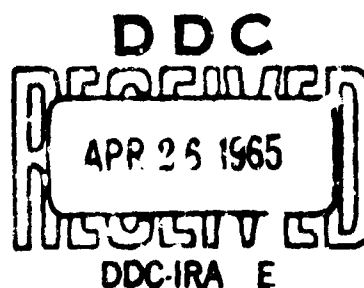
1 January - 31 December 1964

# ELECTROCHEMICAL STUDIES IN THE SYNTHESIS OF N-F COMPOUNDS

Contract No. Nonr-4054(00)

Research Project No. RR001-06-02

ARPA Order No. 399, Program Code No. 2910

April 7, 1965
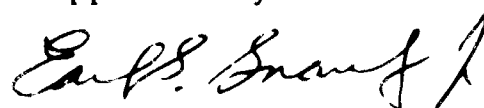
Prepared by:

Larry G. Spears
Larry D. Fiel
Wallace E. Harrell, Jr.
Margaret H. Northrup

Approved by:

*Earl S. Snavely, Jr.*

Earl S. Snavely, Jr.
Director of Chemical
Research

TABLE OF CONTENTS

## LIST OF ILLUSTRATIONS

## LIST OF TABLES

# Abstract

This report summarizes the research carried out during the period January through December 1964. Work during the last quarter is emphasized. The goal of this work is to determine the mechanism by which electrochemical fluorination of ammonium and hydrazinium salts occur in anhydrous hydrogen fluoride (AHF). A major portion of the work to date has been done to (1) develop a suitable reference electrode, (2) construct an HF handling system for preparing and maintaining AHF at low electrical conductivities (i.e., $10^{-5}\ \Omega^{-1}\ cm^{-1}$), and (3) select a suitable working electrode. The $Hg/Hg_2F_2$ electrode satisfies the requirements for a reference electrode, and Monel (alloy 400) satisfies the requirements for a working electrode. Monel is now being used as an anode and $Hg/Hg_2F_2$ as a reference electrode in studying the electrolysis of $NH_4F$ in AHF.

## ELECTROCHEMICAL STUDIES IN THE SYNTHESIS OF N-F COMPOUNDS

### I. INTRODUCTION AND BACKGROUND

The objective of this work is to employ electrochemical techniques to determine if the fluorination of ammonium and hydrazinium salts proceeds by a stepwise mechanism or if fluorine is substituted for hydrogen in a random fashion. These data are to be used in establishing if electrochemical fluorination of ammonium and hydrazinium salts can produce fluorine-containing cationic species such as $NH_3F^+$, $NH_2F_2^+$, $NHF_3^+$, $NF_4^+$. and $N_2H_4F^+$. $N_2H_3F_2^+$, etc.

To employ electrochemical techniques, such as reaction order methods, conductivity measurements, pulse techniques, and chrono-potentiometry, successfully for these studies, it is imperative that the following experimental conditions must be known and maintained:

1. A working anode which has a known corrosion rate that is small compared to the rate of fluorination studied.

2. A reference electrode that is reproducible, stable, and reversible, having a potential with thermodynamic significance.

3. An experimental cell capable of maintaining AHF at constant conductivity (i.e., dry and free of foreign ions).

The problems relating to 1, 2, and 3 above have been solved to a sufficient degree to allow reasonable certain interpretation of data concerning the fluorination of $NH_4^+$ and $N_2H_5^+$.

In the search for a working anode to satisfy the requirement of 1, above, twenty materials were investigated for possible use in electrochemical fluorination. These materials included aluminum, antimony, bismuth, cadmium, chromium, cobalt, copper, Hastelloy-F,

iron, magnesium, molybdenum, Monel, platinum, pyrolytic carbon, silver, thallium, titanium, zinc, zirconium, and zirconium diboride. All of these materials except Monel have been rejected for one or more of the following reasons: excessive corrosion, unstable electrochemical behavior, high film electrical resistance, or undesirable interaction with the solvent. Monel is the only material investigated to date which has a sufficiently low corrosion rate, low electrical resistance film, and reproducible behavior to allow its use as a working anode for fluorination studies in AHF.

Anodic polarization curves of Monel in AHF solutions of $NH_4F$ revealed no concentration-dependent plateaus to indicate a stepwise fluorination of the ammonium ion. The reproducibility of these curves was poor, however, due to a change in character of the surface film formed on Monel by anodic polarization above +4.0 volts with respect to the $Hg/Hg_2F_2$ reference electrode. Galvanostatic cathodic reduction measurements have indicated that this change is due to the sorption of fluorine in the fluoride film on the Monel electrode. Since anodic polarization in AHF solutions of $NH_4F$ involves fluorine evolution, fluorination of $NH_4^+$, electrode oxidation, and contaminant oxidation, the clarification of the sorbed layer is important.

## II.     EXPERIMENTAL APPARATUS

A schematic diagram for the $F_2$, HF, and $N_2$ handling system is shown in Figure 1.  In operation, the cleaned and dried conductance cell and electrolytic cells are assembled without the working and reference electrodes.  The entire HF handling system is then treated with fluorine gas to passivate all surfaces that contact HF.  The cells are then purged with dry $N_2$ and the conductance cell filled with HF from the HF tank with the electrolytic cells closed off.  The HF in the Kel-F conductance cell is then electrolyzed using nickel screen electrodes, while bubbling dry $N_2$, until a high resistivity is obtained as shown by measurements with the platinum electrodes.  The AHF is then allowed to distill over into one of the Kel-F electrolytic cells where it is electrolyzed again until a conductivity of $10^{-5} \, \Omega^{-1} \, cm^{-1}$ is reached.  The $Hg/Hg_2F_2$ reference electrode is then introduced into the cell and allowed several hours to come to equilibrium with the AHF before it is used.  Then the working electrode is inserted through the cell lid into the HF.  Nitrogen is bubbled through the cell while the electrode is inserted to prevent diffusion of any contaminant into the cell.  Solid samples (i.e., $NH_4F$ or NaF) are injected through an injection port on the cell lid.  During electrolysis dry $N_2$ is used as a stirrer and a carrier gas.

The gas IR cell being used is made of nickel with Irtran-2 windows, a pathlength of 10 cm, and a volume of 26 cc.  The liquid IR cell is made of Monel with Teflon spacers ard gaskets, Irtran-2 windows, a variable pathlength up to 0.5 mm, and a maximum volume of 0.3 ml.

All the working electrode materials reported are in the form of 1/8" rods unless stated otherwise, and all potentials are volts vs $Hg/Hg_2F_2$ unless otherwise stated.

3
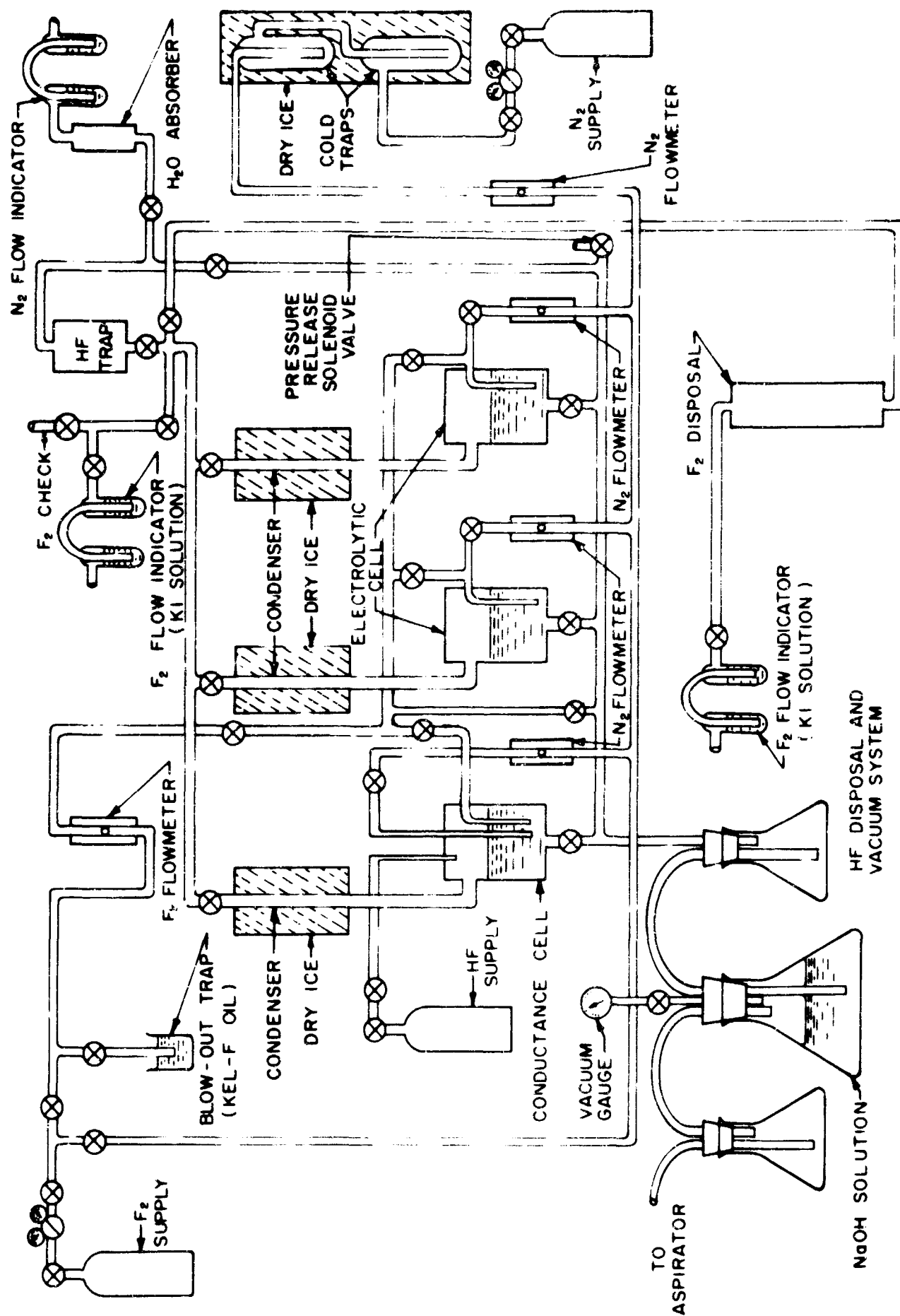
Fig. I – $F_2$, $N_2$ AND HF HANDLING SYSTEM

## III.   REFERENCE ELECTRODES

In aqueous systems the most satisfactory reference electrodes are those consisting of a metal with thermodynamic stability toward water in intimate contact with a sparingly soluble salt of the metal. The best known examples are $Hg/Hg_2Cl_2$ and $Ag/AgCl$.  In many cases where the presence of the anion of the reference electrode is undesirable, or where the use of a salt bridge is inconvenient, an inert metal immersed in the solution may possess sufficient potential stability providing only very low currents are drawn.  Such potential stability is dependent on the presence in solution of small quantities of oxidizable or reducible species (like ions of the metal, hydrogen ions, metal oxides formed on the surface, etc.). The best known examples of this in nonaqueous media is a platinum wire reference electrode.

Reference electrodes investigated during this project have included Pt, $Ni/NiF_2$, $Al/AlF_3$, and $Hg/Hg_2F_2$.  These electrodes were tested in like pairs, one of which was used as a base against which the potentials of both a working electrode and the other like electrode were measured.  These experiments were performed to determine if the small current ($10^{-9}$ amp) in the reference electrode circuit of the potentiostat or ions introduced by dissolution of the working electrode had any adverse effects on the reference electrode.  The average deviations of the open-circuit potentials of the Pt, $Ni/NiF_2$, and $Al/AlF_3$ electrodes were greater than 100 mv, which is excessive for the objectives of this project.  However the deviations in the $Hg/Hg_2F_2$ electrodes had a maximum of only 16 mv (see Table I).

Polarization curves using one $Hg/Hg_2F_2$ electrode as a working electrode and another $Hg/Hg_2F_2$ electrode as the reference electrode were made in 0.01M NaF in HF (Figure 2).  Reversibility

## TABLE I

## POTENTIAL DIFFERENCE OF PAIRS OF $Hg/Hg_2F_2$ ELECTRODES

| ELECTRODE PAIR | ΔE at Open Circuit, volts[a] | | | WORKING ELECTRODE USED |
|---|---|---|---|---|
| | BEFORE POLARIZATION | AFTER POLARIZATION | | |
| | | Anodic | Cathodic | |
| 1[e] | -0.014 | ---- | ---- | Aluminum, platinum |
| 2 | -0.008 | +0.002 | -0.016 | Aluminum |
| 3[e] | +0.011 | ---- | ---- | Magnesium |
| 4 | +0.003 | +0.001[b] | +0.004[c] | $Hg/Hg_2F_2$ |
| 5 | +0.014 | +0.014[b] | +0.012[c] | $Hg/Hg_2F_2$ [d] |

[a] The sign refers to the potential of the electrode in the potentiostat circuit with respect to a like electrode at open circuit.

[b] Open circuit potential after polarization to +1.0 v vs $Hg/Hg_2F_2$

[c] Open circuit potential after polarization to -1.0 v vs $Hg/Hg_2F_2$

[d] Cell contained 0.01M NaF in anhydrous HF.

[e] For Electrode Pairs 1 and 3, no values were recorded after polarization.
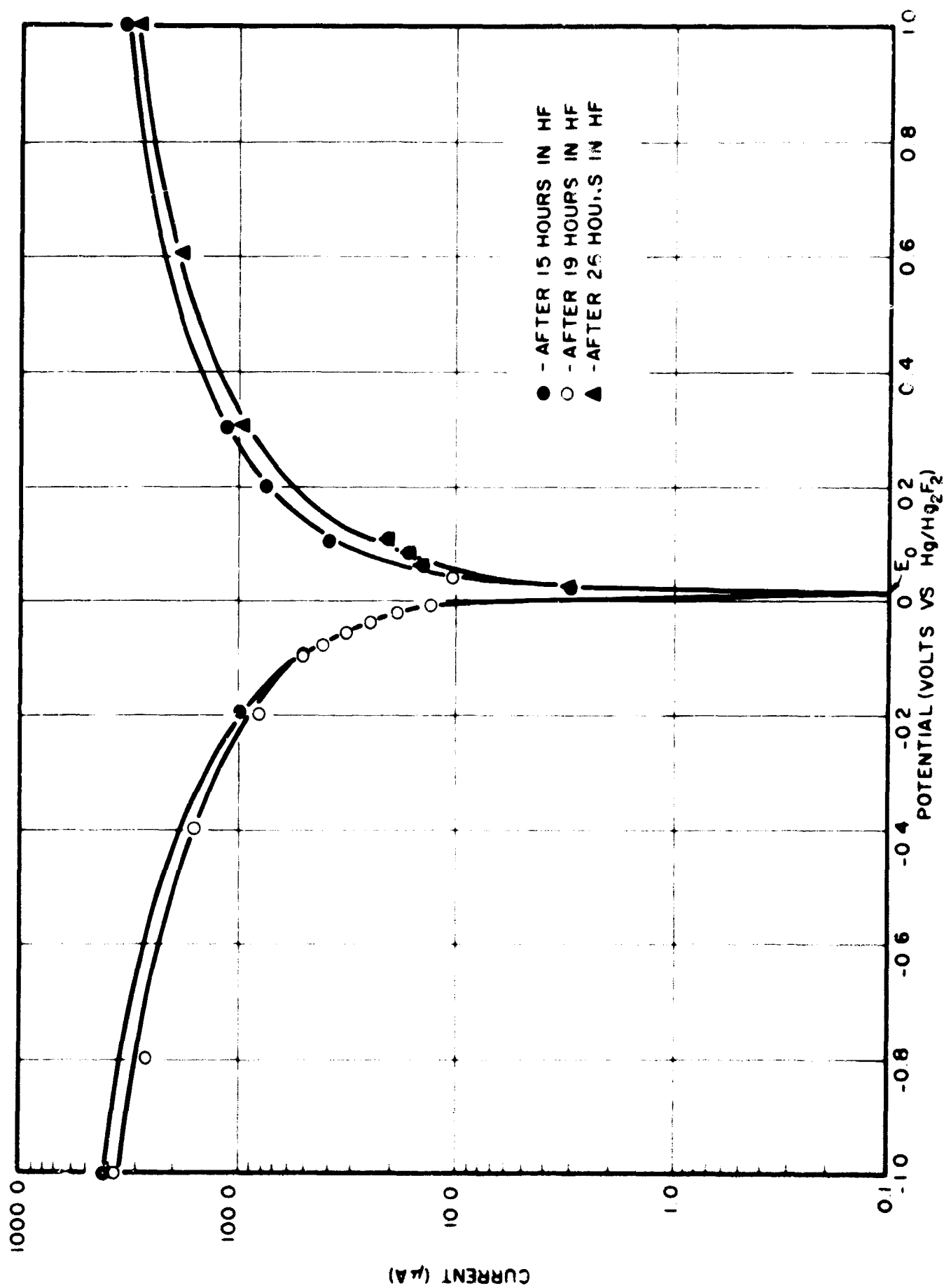
Fig. 2 - POLARIZATION CURVES OF Hg/Hg₂F₂ REFERENCE ELECTRODE IN 0.01M NaF IN AHF

of the electrodes is indicated by the symmetry of the curves and the instantaneous return to open-circuit potential from +1.0 v and -1.0 v upon removal of the polarizing current. Potential decay of the electrodes was faster than the pen speed of the recorder (1 second full scale). The curves in Figure 2 also show that polarization of the electrodes is insignificant for currents which will be encountered ($10^{-9}$ amp) in the potentiostat reference circuit.

New $Hg/Hg_2F_2$ reference electrodes vary widely in potential difference but this decreases to within 0.014 v in a few hours as shown in Figure 3. It is assumed that this behavior is due to the establishment of equilibrium between the $Hg_2F_2$ and Hg in the AHF and to effects of traces of $Hg_2O$ (which form $H_2O$ and HF in the electrode).

Construction details for the $Hg/Hg_2F_2$ reference electrode are shown in Figure 4. It is necessary to build new electrodes each time the electrolysis cell is disassembled because $Hg_2F_2$ is decomposed by moist air.

In summary, both the electrochemical properties and the physical construction of the $Hg/Hg_2F_2$ make it satisfactory for use as a reference electrode in AHF.
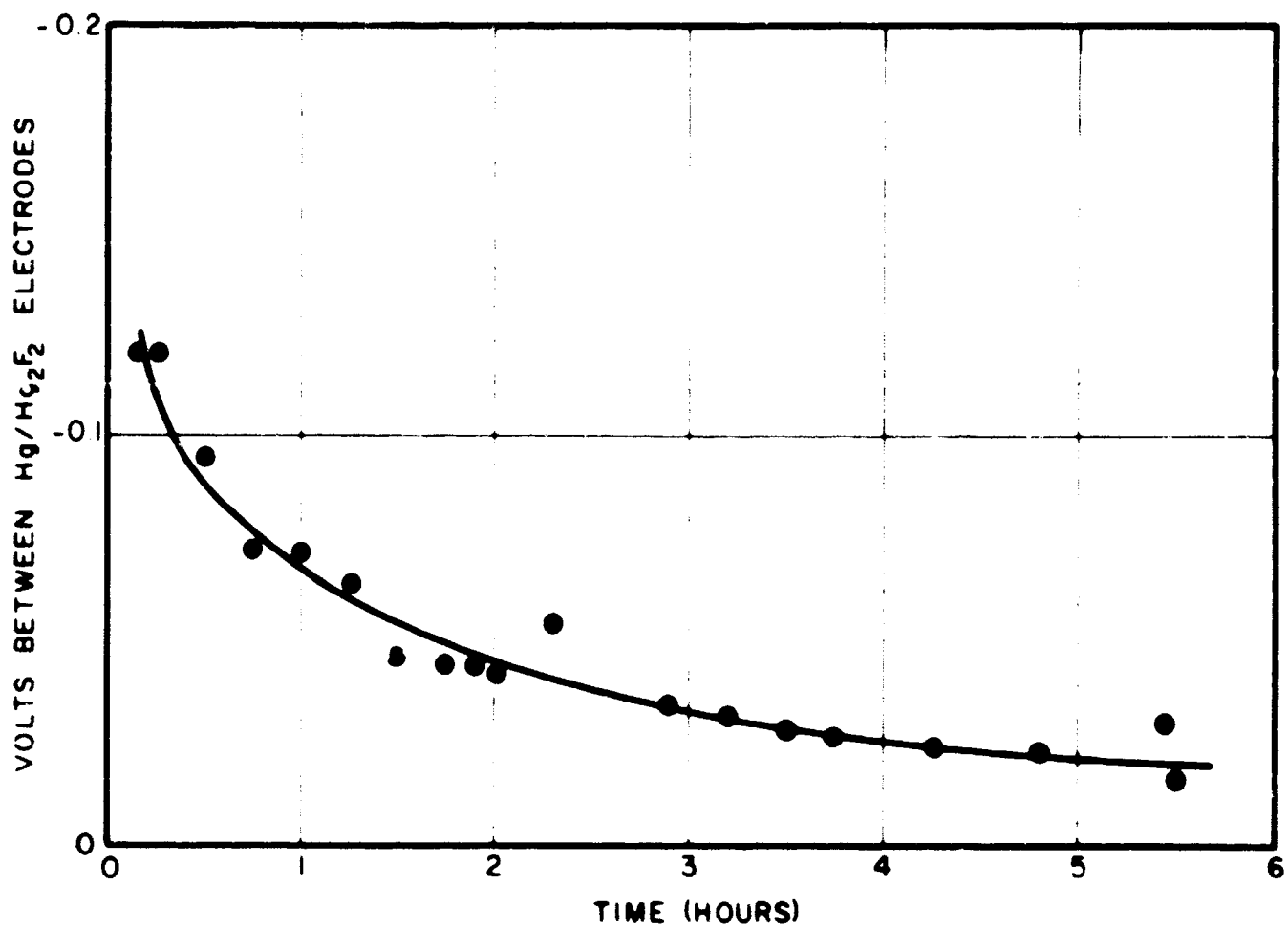
Fig 3- CHANGE IN OPEN-CIRCUIT POTENTIAL
OF Hg/Hg$_2$F$_2$ REFERENCE ELECTRODE
WITH TIME
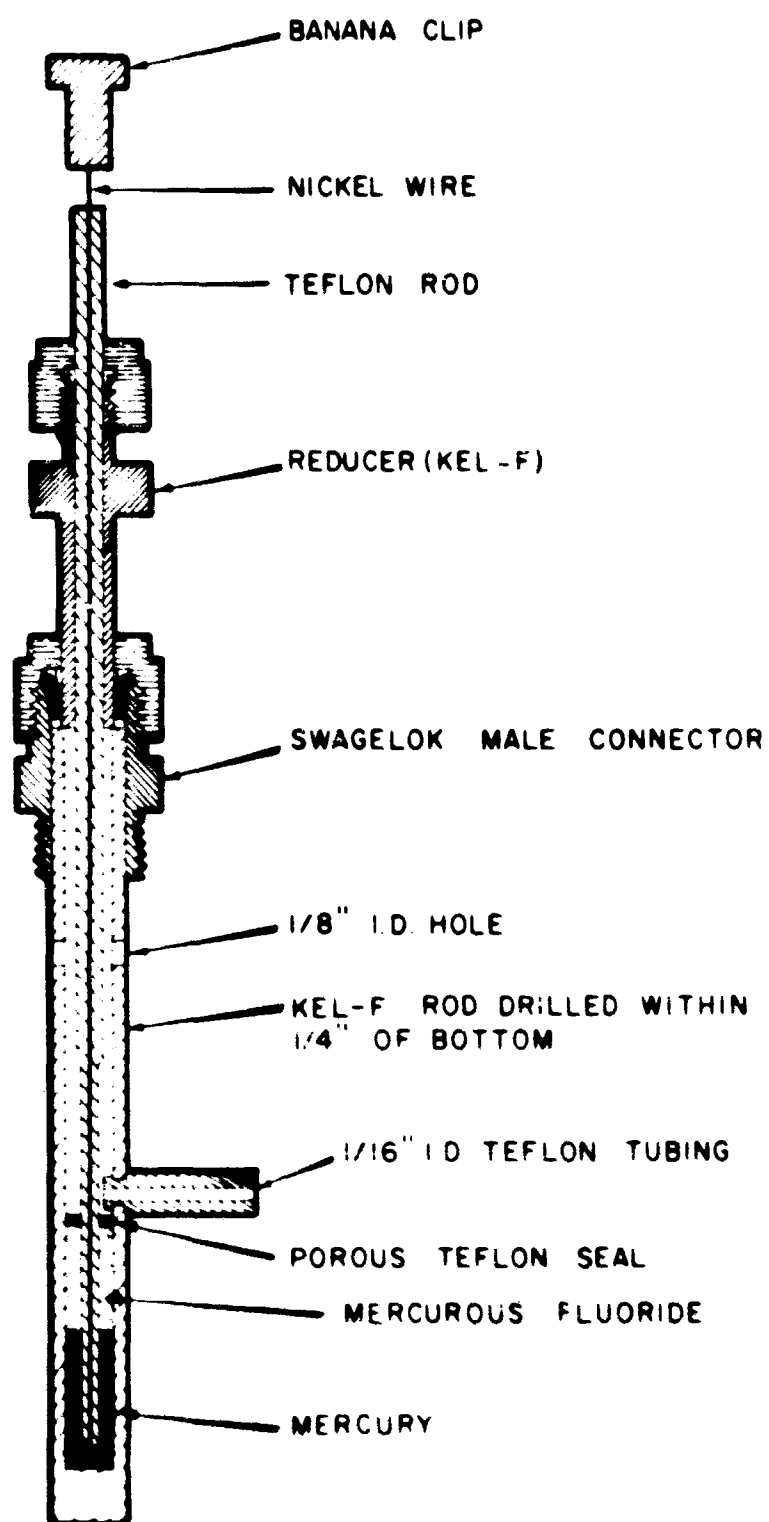
Fig. 4 - REFERENCE ELECTRODE $Hg/Hg_2F_2$

Labels in figure:
- BANANA CLIP
- NICKEL WIRE
- TEFLON ROD
- REDUCER (KEL-F)
- SWAGELOK MALE CONNECTOR
- 1/8" I.D. HOLE
- KEL-F ROD DRILLED WITHIN 1/4" OF BOTTOM
- 1/16" I.D. TEFLON TUBING
- POROUS TEFLON SEAL
- MERCUROUS FLUORIDE
- MERCURY

10

IV.    ELECTROCHEMICAL FLUORINATION OF $NH_4F$ IN ANHYDROUS HYDROGEN
        FLUORIDE WITH MONEL ANODES

Studies were made to determine if the electrochemical
fluorination of $NH_4F$ in AHF proceeded in a stepwise fashion as a
function of potential.  Polarization curves were obtained, after
the injection of a certain amount of dry $NH_4F$, by use of an X-Y
recorder and a motor-driven potentiometer (Figure 5).  In these
curves a plateau similar to a diffusion limited region consistently
appeared at 3.0 to 5.0 v.  The current density on this plateau is
independent of $NH_4F$ concentration or any contaminant added with
the $NH_4F$.  The effects of concentration and resistance polarization
with decreasing $NH_4F$ concentration are clearly seen; however, no
other evidence of depolarization of the electrode by addition of
$NH_4F$ was detected.  Since there were no concentration-dependent
plateaus in the anodic polarization curves (up to +8.0 v vs
$Hg/Hg_2F_2$) of Monel in AHF solutions of $NH_4F$, the fluorination of
$NH_4^+$ apparently does not proceed in a stepwise manner as a function
of the applied potential.  It thus appears, that $NH_4^+$ is fluorinated
by chemical reaction in AHF.  If the fluorination of $NH_4^+$ does
proceed by chemical reaction, it is still possible to obtain the
cationic species $NH_3F^+$, $NH_2F_2^+$, $NHF_3^+$, and $NF_4^+$.

Further studies were made to determine the nature of the
plateau region mentioned above.  A typical steady-state polarization
curve of Monel in AHF is shown in Figure 6.  The presence of $NH_4F$
in the HF, results in a plateau region around +3.8 v (see Curve A
of Figure 7).  Curve B of Figure 7 shows the effect that the
addition of 1% water to the $NH_4F$-HF solution has on the +3.8 v
plateau region.  It is possible that this plateau region is due
to a sorbed species (possibly fluorine) on the metal fluoride
coating of the Monel electrode.  From Curve B it may be postulated
that the sorbed species reacted with the added $H_2O$, thus doing
away with the plateau region.

11
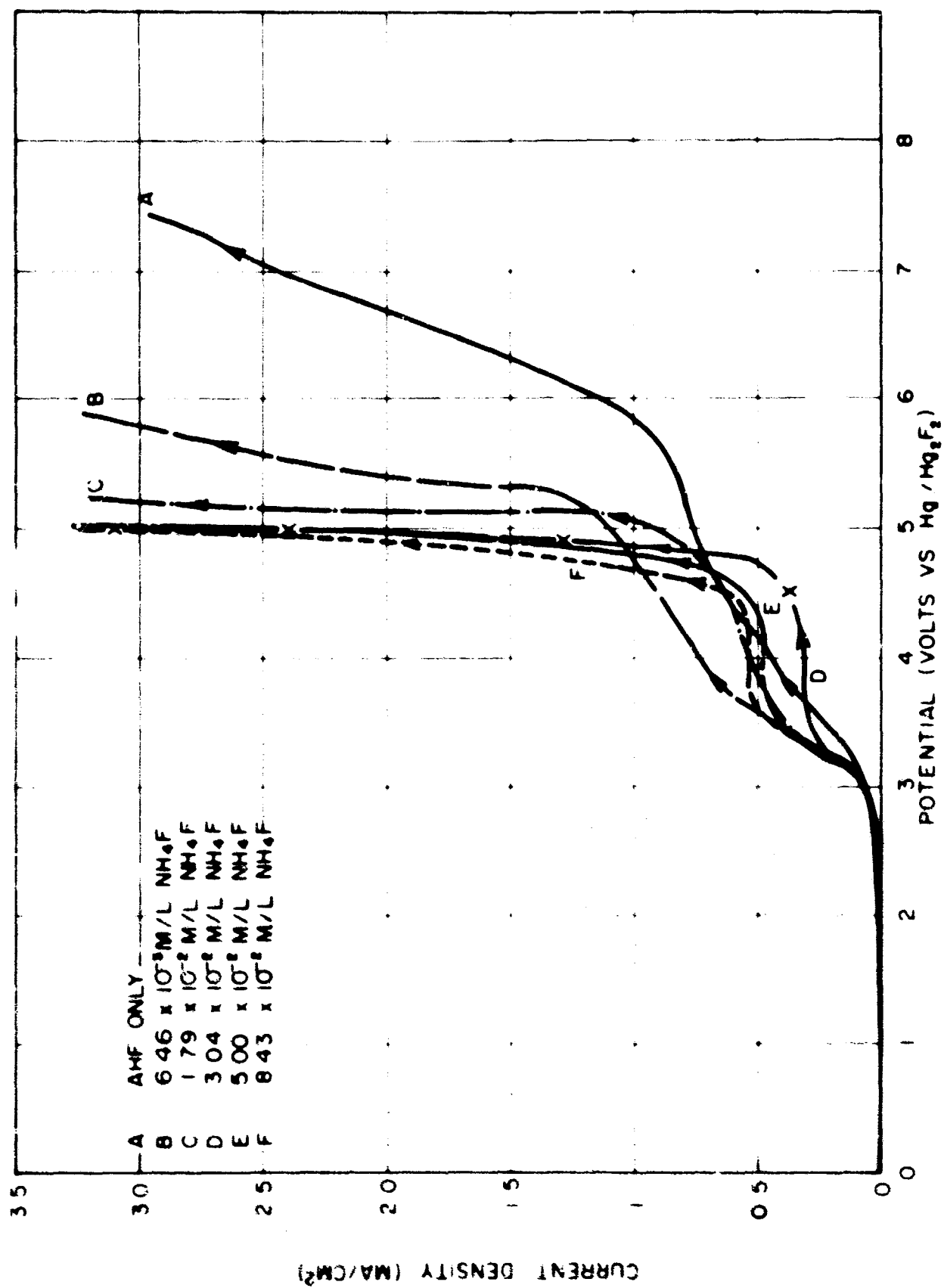
Fig 5 - POLARIZATION CURVES FOR MONEL WITH NH$_4$F ADDED

A    AHF ONLY
B    6.46 × 10$^{-3}$ M/L NH$_4$F
C    1.79 × 10$^{-2}$ M/L NH$_4$F
D    3.04 × 10$^{-2}$ M/L NH$_4$F
E    5.00 × 10$^{-2}$ M/L NH$_4$F
F    8.43 × 10$^{-2}$ M/L NH$_4$F

POTENTIAL (VOLTS VS Hg / Mg$_2$F$_2$)

CURRENT DENSITY (MA/CM$^2$)

12
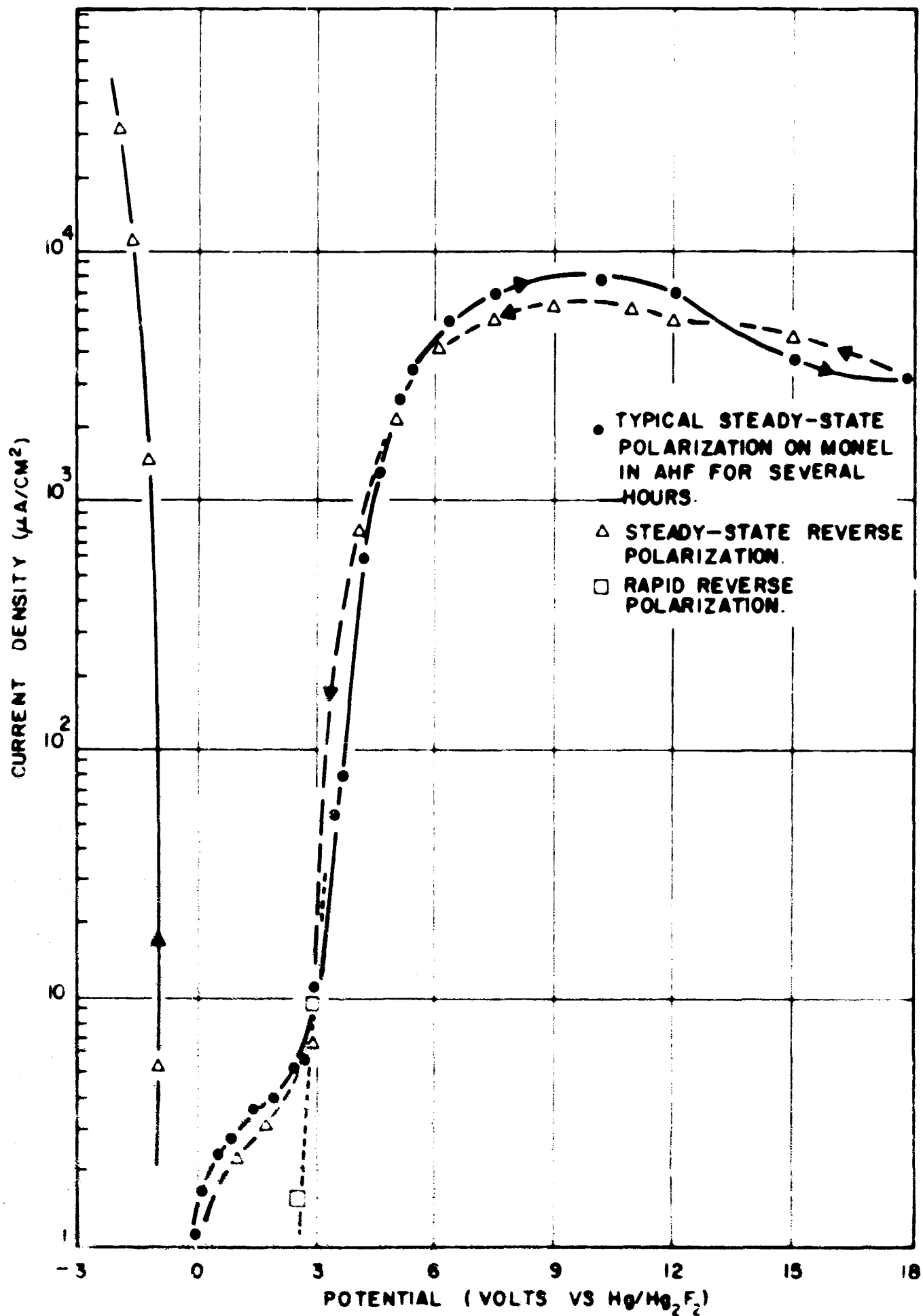
Fig. 6 -POLARIZATION CURVES FOR MONEL IN AHF

13
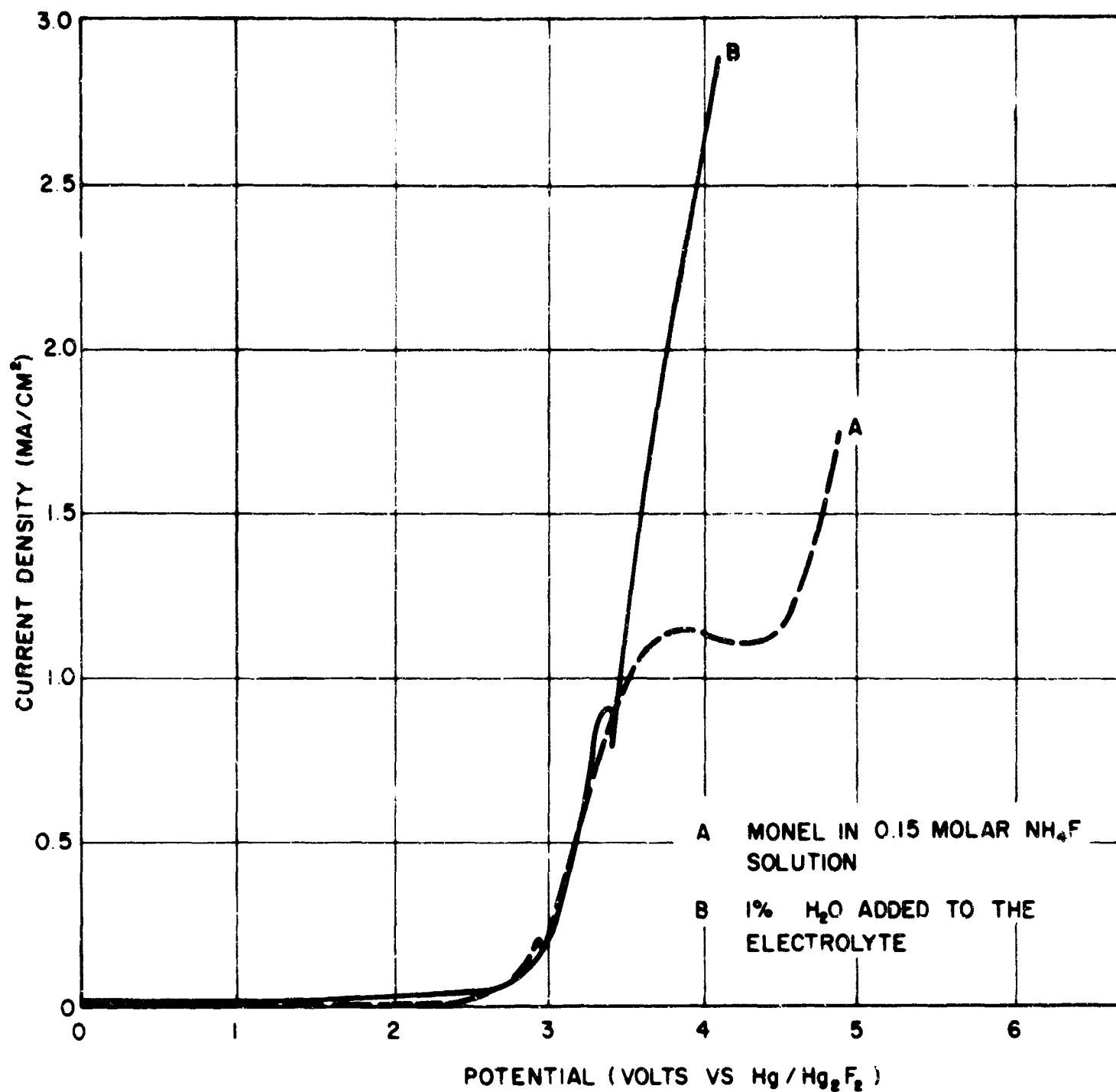
Fig. 7 -EFFECT OF H₂O ON THE POLARIZATION CURVE FOR MONEL
IN HF+NH₄F

14

Galvanostatic cathodic stripping curves of Monel polarized
anodically in AHF (Figure 8) and in AHF and $NH_4F$ solutions
(Figure 9) were recorded.  The potential arrests at approximately
+2.0 v is in the region of the reduction potential for fluorine.
The total charge required for reduction of the film formed by
anodic bias of the Monel anode is not reproducible when equal
charges are passed at the anodic potential.  As shown in Figure 10,
the charge required for reduction depends on the total charge
passed at +6.0 v rather than the increment of charge passed between
reductions.  These data are summarized in Table II.  These results
indicate that a portion of the film formed at +6.0 v is not reduced
under the conditions employed.  From the data in Table II and the
curves in Figure 10, it appears a species other than the metal
fluoride is being reduced during the cathodic reduction experiments.

## TABLE II

### CHARGE REQUIRED FOR REDUCTION OF ANODIC FILMS FORMED
### ON MONEL IN AHF SOLUTIONS OF $NH_4F$

COULOMBS PASSED

| +6.0 v($C_+$) | Cathodic($C_-$) | $(C_-/C_+) \times 10^6$ | $(C_-/\Sigma C_+) \times 10^6$ |
|---|---|---|---|
| 47.3 | 6,200 $\times$ $10^{-6}$ | 133 | 133 |
| 43.2 | 13,050 x $10^{-6}$ | 302 | 144 |
| 35.1 | 21,750 x $10^{-6}$ | 619 | 173 |
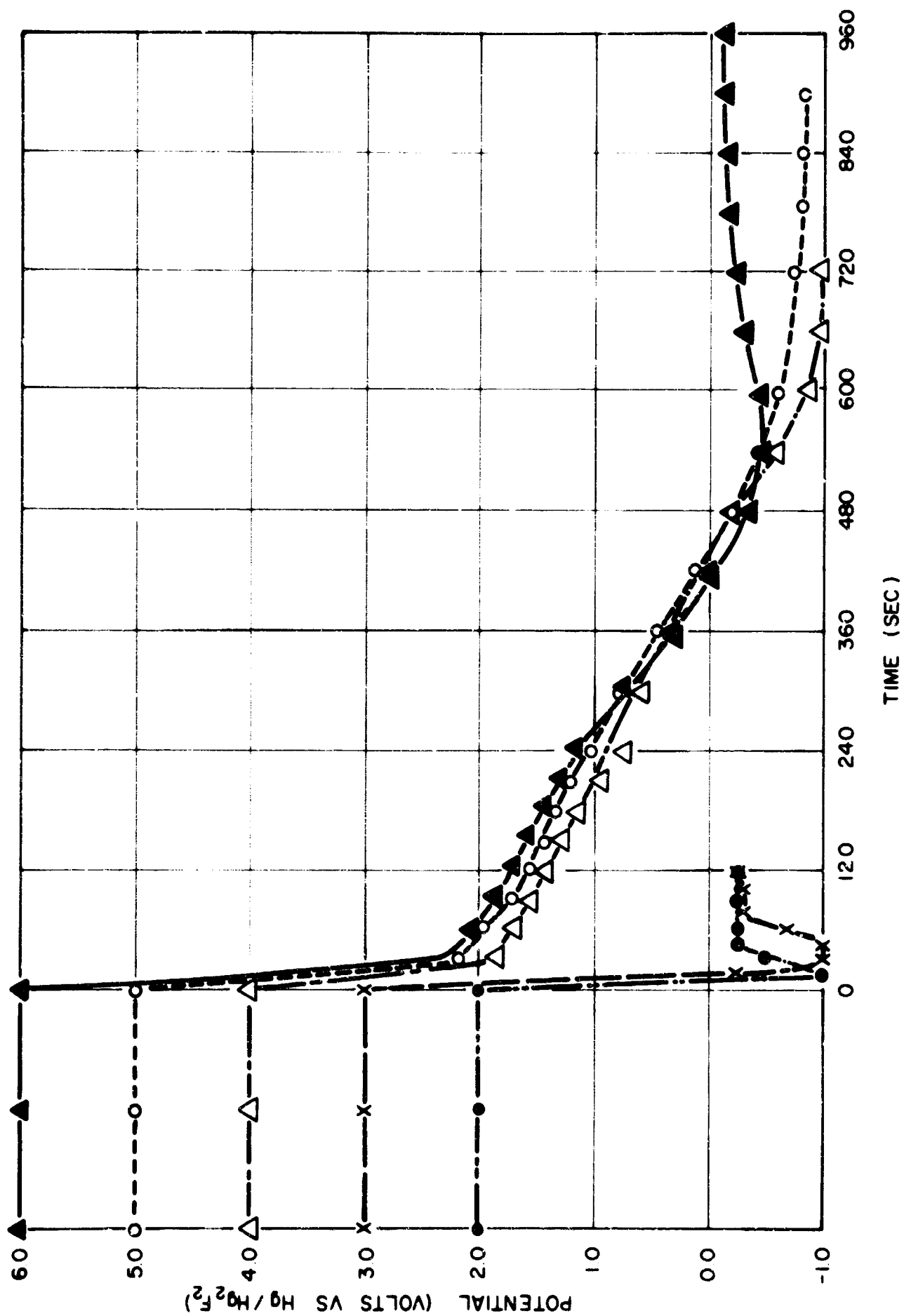
Fig. 8 - CATHODIC STRIPPING OF MONEL IN AHF

16

TRACOR, INC          DWG A 729-132
AUSTIN, TEXAS    LDF/LBH    11/11/84
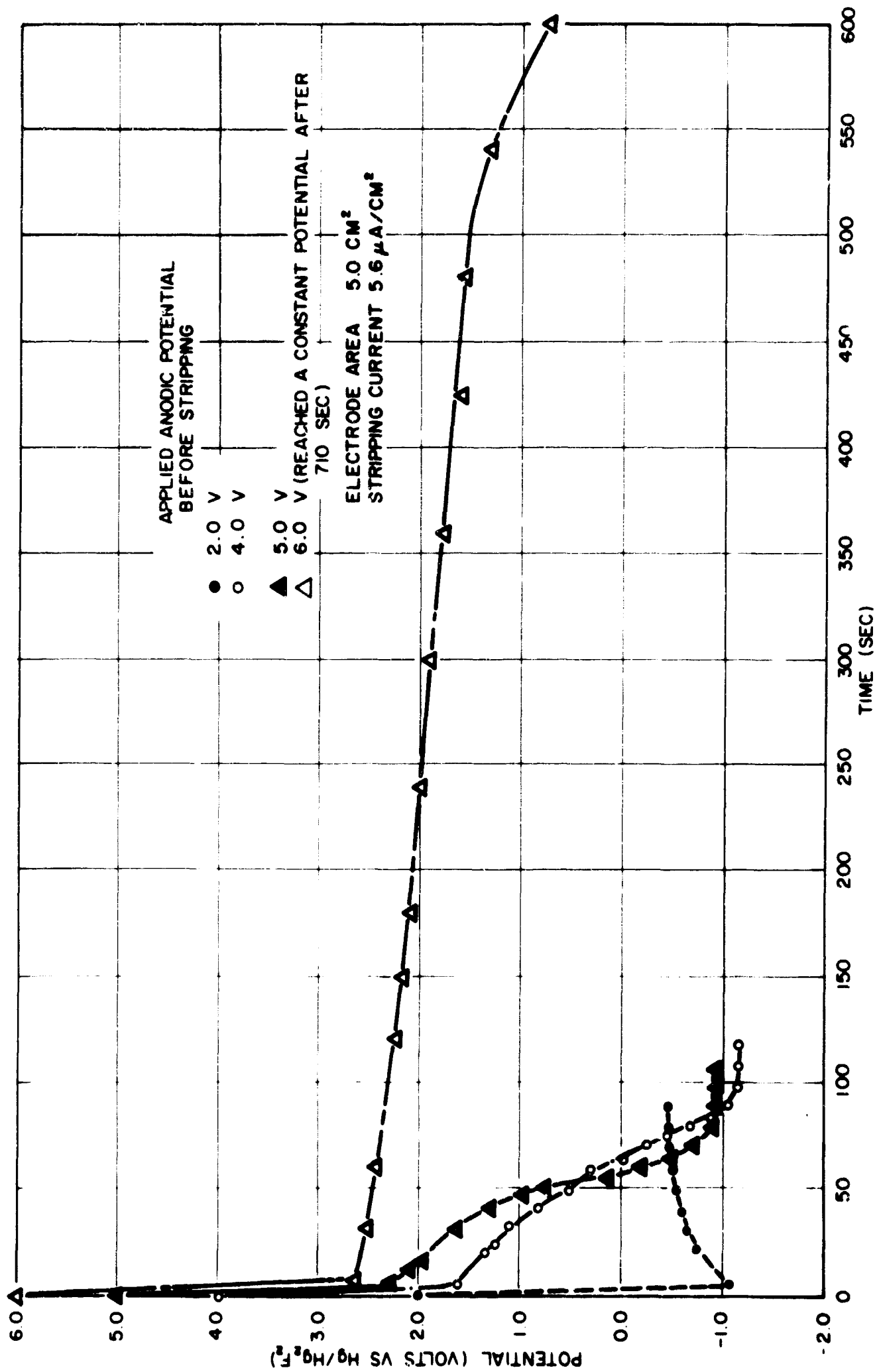
Fig. 9-STRIPPING CURVES FOR MONEL ELECTRODES POLARIZED ANODICALLY IN 0.021M NH₄F IN AHF

APPLIED ANODIC POTENTIAL
BEFORE STRIPPING

● 2.0 V
○ 4.0 V
▲ 5.0 V
△ 6.0 V (REACHED A CONSTANT POTENTIAL AFTER 710 SEC )

ELECTRODE AREA 5.0 CM²
STRIPPING CURRENT 5.6 µA/CM²

POTENTIAL (VOLTS VS Hg/Hg₂F₂)

TIME (SEC)

17

Fig. 10- CATHODIC STRIPPING OF MONEL ELECTRODES FROM +6.0 V IN 2.13 x 10⁻² M NH₄F IN AHF

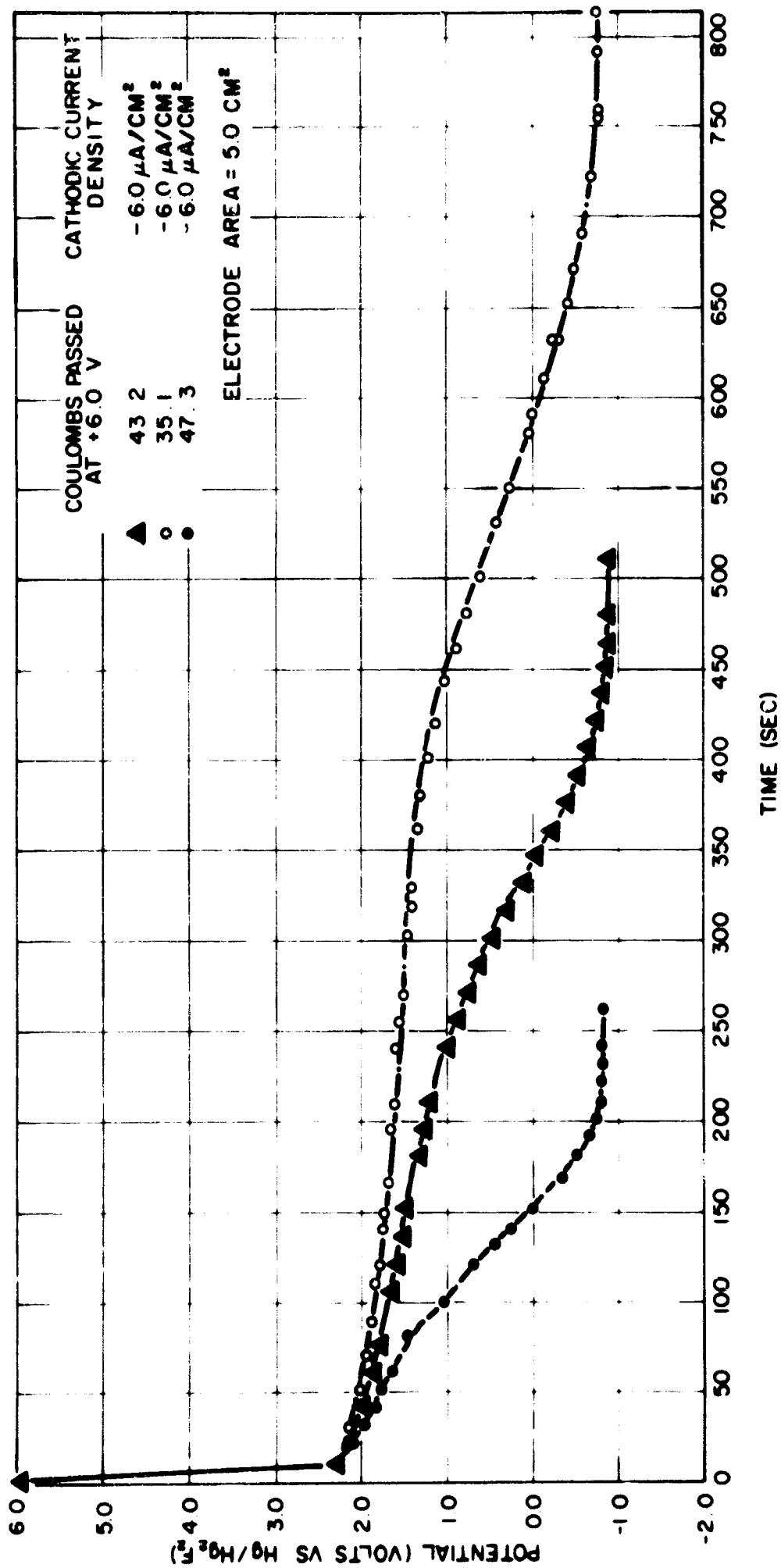If the potential arrest at +2.0 v is due to the reduction of fluorine which is sorbed on the fluoride film, it should be possible to reach a state where the fluoride film would be saturated with fluorine as long as the applied anodic bias is above the fluorine evolution potential. This effect is shown in Figure 11, runs 1 and 2. It should be noted that 154 coulombs were passed at +6.0 v and the sorbed fluorine reduced before the first run was made. A flow of dry nitrogen at the rate of 22 cc/min was used to stir the solution during the experiments. Once the film is saturated, it should be possible to decrease the number of coulombs applied anodically and thus have a decrease in the number of coulombs required to reduce the sorbed fluorine. This can be seen in runs 3 through 8. Here also it is observed that fluorine and not the fluoride film is being reduced. Weight losses were determined after each run and indicated that at least 90% of the applied anodic current was going to fluorine evolution.

A comparison between the number of applied anodic coulombs and the number of reduction coulombs required to reduce the sorbed species was made. These results are given in Figure 12 and Table III. These experiments were made using a 0.1M solution of $NH_4F$ in AHF. It was noted that the number of reduction coulombs required after applying 6.0 v for 2 sec and 4.0 v for 30 sec was the same. This would be expected because the same amount of fluorine should have been produced for either run since the number of applied anodic coulombs was the same. Figure 13 shows that the amount of fluorine required to saturate the fluoride film at +6.0 v and +8.0 v is approximately the same. Thus there is no significant change in the thickness of the fluoride film formed at +6.0 v and +8.0 v.
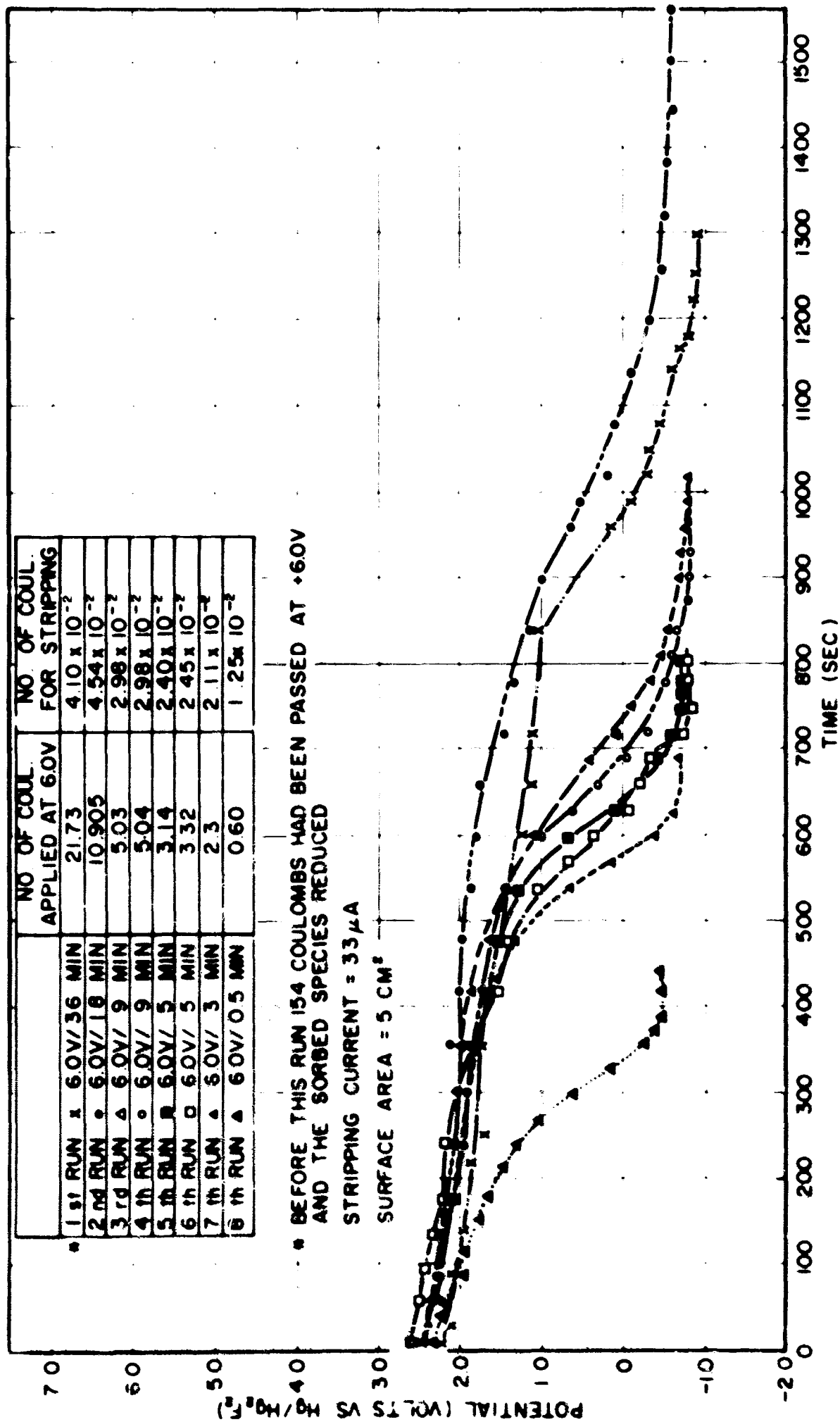
Fig.11 - CATHODIC REDUCTION CURVES FOR MONEL IN $2.16 \times 10^{-3}$ M $NH_4F$ IN AHF

|  | NO. OF COUL.<br>APPLIED AT 6.0V | NO. OF COUL.<br>FOR STRIPPING |
|---|---|---|
| 1st RUN × 6.0V/36 MIN | 21.73 | $4.10 \times 10^{-2}$ |
| 2nd RUN • 6.0V/18 MIN | 10.905 | $4.54 \times 10^{-2}$ |
| 3rd RUN △ 6.0V/9 MIN | 5.03 | $2.98 \times 10^{-2}$ |
| 4th RUN • 6.0V/9 MIN | 5.04 | $2.98 \times 10^{-2}$ |
| 5th RUN ▪ 6.0V/5 MIN | 3.14 | $2.40 \times 10^{-2}$ |
| 6th RUN □ 6.0V/5 MIN | 3.32 | $2.45 \times 10^{-2}$ |
| 7th RUN ▲ 5.0V/3 MIN | 2.3 | $2.11 \times 10^{-2}$ |
| 8th RUN ▲ 6.0V/0.5 MIN | 0.60 | $1.25 \times 10^{-2}$ |

* BEFORE THIS RUN 154 COULOMBS HAD BEEN PASSED AT +6.0V AND THE SORBED SPECIES REDUCED

STRIPPING CURRENT = 33 $\mu$A

SURFACE AREA = 5 $CM^2$

20

Fig. 12 - NO. OF REDUCTION COULOMBS REQUIRED AFTER ANODIC BIAS
OF MONEL AT +6.0V IN 0.1M NH₄F IN AHF

21

TRACOR, INC    DWG 729-163
AUSTIN, TEXAS   4/8/65    L65/L6H

## TABLE III

### SUMMARY OF THE AVERAGE VALUE OBTAINED FROM THE CATHODIC REDUCTION MEASUREMENTS MADE ON MONEL IN A SOLUTION OF 0.01M $NH_4F$ IN AHF

| ANODIC POTENTIAL/ SEC. APPLIED | NO. OF REDUCTION COUL. REQUIRED x $10^3$ ($C_1$) | NO. OF COUL. APPLIED ANODICALLY ($C_2$) | $C_1/C_2$ x 100 |
|---|---|---|---|
| 6.0 v/30 sec | 5.95 | 2.55 | 0.233 |
| 6.0 v/15 sec | 4.25 | 1.22 | 0.348 |
| 6.0 v/5 sec | 2.96 | 0.35 | 0.845 |
| 6.0 v/2 sec | 1.84 | 0.136 | 1.35 |
| 4.0 v/30 sec | 1.87 | 0.135 | 1.36 |
| 4.0 v/15 sec | 1.12 | 0.063 | 1.75 |
| 4.0 v/11 sec | 0.918 | 0.044 | 2.09 |
| 4.0 v/5 sec | 0.740 | 0.015 | 4.93 |
| 4.0 v/3 sec | 0.442 | 0.008 | 5.46 |
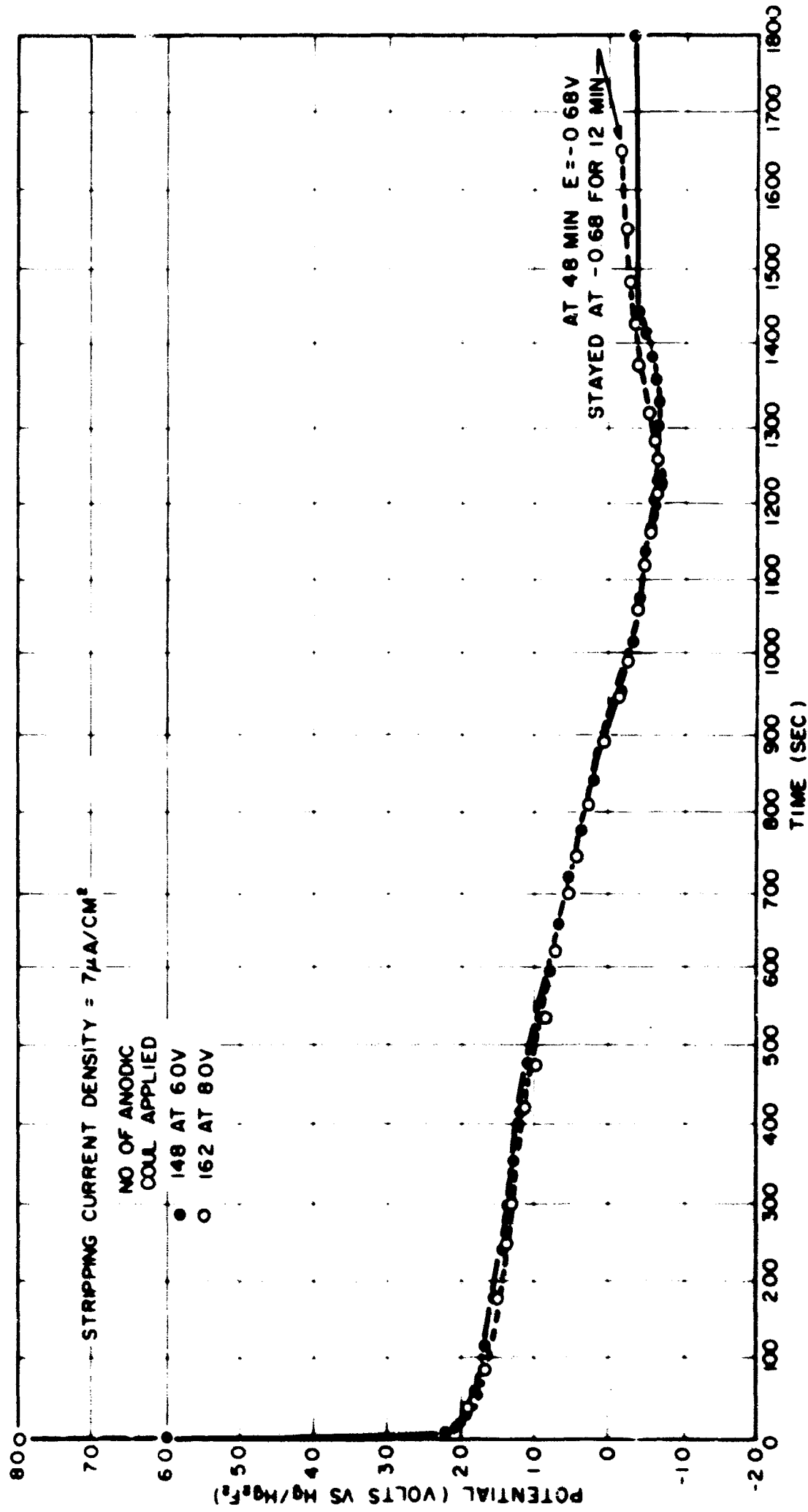
Fig. 13 - CATHODIC STRIPPING CURVES FOR MONEL IN 0.1M NH₄F IN AHF

STRIPPING CURRENT DENSITY = 7μA/CM²

NO. OF ANODIC
COUL. APPLIED
● 148 AT 6.0V
○ 162 AT 8.0V

AT 48 MIN E=-0.68V
STAYED AT -0.68 FOR 12 MIN

POTENTIAL (VOLTS VS Hg/Hg₂F₂)

TIME (SEC)

23

TRACOR, INC DWG 729-159
AUSTIN, TEXAS 1/12/68

Figure 14 shows the effect of the amount of reducing current used upon the number of reduction coulombs required to reduce the sorbed fluorine after applying 31.5 coul at +6.0 v. The limiting region between 300 to 500 $\mu$a corresponds to the reduction of only the sorbed fluorine in the fluoride film. The rise in the curve between 30 to 200 $\mu$a is due to reduction of species in solution in addition t sorbed reproducible species.

Figure 15 shows the decay of the open-circuit potential of Monel after applying 6.0 v for 65 min. It is easy to see that the reduction current involved here would not have any significant effect on the galvanostatic cathodic reduction curves.

Electrode film resistance measurements show a significant difference under anodic conditions and after stripping as shown in Figure 16. Film resistances were calculated from the instantaneous change in potential observed on application of a 10 $\mu$sec constant-current, 3.6 ma pulse to the electrode. The potential changes were recorded by photographs of oscilloscope traces. Since the concentration of $NH_4F$ employed, 0.01M, was small, the solution resistance was relatively high and therefore made a significant contribution to the measured electrode film resistance. However, the solution concentration was not changed significantly by the passage of low currents for short periods of time; therefore, contribution of solution resistance is constant and changes in the values measured for different electrode treatments are due to changes in the electrode film resistance. As shown in Figure 6, application of cathodic current resulted in a steady decrease in film resistance, while anodic polarization to +4.0 v resulted in a rapid increase to a constant value. The average change in film resistance observed between the anodic state and stripped state was $\pm 6.0$ $\Omega$ or 30 $\Omega/cm^2$. These results and results of the cathodic stripping measurements described earlier in this report indicate that the change in film resistance is due to saturation and discharge of fluorine in the electrode corrosion product film.
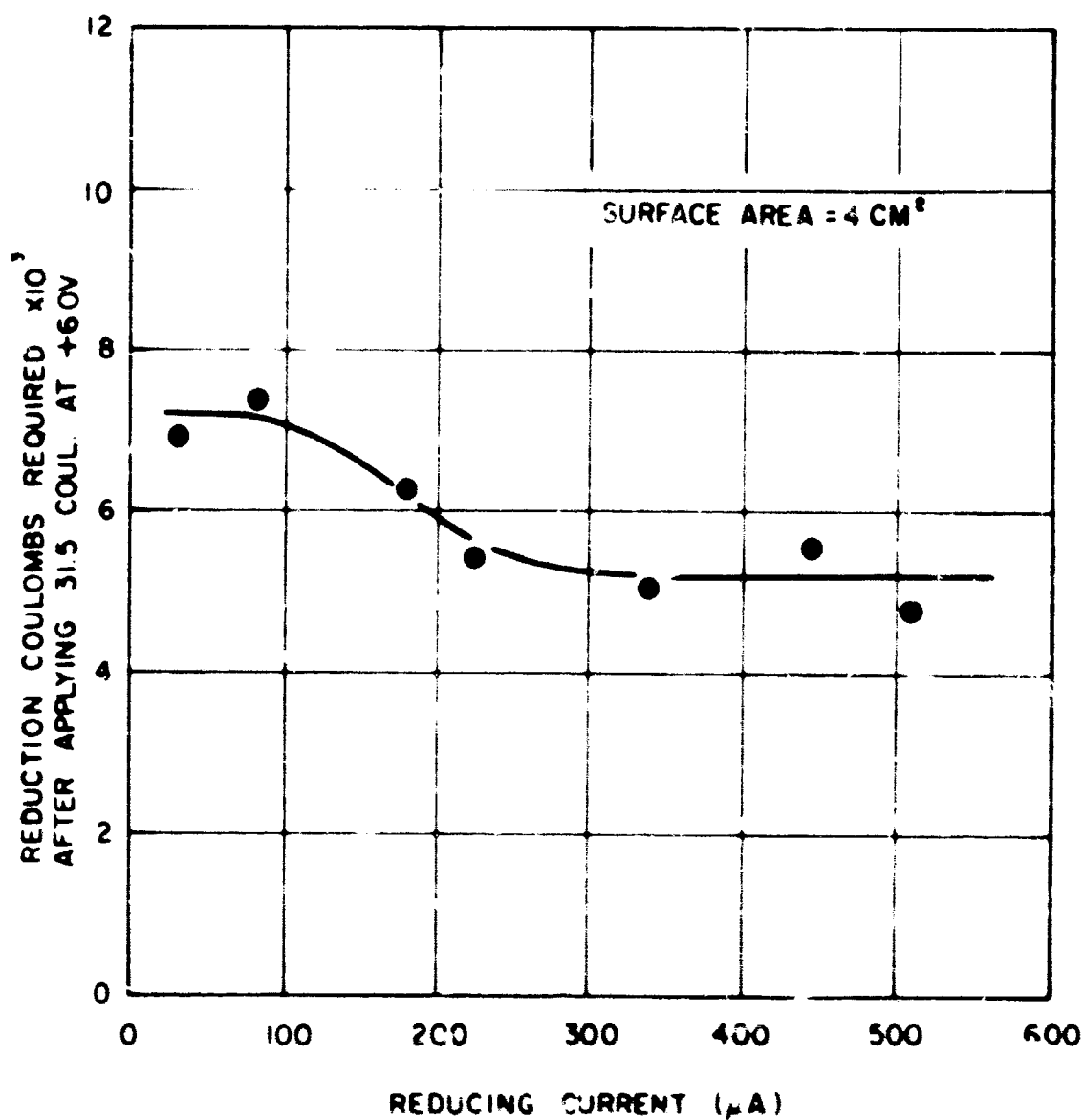
Fig. 14—EFFECT OF THE REDUCING CURRENT ON THE NO. OF
REDUCTION COULOMBS REQUIRED AFTER APPLYING
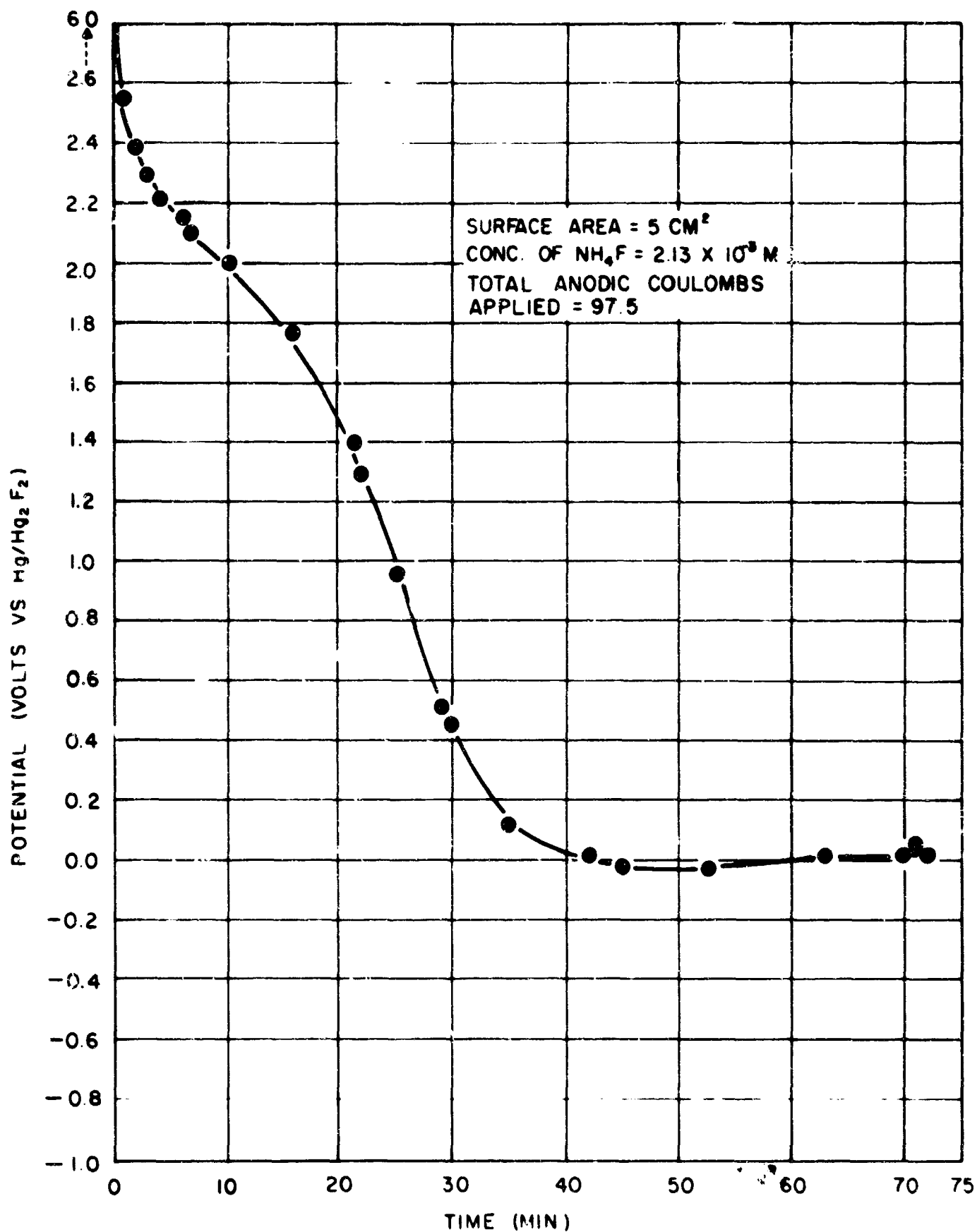31.5 COUL AT +6.0V IN 0.1M NH₄F IN AHF

25

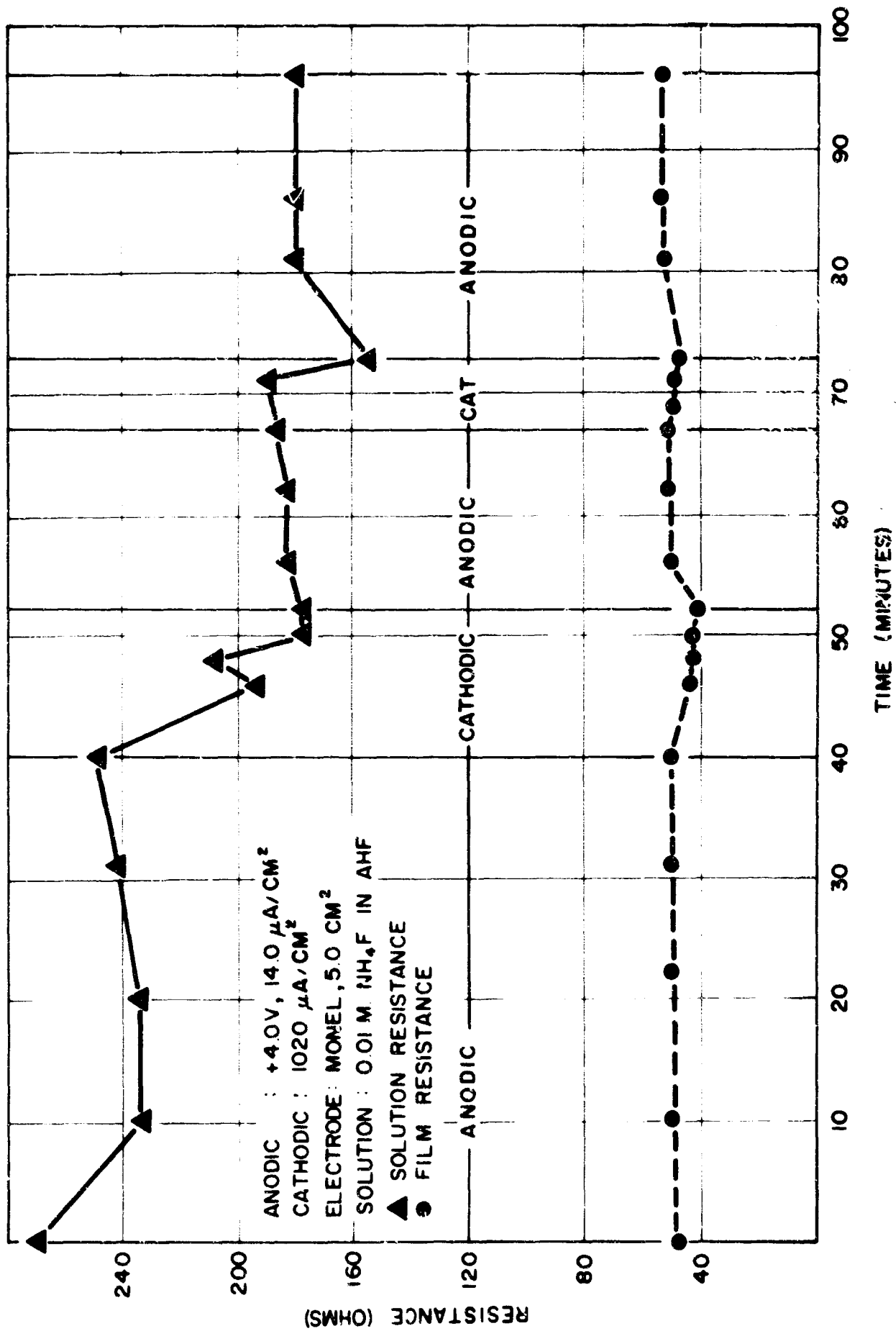Fig. 15—DECAY OF THE MONEL OPEN CIRCUIT POTENTIAL AFTER APPLYING +6.0V/65 MIN

26

Fig. 16 – SOLUTION AND ELECTRODE FILM RESISTANCE AS A FUNCTION OF
ANODIC AND CATHODIC CURRENT

27

## V.     HF CONDUCTIVITY

The maintenance of HF of high purity in the electrolysis cells is important in obtaining reproducible results and in interpreting the data obtained.   In the past quarter several experiments were performed to check the effectiveness of cold traps in purifying the carrier gas $(N_2)$ used in the AHF cells. The effects of pure helium, passed through a liquid nitrogen cold trap, were compared to nitrogen passed through a dry ice cold trap. Each gas was bubbled through the cell at a rate of 40 cc/min (twice the normal rate used) for 15 hours, while the conductivity of the HF was monitored by measurements with a pair of platinum electrodes. Both runs showed a decrease in resistivity of approximately 250 $\Omega$-cm but returned to their initial values of approximately 4000 $\Omega$-cm after the gas was shut off and the cell allowed to return to its equilibrium temperature of $-20^{\circ}C$.   The values recorded for these two runs are shown in Figure 17.   Thus we have concluded that any increase in the conductivity was due only to a slight temperature increase caused by the warmer nitrogen or helium gas bubbled through the electrolytic cell.   The cell temperature returned to its equilibrium temperature slowly due to the poor thermal conductivity of Kel-F.

The conductivity of the AHF in the new Kel-F electrolytic cells was checked for periods up to 15 hours, with the cell closed off, to determine if there was any water diffusion through the cell wall.   The initial resistivity for these runs was about 9000 $\Omega$-cm in each case.   The results showed a maximum decrease of 190 $\Omega$-cm for a 15-hour period.   Ukaji and Kageyama (1) developed an empirical equation relating the $H_2O$ content of AHF to its resistivity as follows:

$$\log x = 1.808 - 1.528 \log R$$

where
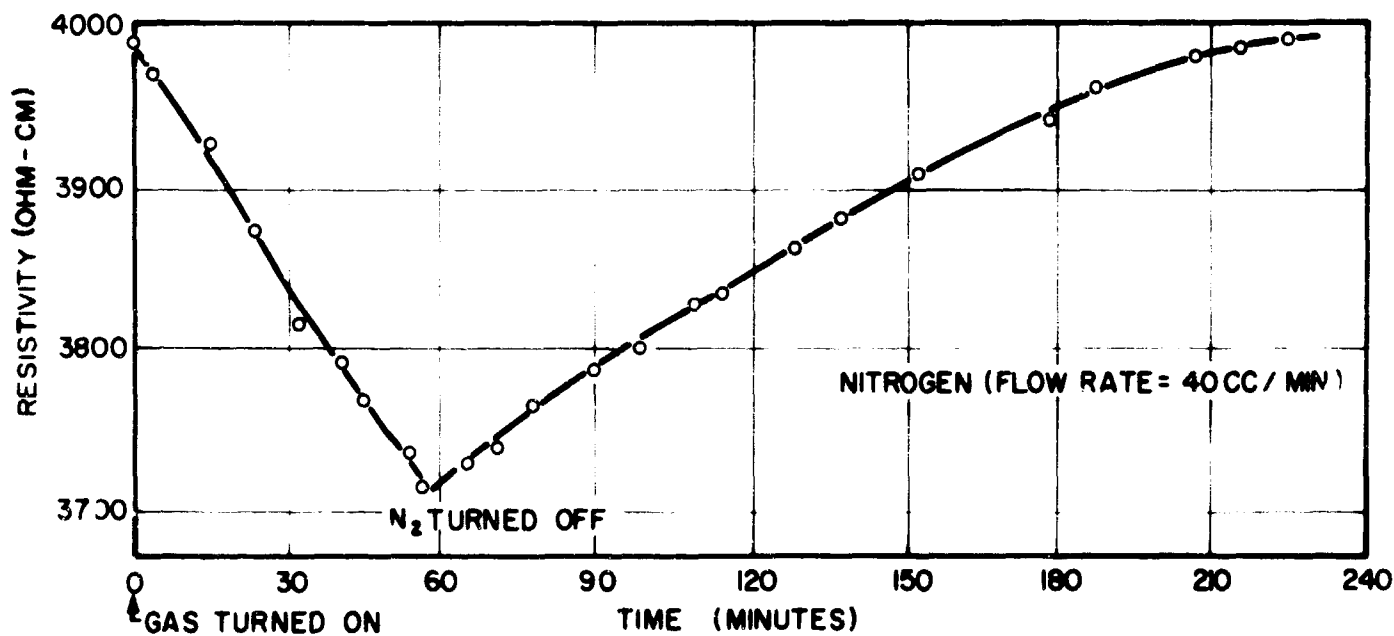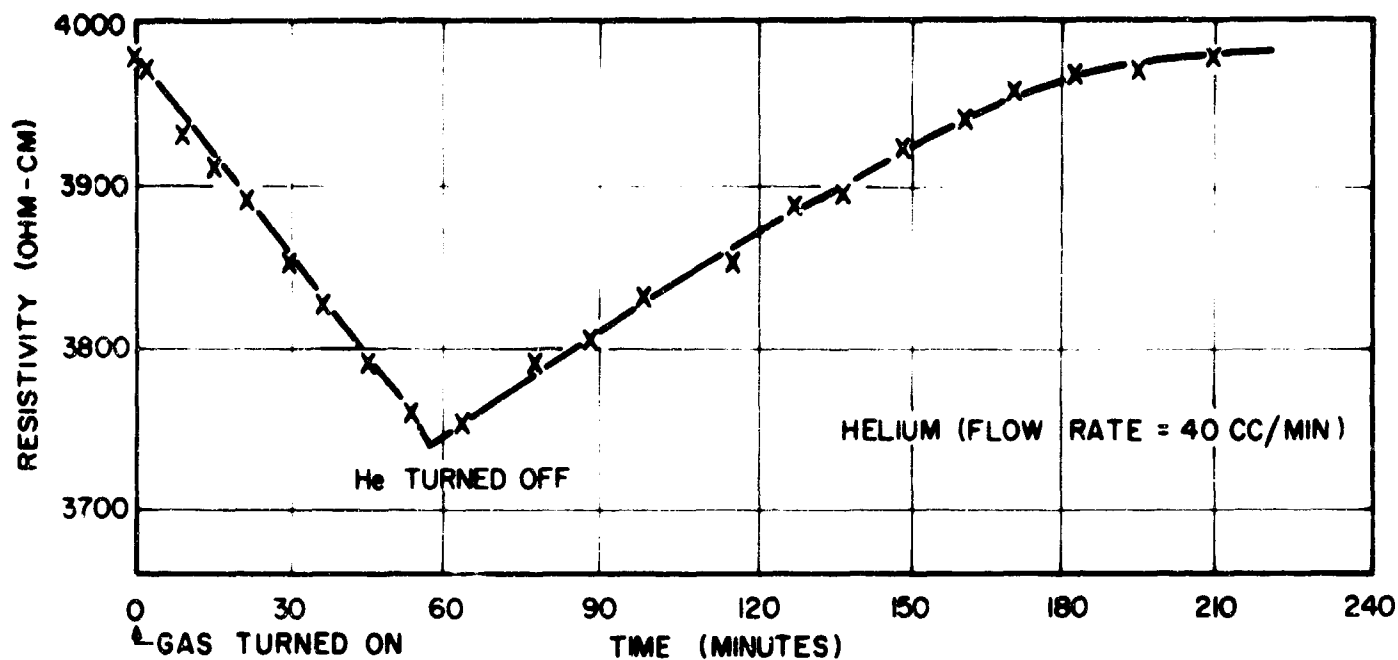
R = resistivity                    $x = \%\ H_2O$ by weight.

Fig.17-EFFECTS OF N$_2$ AND He ON THE RESISTIVITY OF THE AHF

29

Using this equation, a diffusion rate of $1.73 \times 10^{-7}$ ml/hr can be calculated as a result of the 190 $\Omega$-cm decrease in resistivity. Thus any water diffusion during a normal working day is negligible. This will allow more accurate interpretations of conductivity changes in the electrolytic cells.

It has not been possible to obtain HF with a conductivity less than $10^{-2}$ mho/cm by the NaF trapping procedure; therefore, this has been replaced by pre-electrolysis in the cells. By electrolyzing the HF in the electrolytic cells before it is used, very pure AHF was obtained. One example of this is that the resistivity of the HF increased from 300 to 8000 $\Omega$-cm after a potential of 7.0 volts and a current of 18 ma was applied across the nickel screens for 15 hours. Periods of approximately 20 hours are needed to get a resistivity of greater than $10^4$ $\Omega$-cm. According to Ukaji and Kageyama's equation (1) this corresponds to $5 \times 10^{-5}$ ml of water present in the electrolytic cell, which contains 100 ml of AHF.

When a clean Monel electrode was introduced into the cell, the conductivity increased by at least a factor of two. This was presumably due to metal ion contamination on corrosion of the Monel in the AHF. When the first rapid polarization curve was run on a Monel electrode after it had been in the cell for 100 minutes, the resistivity decreased an additional amount from 2900 to 2710 $\Omega$-cm.

The addition of small amounts of water or $NH_4F$ to AHF had similar effects on the resistivity of the AHF   Eight milligrams $(2.16 \times 10^{-3}$ M/l) of $NH_4F$ were added to the AHF and the resistivity decreased from 8000 to 45 $\Omega$-cm. When 0.05% water was added to AHF, the resistivity decreased from 6000 to 68 $\Omega$-cm. From these data the equivalent conductance of water in HF was calculated to be 528 and 447 mhos-cm$^2$ for 0.05 and 0.1%, respectively. These are similar to values obtained for solutions of strong acids in water.

30

## VI.  ANALYTICAL WORK

The products which may be formed by the electrochemical fluorination of ammonia in AHF include gaseous products ($NF_3$, $NHF_2$, and $NH_2F$) and soluble products ($NHF_3^+$, $NH_2F_2^+$, etc.). A determination of the distribution of these products as a function of electrode and electrolyte parameters is necessary to describe the kinetics and mechanism of the electrode reactions. At the present, these goals are being achieved by the use of gas chromatography and infrared spectra for analyses of the vapor phase and by electrochemical measurements and infrared spectra for the solution phase. Results for the electrochemical measurements were given in earlier sections of this report.

The selection of materials for IR gas and liquid cell windows for this work is very limited because of the high reactivity of the compounds studied. Materials investigated were Kel-F, NaCl coated with Kel-F grease, $BaF_2$, and Irtran-2 (poly-zinc sulphide). The most satisfactory of these is Irtran-2, which gives excellent spectra for gaseous HF (Figure 18) and $NF_3$ (Figure 19). After exposure to HF and $NF_3$, the background spectrum of Irtran-2 reproduced the background obtained before exposure indicating a high degree of stability in the presence of fluorinated compounds. A calibration curve to be used for the analysis of $NF_3$ in gaseous products is shown in Figure 20. Preliminary experiments with the chromatograph have indicated that a 20-foot long, 1/4-inch diameter Monel column packed with #40 Kel-F grease on shredded Teflon gives satisfactory results for the analysis of fluorinated mixtures. Calibration IR curves using HF gas and $NF_3$ are being made using the gas chromatograph.
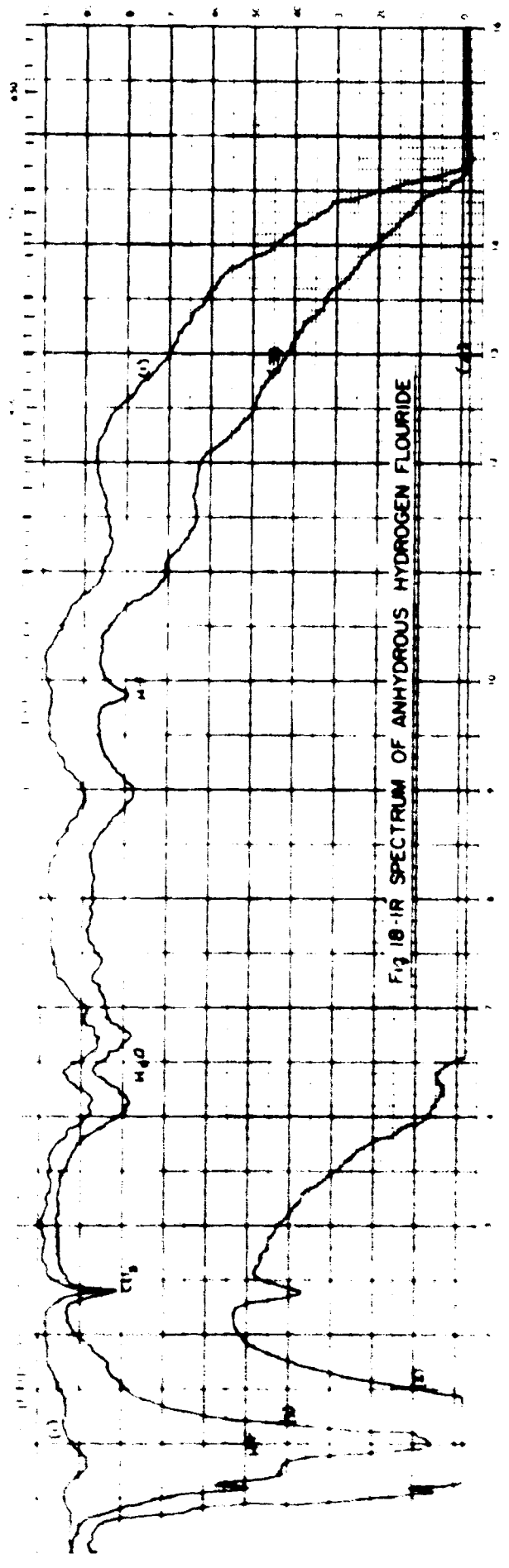
31

Fig 18-IR SPECTRUM OF ANHYDROUS HYDROGEN FLUORIDE
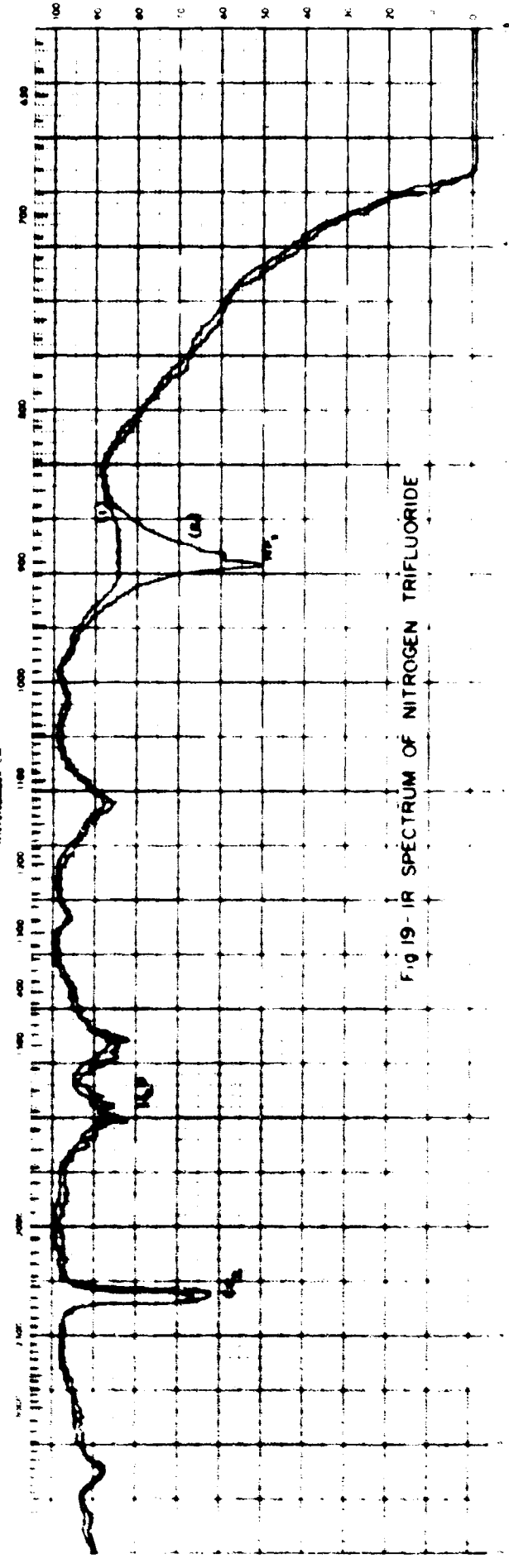
Fig 19-IR SPECTRUM OF NITROGEN TRIFLUORIDE

Fig. 20-ABSORBANCE OF NF₃ AT 11.02 μ
IN A 10 CM GAS CELL WITH
IRTRAN-2 WINDOWS

33

## VII. SUMMARY OF ELECTRODE MATERIALS

Twenty electrode materials were investigated during the past report year for possible use as an anode material in AHF. The behavior of these materials can be divided into four distinct classes.

Class I — Materials which exhibited a high corrosion rate in AHF.
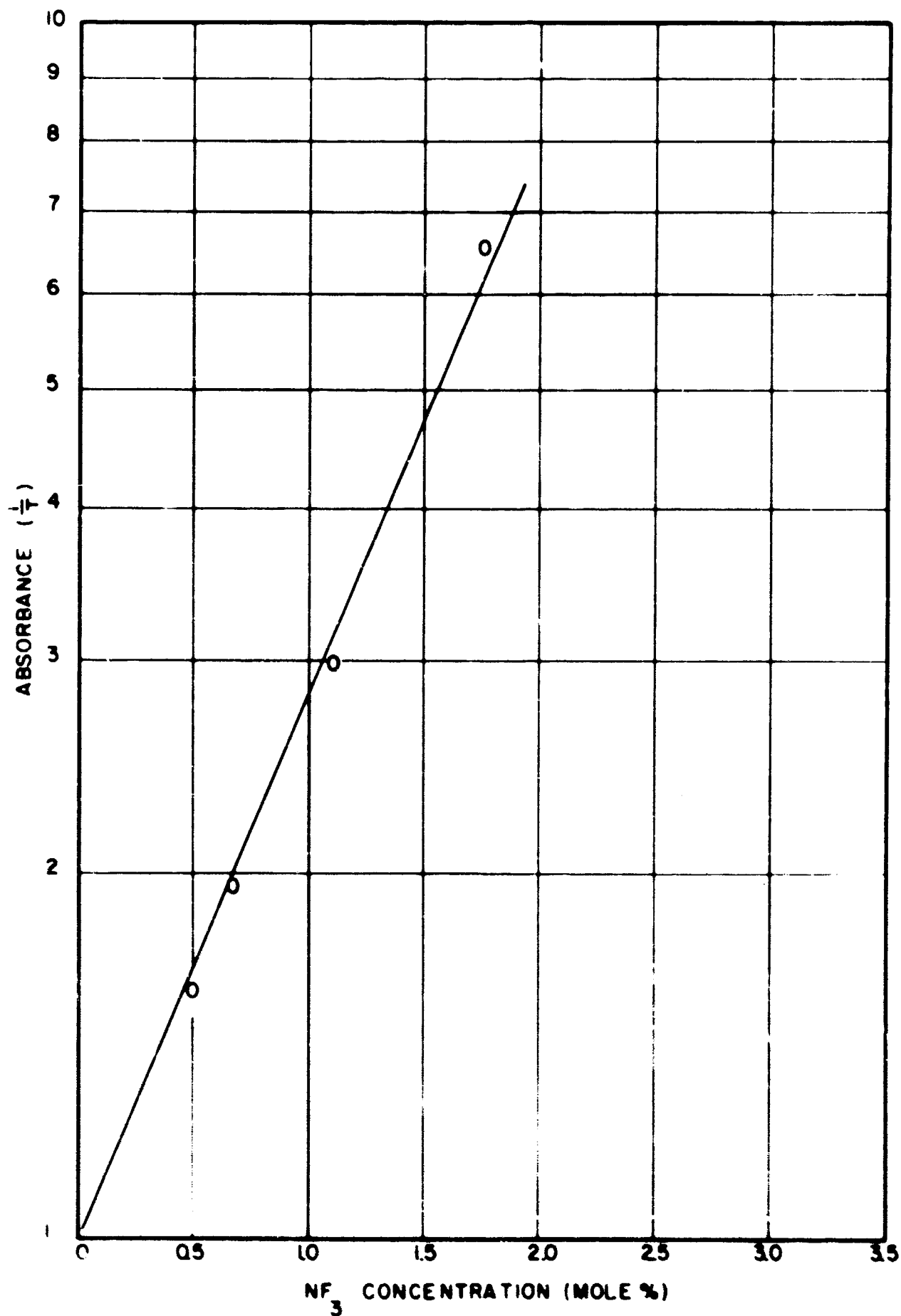
Class II — Materials which exhibited a low corrosion rate in AHF due to formation of a passive nonconducting film.

Class III — Materials which exhibited a low corrosion rate in AHF due to formation of a passive conducting film. Anodic fluorine evolution was observed from these materials.

Class IV — Materials which exhibited a negligible corrosion rate in AHF at open circuit but were severely damaged by fluorine evolution during anodic polarization.

The Class I materials are antimony, bismuth, cadmium, molybdenum, silver, zirconium diboride, and thallium. High current densities (on the order of $10^5$ $\mu a/cm^2$) at low potentials was the dominant characteristic of polarization curves of these metals (except thallium which dissolved too rapidly for a polarization curve to be obtained) in AHF as shown in Figures 21-26. Weight change data on cadmium and molybdenum at open circuit and at anodic bias are shown in Figures 27 and 28. Weight loss studies at anodic bias showed that the corrosion current efficiency was nearly 100% for antimony, bismuth, cadmium, and molybdenum (see Table IV). The high weight loss rates of silver and thallium in AHF at open

34

Fig.21-POLARIZATION CURVES FOR ANTIMONY IN AHF

The figure shows polarization curves for antimony in AHF. The vertical axis is labeled CURRENT DENSITY ($\mu A/CM^2$) ranging from $10$ to $10^5$. The horizontal axis is labeled POTENTIAL ( VOLTS VS Pt ) ranging from -1 to 6. Legend: ●Sb IN AHF 2.5 HOURS BEFORE RAPID POLARIZATION
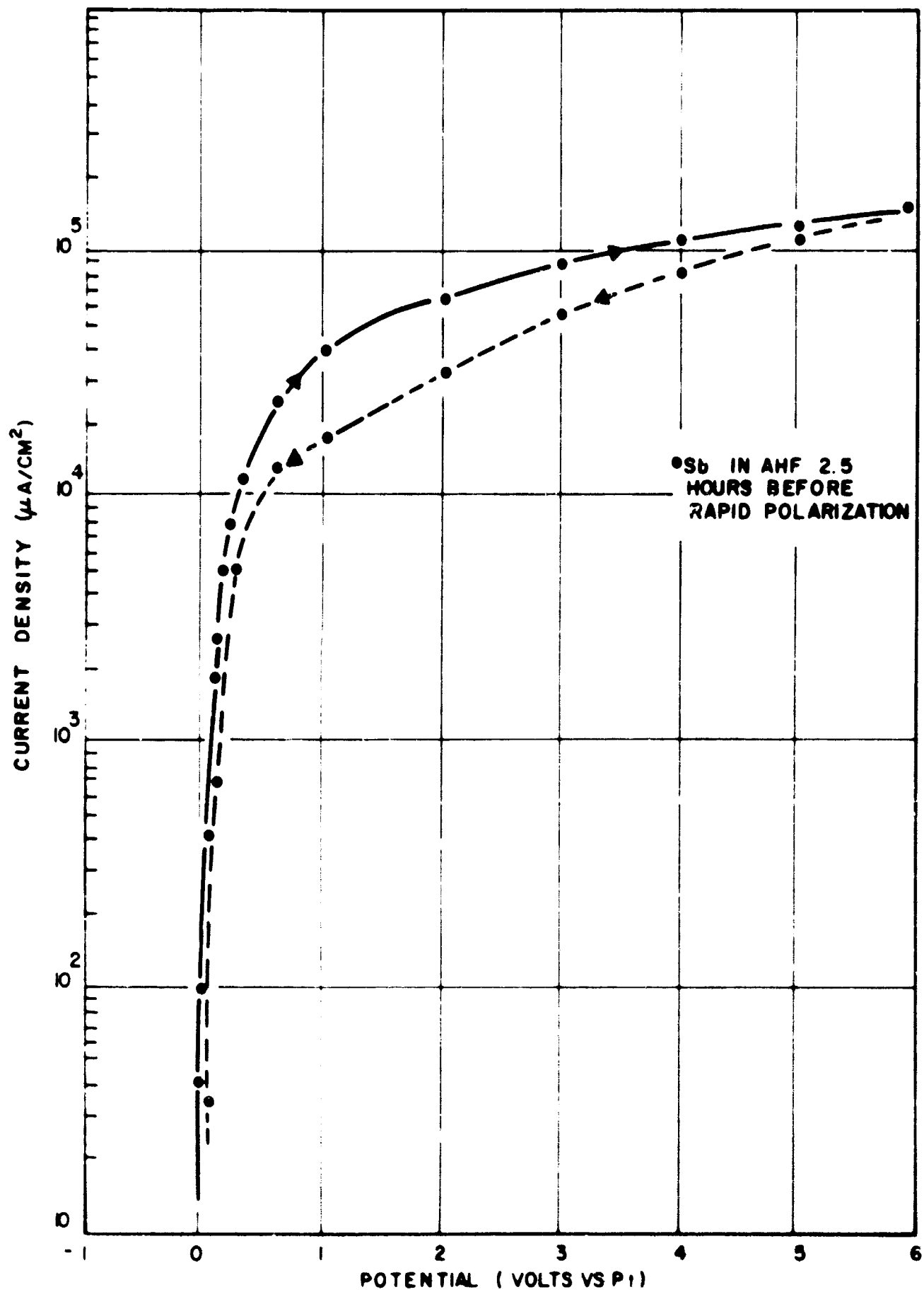
Fig.22 - POLARIZATION CURVES FOR BISMUTH IN AHF
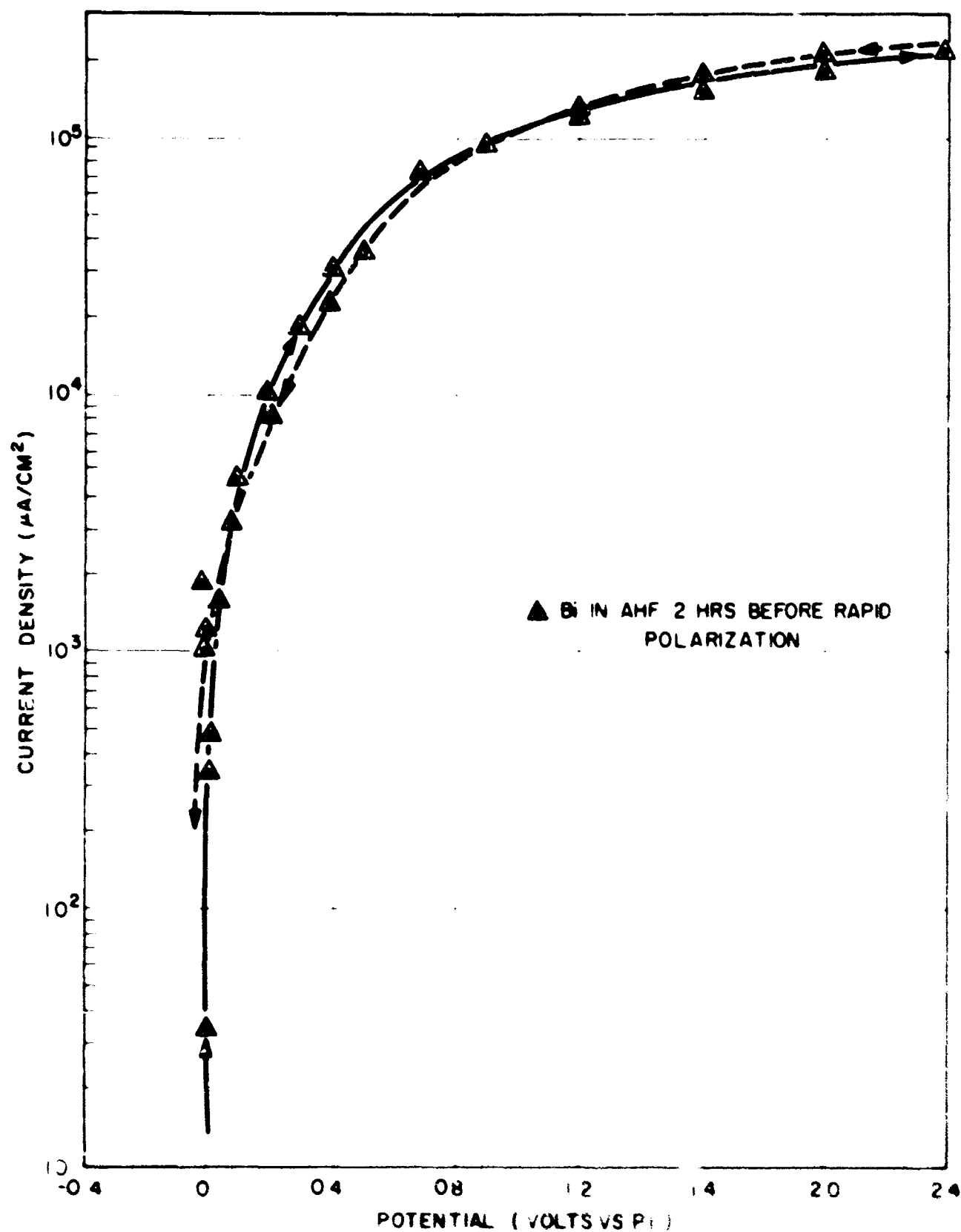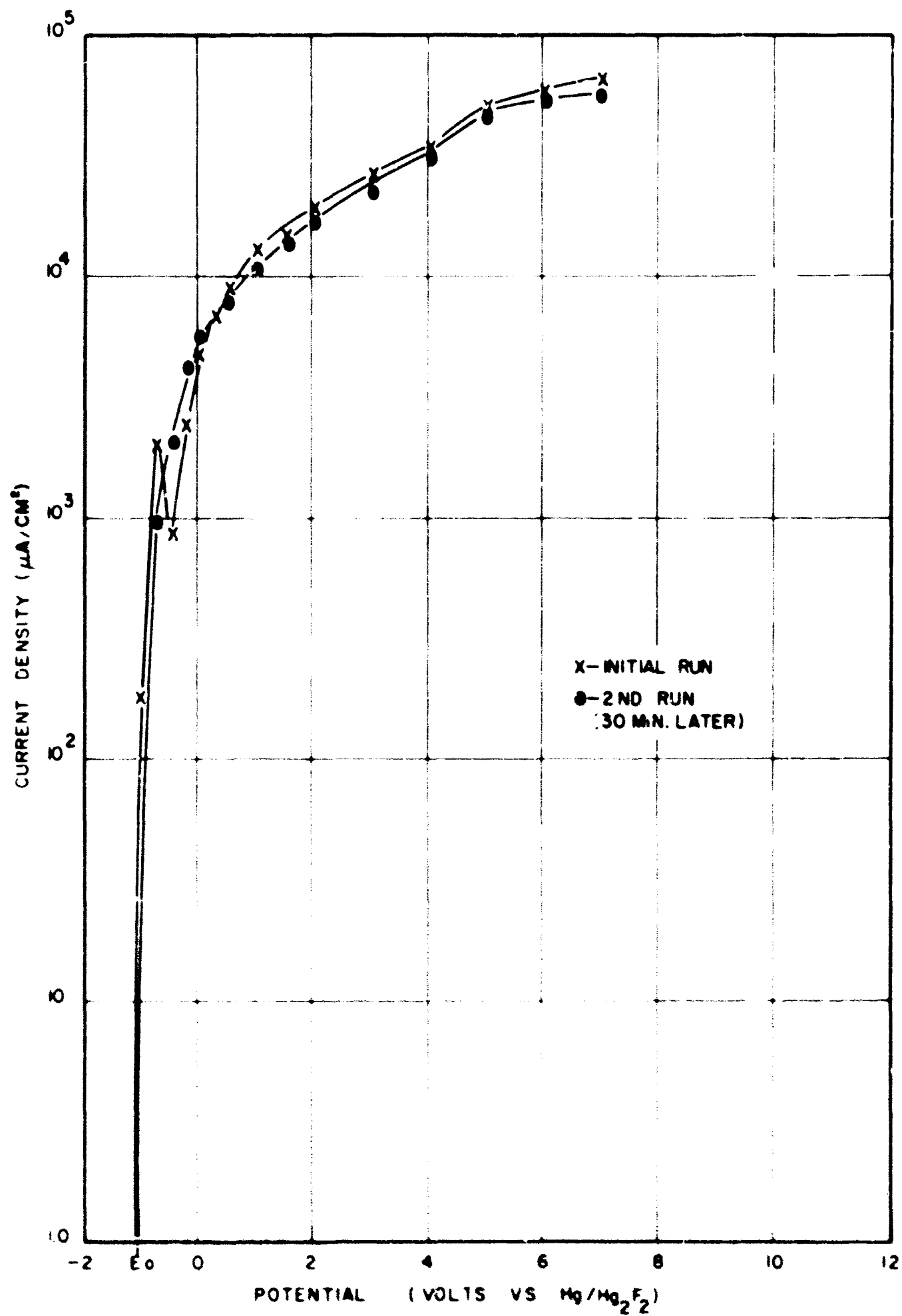
Fig.23-ANODIC POLARIZATION OF CADMIUM
IN 0.0125M NaF IN AHF
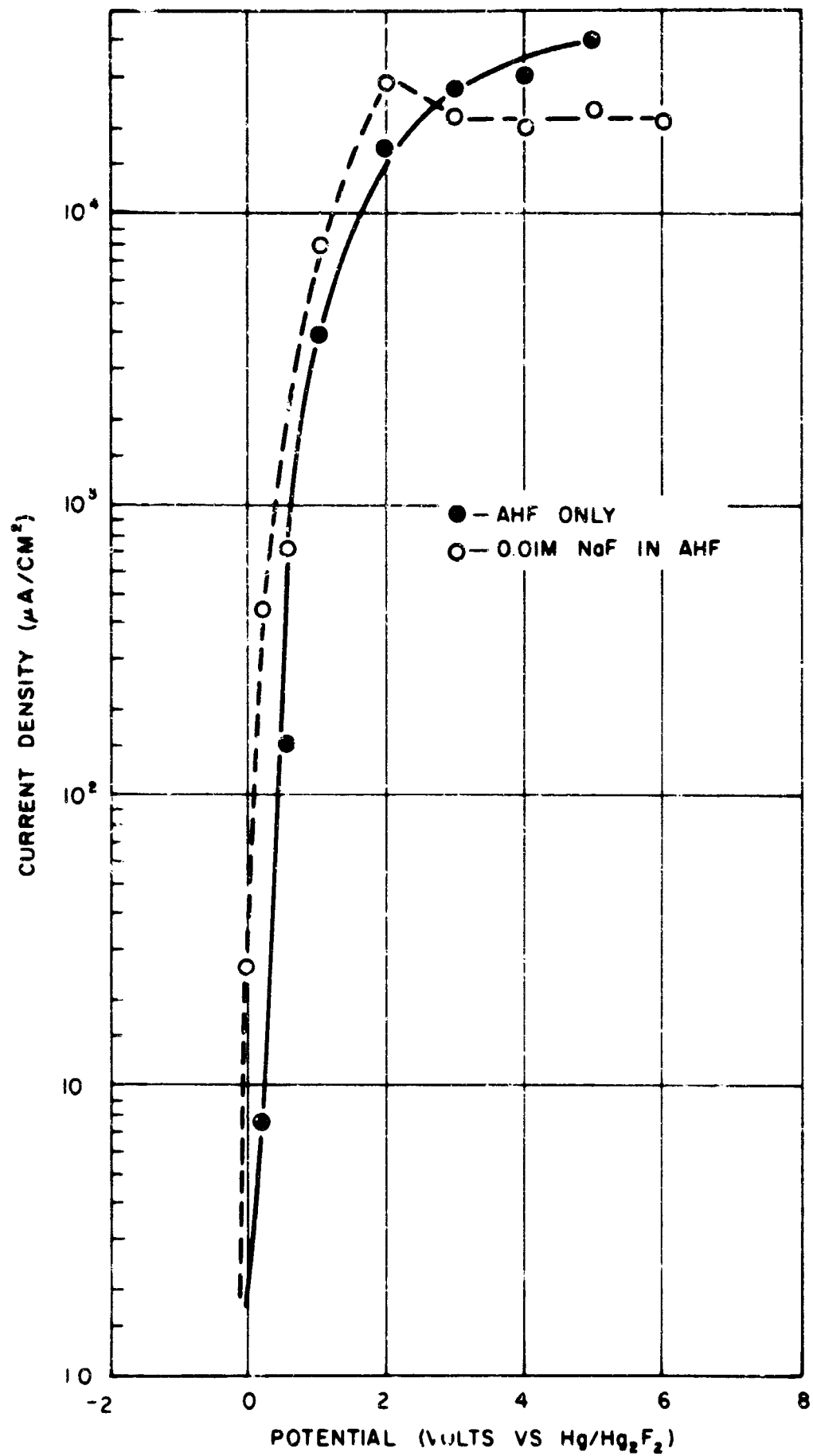
Fig. 24-ANODIC POLARIZATION OF MOLYBDENUM

38
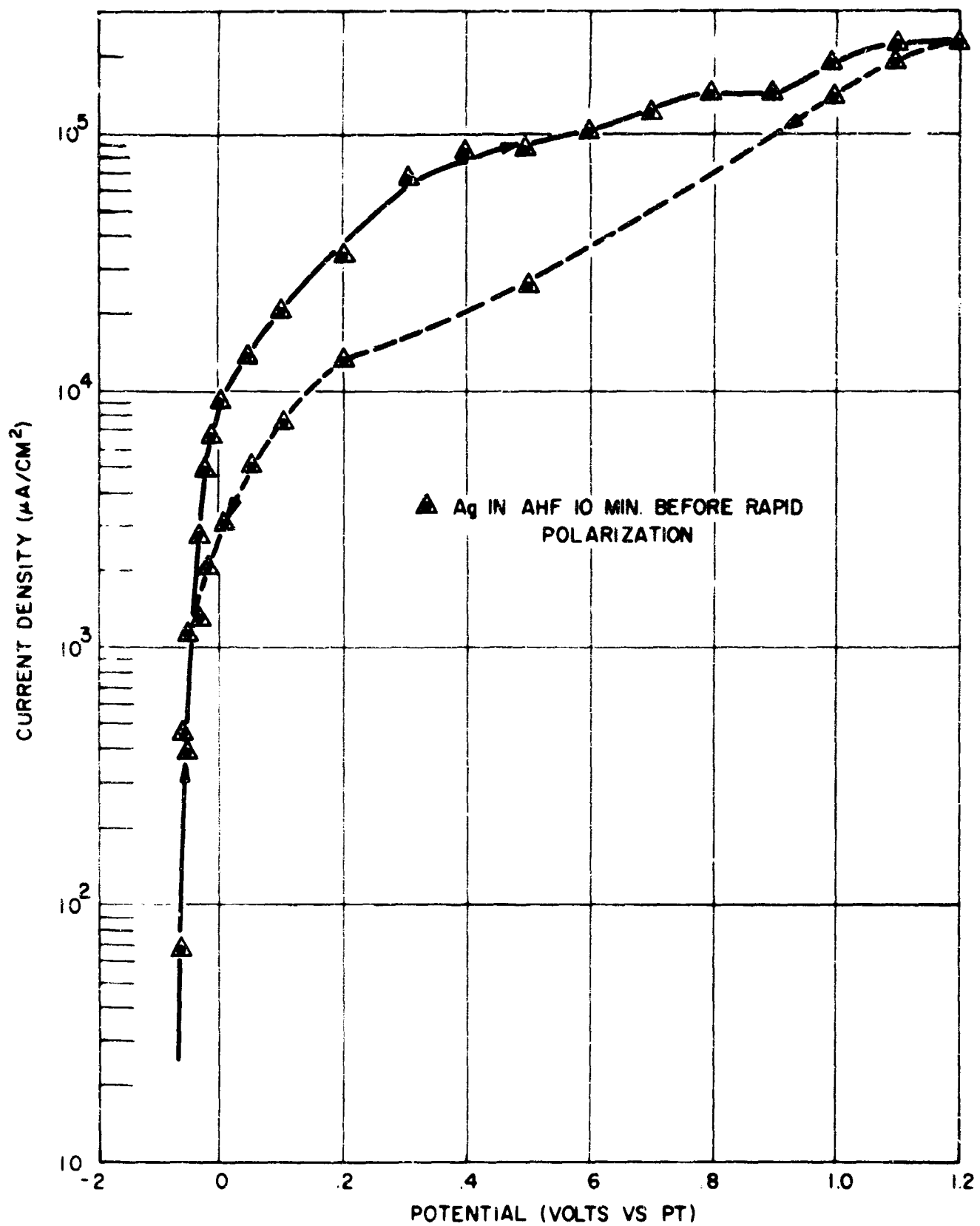
Fig. 25-POLARIZATION CURVES FOR SILVER IN AHF
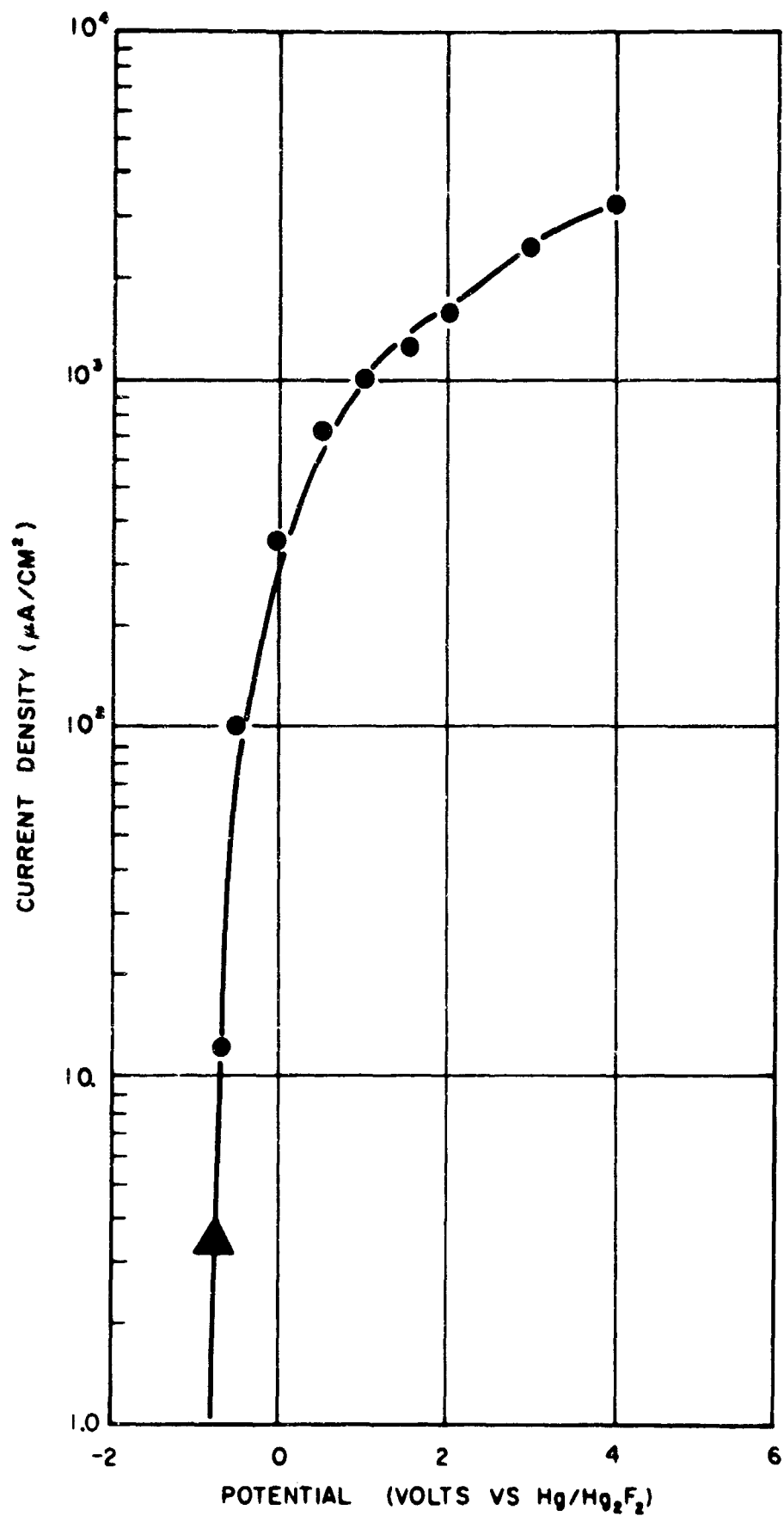
Fig. 26 - ANODIC POLARIZATION OF ZIRCONIUM DIBORIDE IN AHF

40
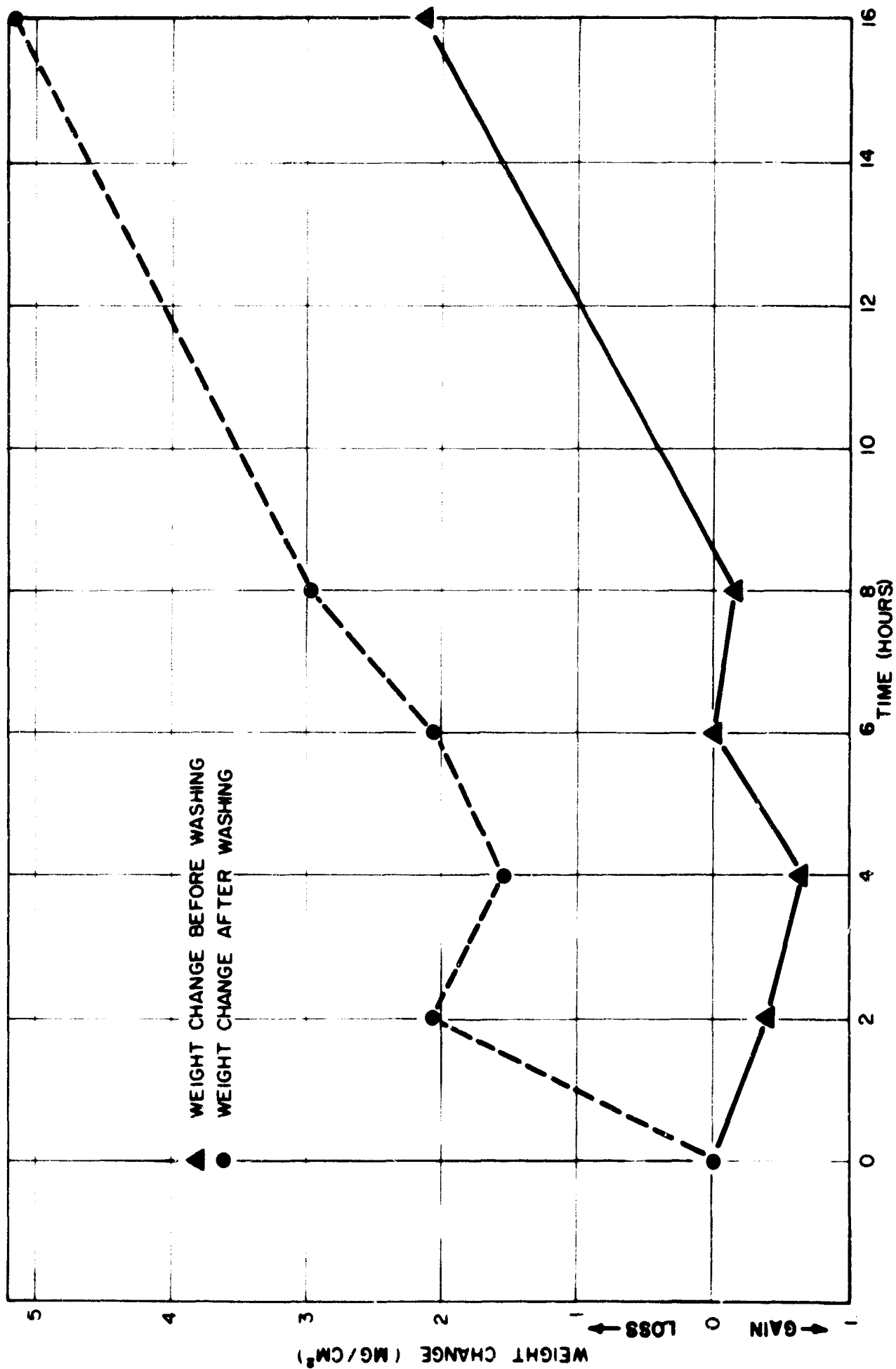
Fig. 27 – WEIGHT CHANGES OF CADMIUM IN AHF

WEIGHT CHANGE BEFORE WASHING

WEIGHT CHANGE AFTER WASHING

WEIGHT CHANGE (MG/CM²)

←GAIN    LOSS→

TIME (HOURS)

41
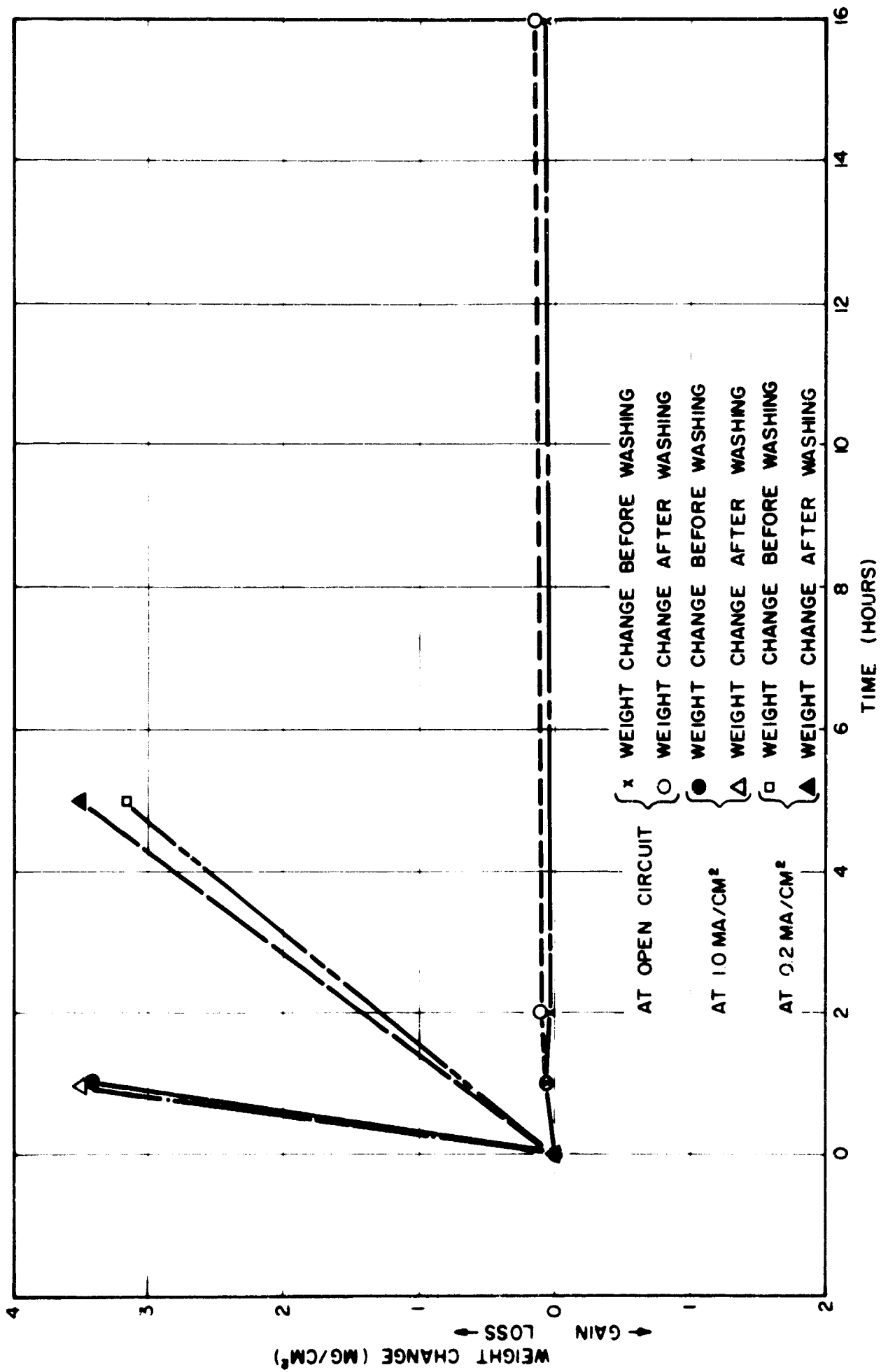
Fig.28-WEIGHT CHANGES OF MOLYBDENUM IN AHF

Legend:

AT OPEN CIRCUIT
- × WEIGHT CHANGE BEFORE WASHING
- ○ WEIGHT CHANGE AFTER WASHING

AT 1.0 MA/CM²
- ● WEIGHT CHANGE BEFORE WASHING
- △ WEIGHT CHANGE AFTER WASHING

AT 0.2 MA/CM²
- □ WEIGHT CHANGE BEFORE WASHING
- ▲ WEIGHT CHANGE AFTER WASHING

TIME (HOURS)

WEIGHT CHANGE (MG/CM²)
GAIN ← LOSS →

42

## TABLE IV

### DATA ON CLASS I MATERIALS

| METAL | METAL FLUORIDE | SOLUBILITY OF METAL FLUORIDE IN AHF[a] (g/100 g AHF) | TEMP °C | WEIGHT LOSS RATE AT ANODIC BIAS (mg/cm$^2$/hr) Exptl. | Calc. | WEIGHT LOSS RATE AT OPEN CIRCUIT (mg/cm$^2$/hr) |
|---|---|---|---|---|---|---|
| Sb | $SbF_3$ | 0.191 ± 0.003 | -23.8 | 11.63[c] | 10.15 | --- |
| Bi | $BiF_3$ | 0.010 ± 0.003 | -23.1 | 24.6[d] | 21.0 | ---- |
| Cd | $CdF_2$ | 0.189 ± 0.001 | -23.2 | 76.5[e] | 62.5 | 0.3 |
| Mo | $MoF_6$ | 0.018[b] | -23.0 | 15.1[f] | 14.8 | 0.01 |
| Ag | $AgF$ | 27.2 ± 0.7 | -25.0 | ---- | ---- | 6.6 |
| Ag | $AgF_2$ | 0.024 ± 0.001 | -24.2 | ---- | ---- | |
| Tl | $TlF$ | 305 ± 15 | -25.2 | ---- | ---- | |
| Tl | $TlF_3$ | 0.027 ± 0.003 | -25.2 | ---- | ---- | 61.0 |
| $ZrB_2$ | ---- | ----------- | ---- | 0.96[b] | 1.80 | ---- |

[a] See Reference 2.

[b] This value calculated at TRACOR, Inc. (see Page 47).

[c] 2.0 v vs Pt.

[d] During polarization.

[e] 2.0 v vs $Hg/Hg_2F_2$.

[f] 1.0 ma applied current.

TRACOR, Inc.
Austin, Texas

43

circuit are expected because of the high solubility of AgF and TlF in HF. Zirconium diboride (a 0.001 inch thick plasma sprayed coating of zirconium diboride on a 0.125 inch zirconium rod) in AHF showed a weight loss of 1.98 $mg/cm^2$ during a two-hour anodic run. The calculated corrosion current weight loss for the run was 3.6 $mg/cm^2$. Thallium dissolved in AHF at open circuit at a tremendous rate (61.0 $mg/cm^2/hr$). Attempts were made to take advantage of the lower solubility of $TlF_3$ to passivate the electrode by immersing it under applied anodic bias of +10.0 v to oxidize the corrosion product to $TlF_3$. These attempts were unsuccessful as excessive dissolution rates were also observed under these conditions.

An estimate of the solubility of $MoF_6$ was obtained from anodic corrosion studies of molybdenum in AHF. The conductivity of the AHF was monitored during the anodic corrosion runs until it reached a constant value. This was taken to be the point at which the solution was saturated with $MoF_6$. The measured weight losses up to this time were used to determine the solubility, which was found to be 0.018 g/100g AHF at $-20^{\circ}C$.

All materials in this class were rejected as anode materials due to their high corrosion rates in AHF.

The Class II materials are aluminum, chromium, cobalt, copper, Hastelloy-F, iron, magnesium, titanium, zinc, and zirconium. Low current densities(on the order of $10^2$ $\mu a/cm^2$) over the entire potential range was the dominant characteristic of polarization curves of these metals in AHF and in AHF with NaF, $NaHF_2$, and/or $NH_3$ added as shown in Figures 29-38. There was no appreciable increase in the current density upon addition of NaF, $NaHF_2$, or $NH_3$ as a supporting electrolyte. Thus, current is limited by a high electrode film resistance rather than the resistance of the AHF.
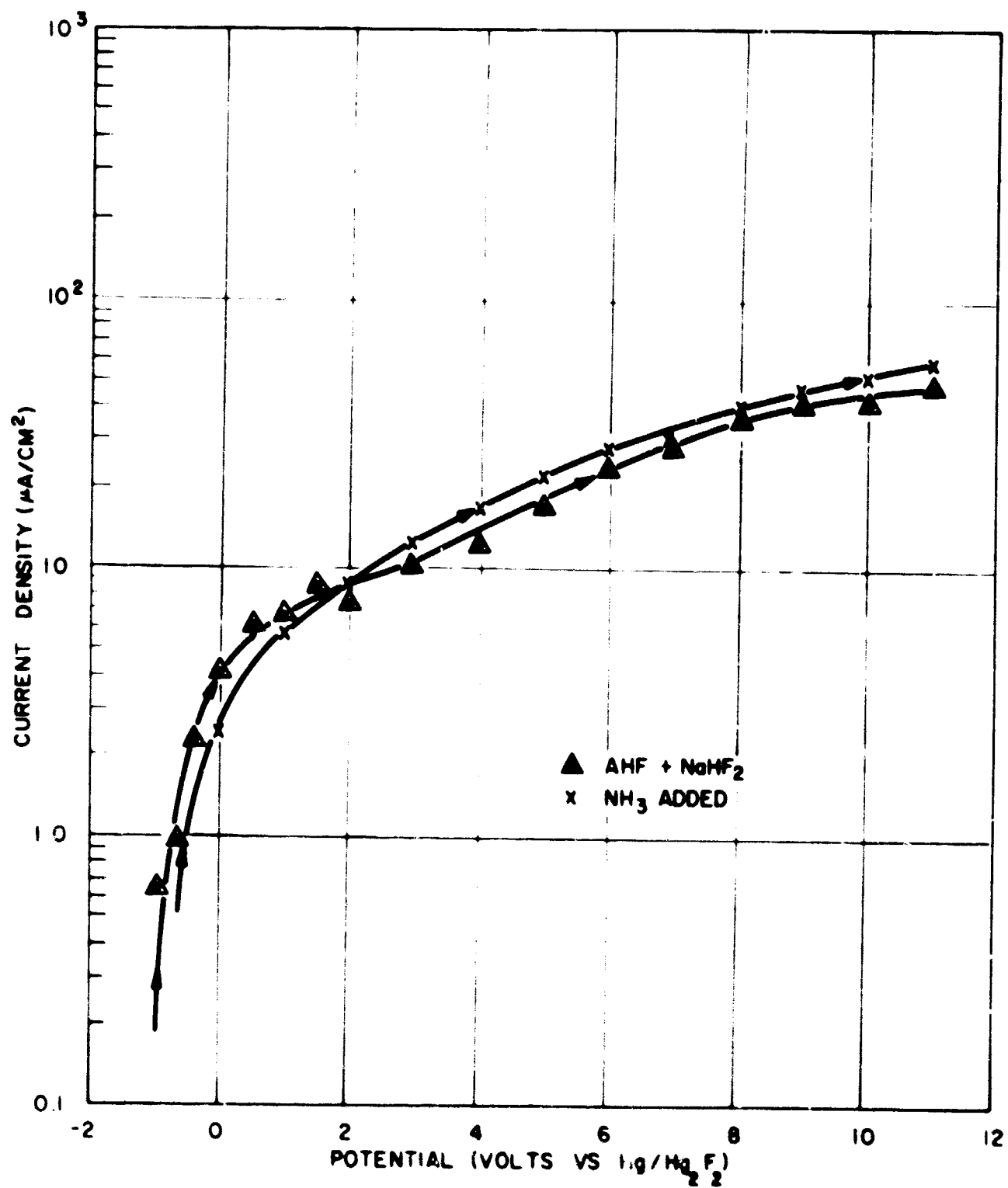
Fig.29-POLARIZATION CURVES FOR ALUMINUM IN AHF
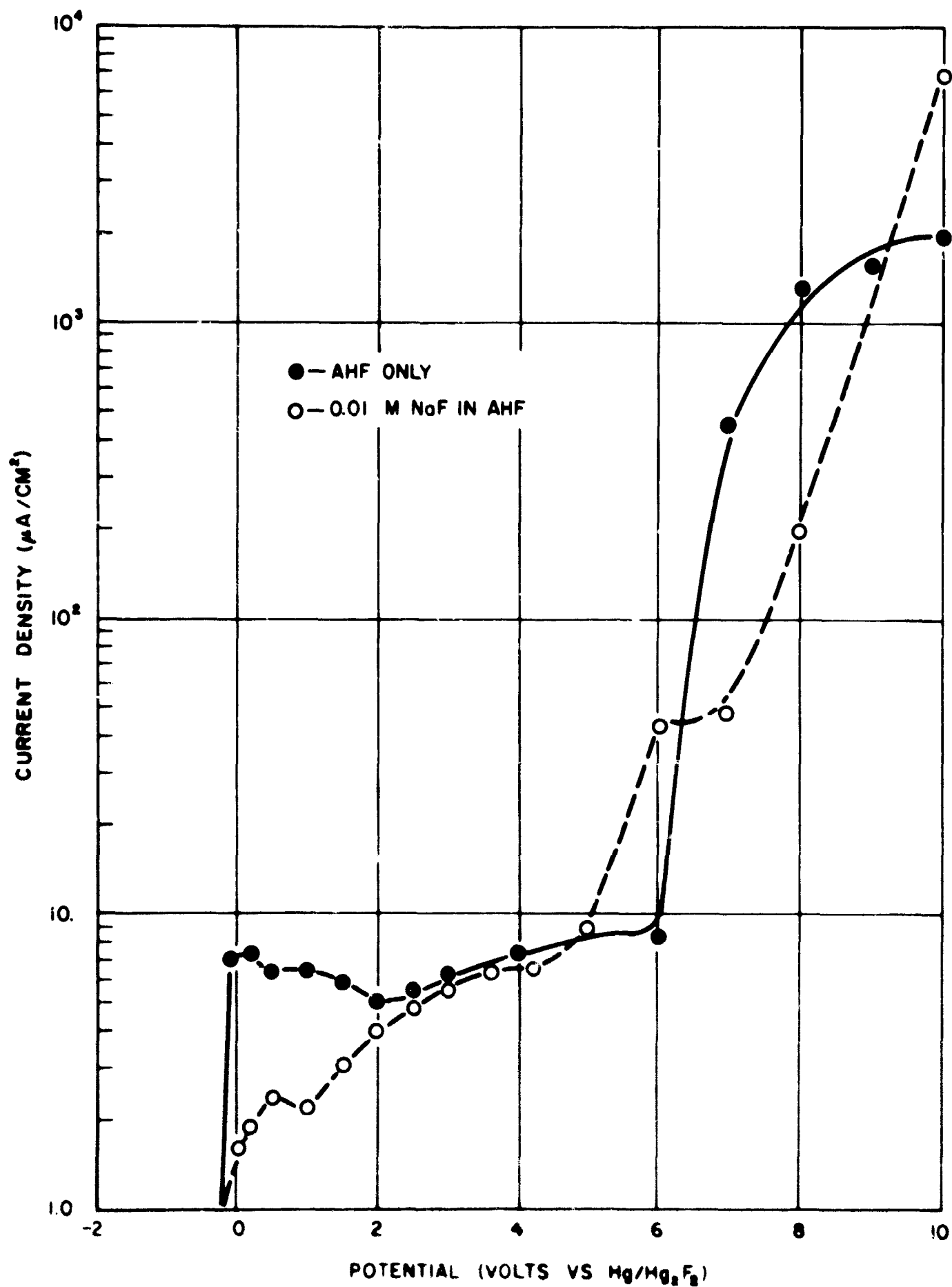
45

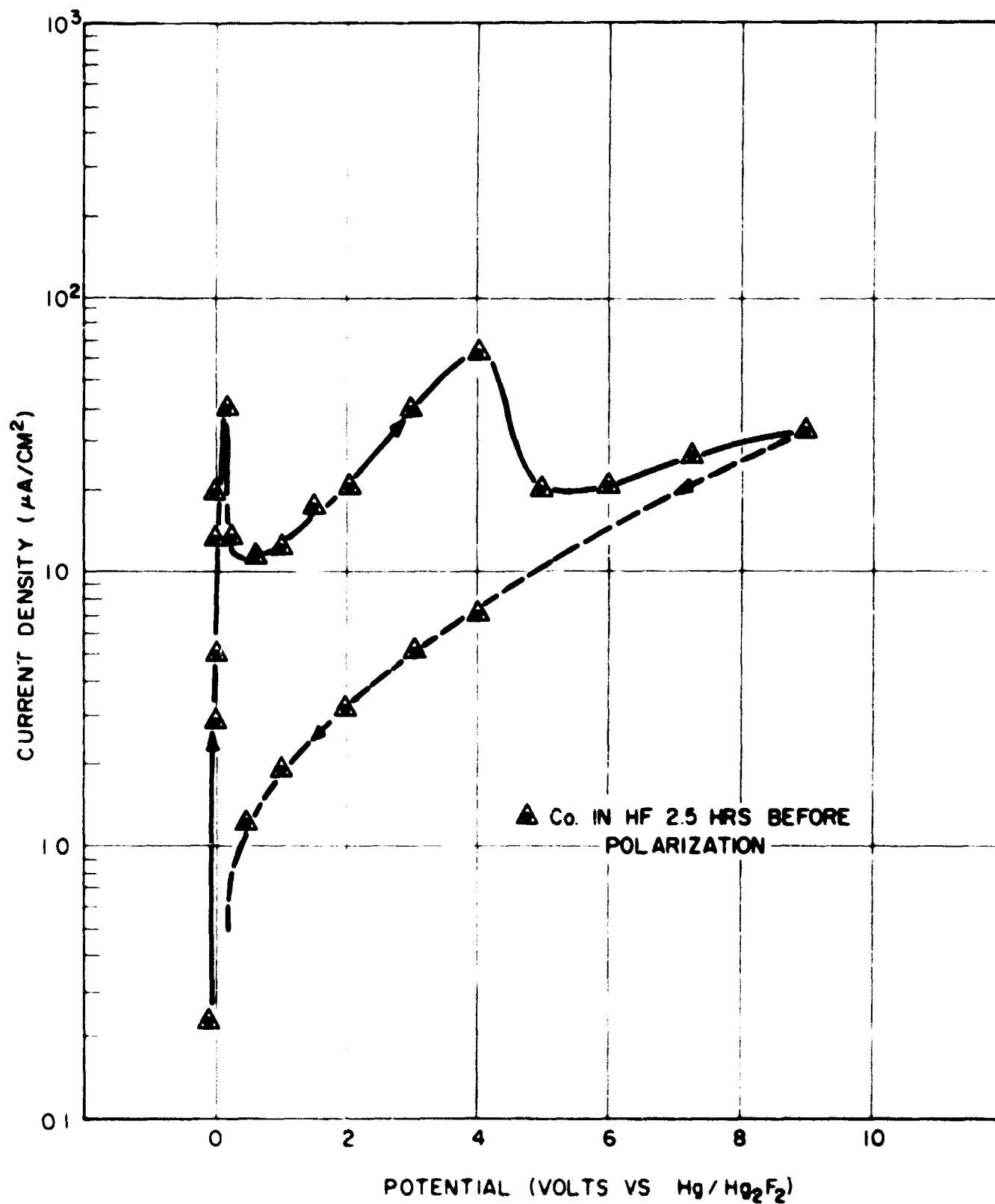Fig. 30—ANODIC POLARIZATION CURVES FOR CHROMIUM

Fig. 31 - POLARIZATION CURVES FOR COBALT IN AHF +
NaHF$_2$

47
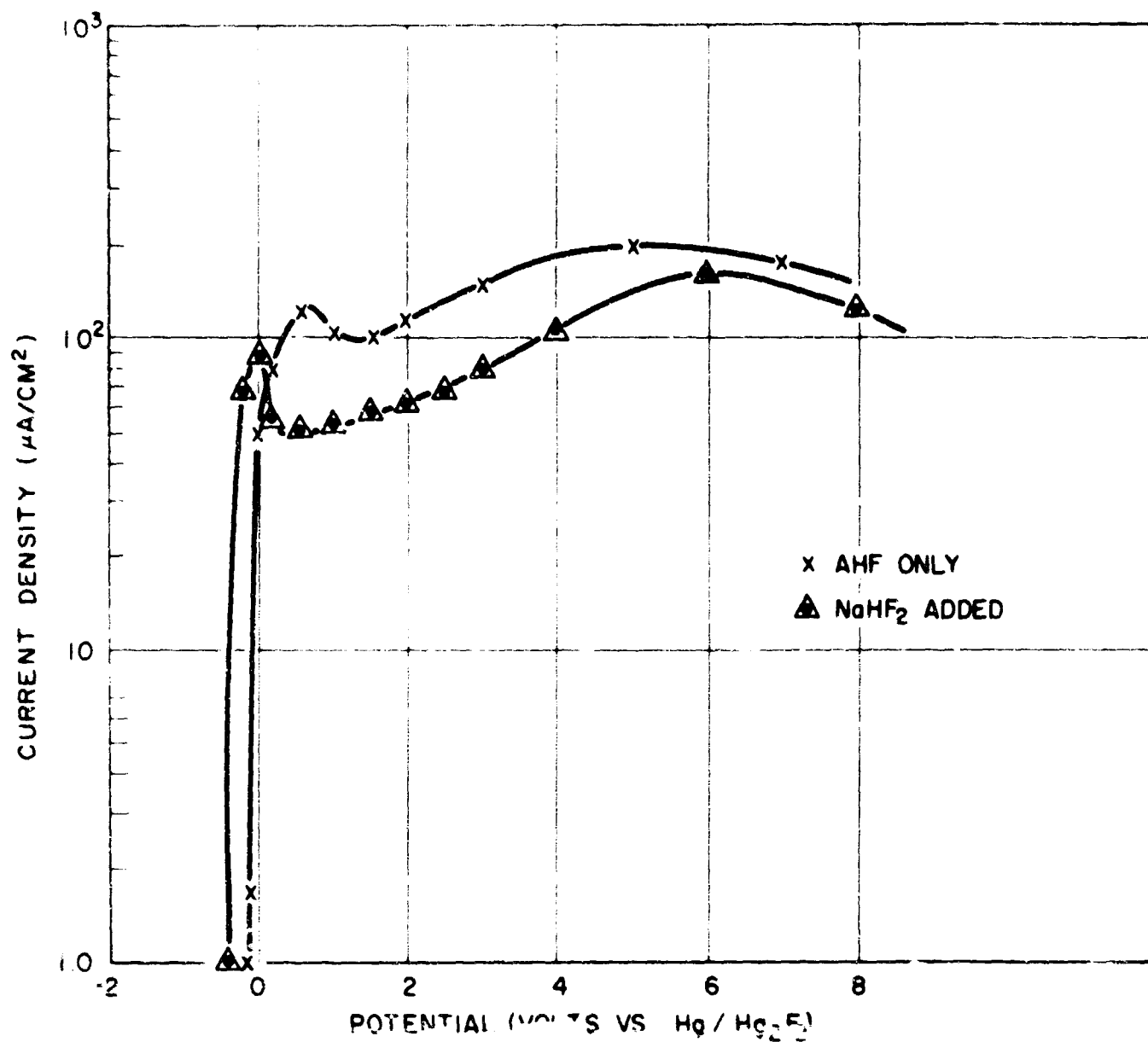
Fig. 32 - POLARIZATION CURVES FOR COPPER IN
AHF

48
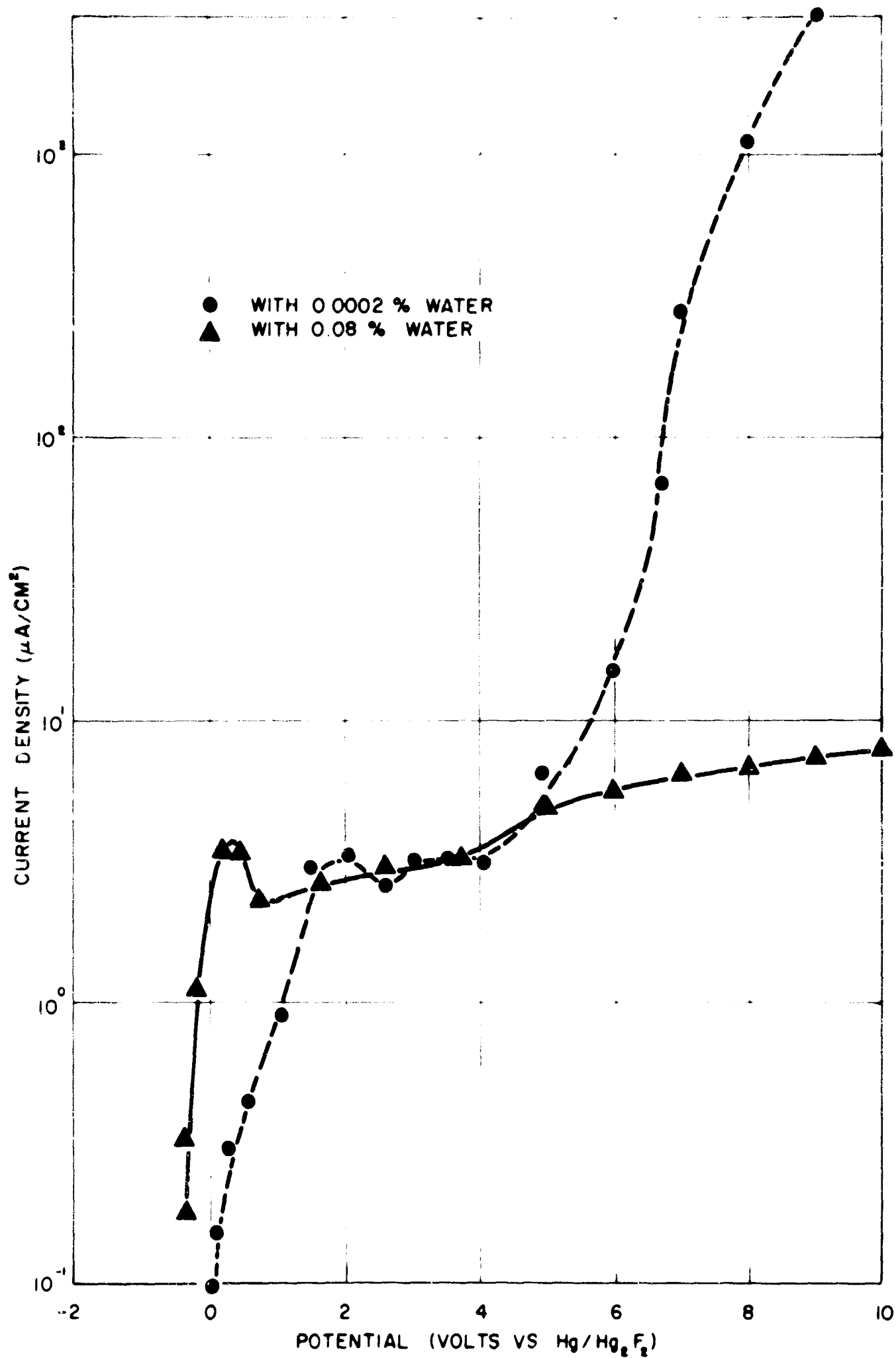
Fig. 33 - POLARIZATION CURVES FOR HASTELLOY-F IN AHF

TRACOR, INC    DWG 729-137

AUSTIN, TEXAS    1/12/88    LDF/LBH
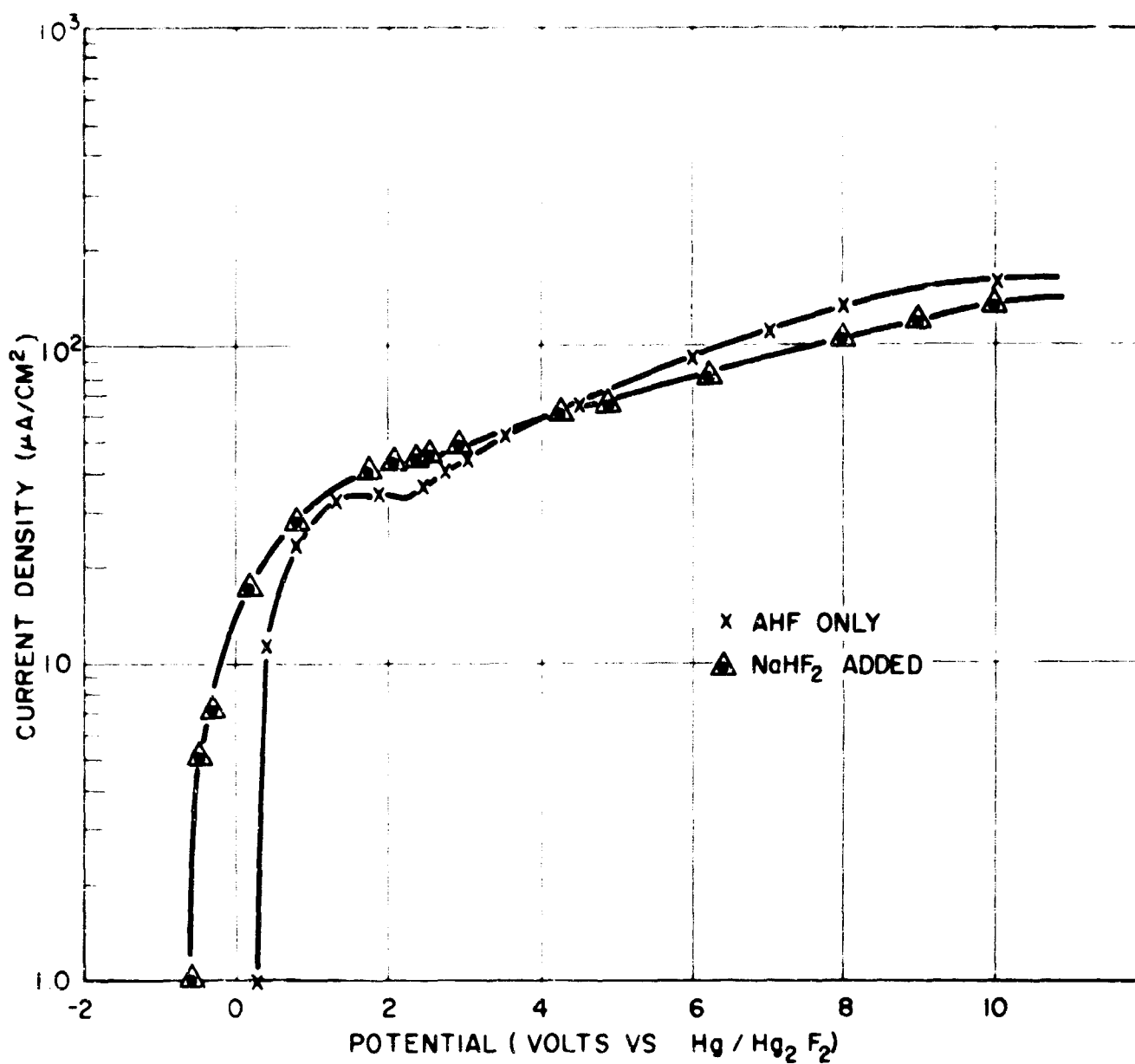
Fig. 34 - POLARIZATION CURVES FOR IRON IN
AHF
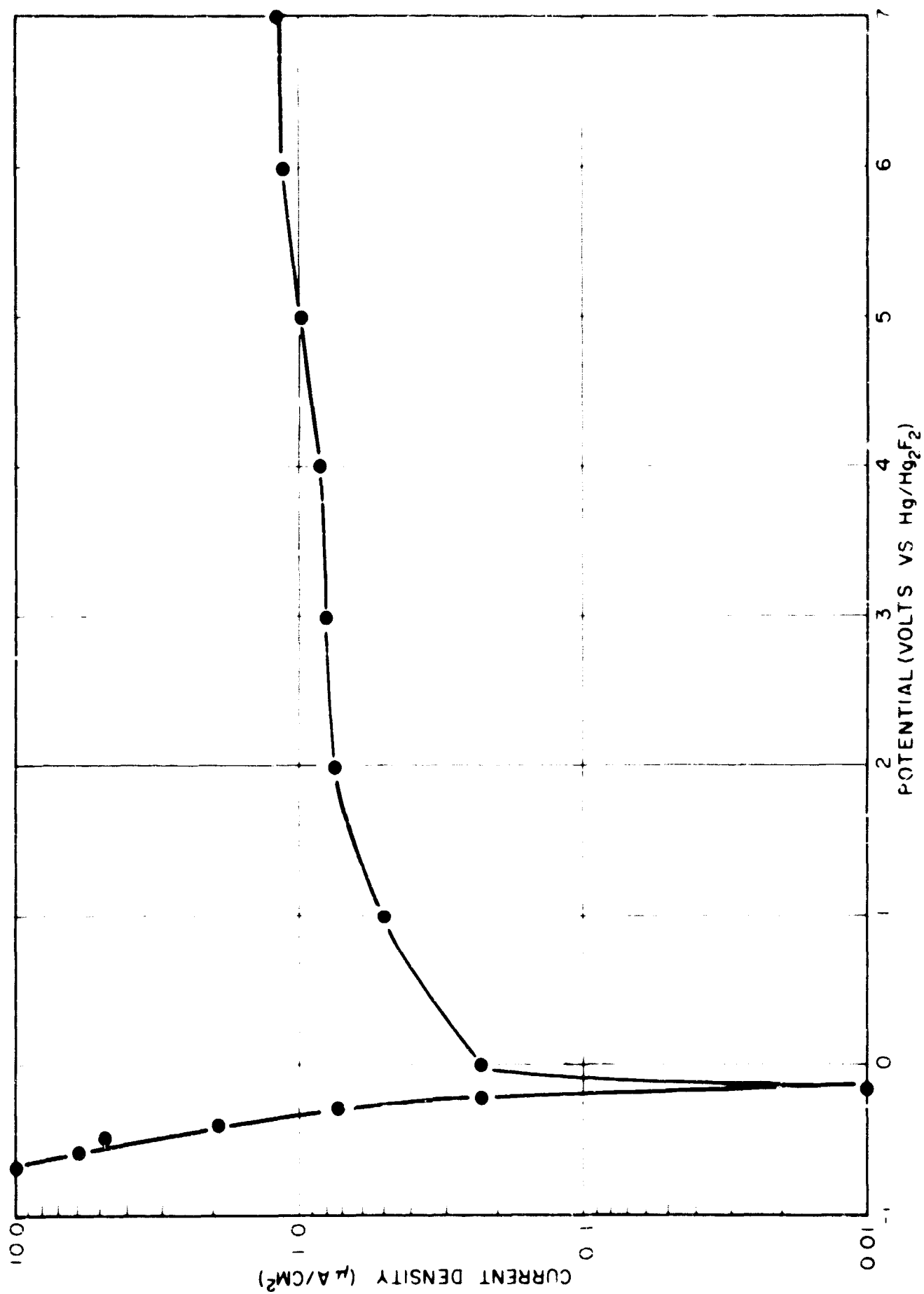
Fig. 35-POLARIZATION CURVES FOR MAGNESIUM IN ANHYDROUS HF

Fig. 36-POLARIZATION CURVES FOR TITANIUM IN AHF

The figure's axes and legend read:

CURRENT DENSITY ($\mu A/CM^2$) on the vertical axis, with values $10^3$, $10^2$, $10$, $1$.

POTENTIAL (VOLTS VS Pt) on the horizontal axis, with values -2, 0, 2, 4, 6, 8, 10.

Legend:
△ Ti IN 0 5 HRS BEFORE RAPID POLARIZATION
x Ti IN 0 75 HRS BEFORE SLOW POLARIZATION

Fig. 37 — ANODIC POLARIZATION OF ZINC

Fig 38 - POLARIZATION OF ZIRCONIUM IN
AHF

The only two exceptions to having the low current density over the entire range were chromium and Hastelloy-F, which exhibited a sharp increase in current density past 6.0 v vs $Hg/Hg_2F_2$. Weight change data at +8.0 v vs $Hg/Hg_2F_2$ showed that this high current density was due to metal corrosion on both the chromium and Hastelloy-F electrodes. A possible explanation for this is that $CrF_2$ is formed at the lower potentials and is not soluble in AHF, but at the higher potentials the $Cr^{+2}$ is oxidized to $Cr^{+3}$ which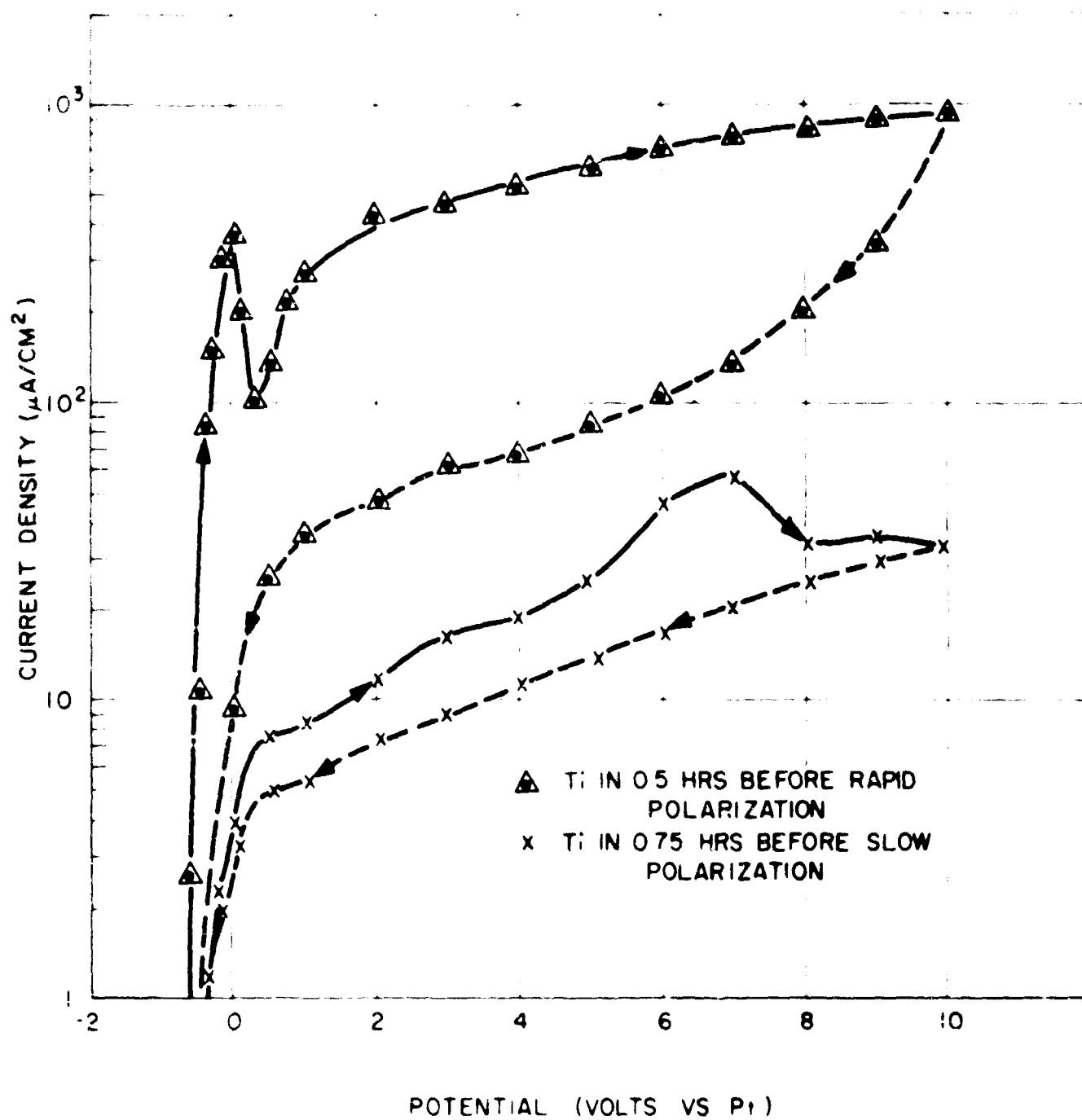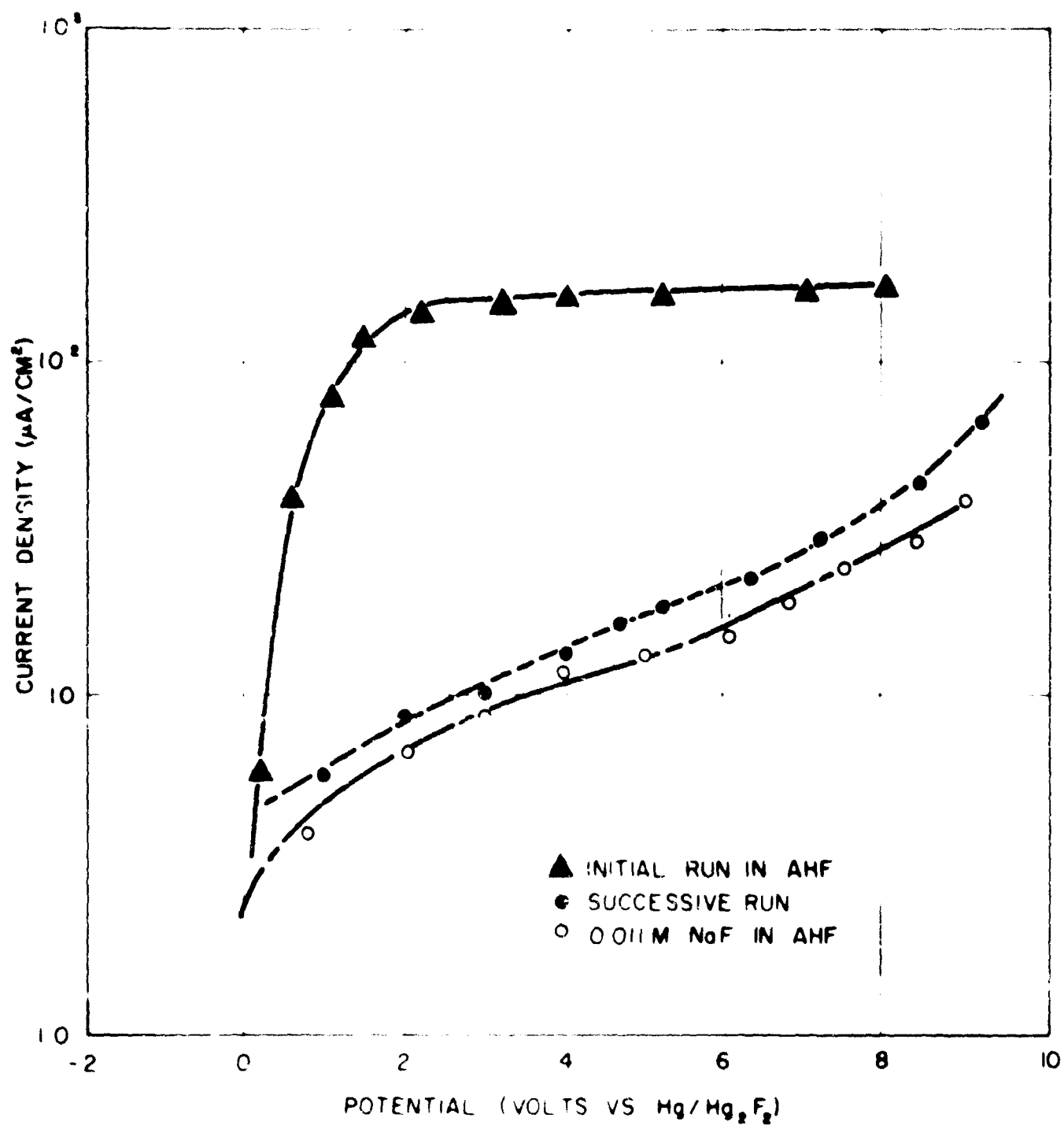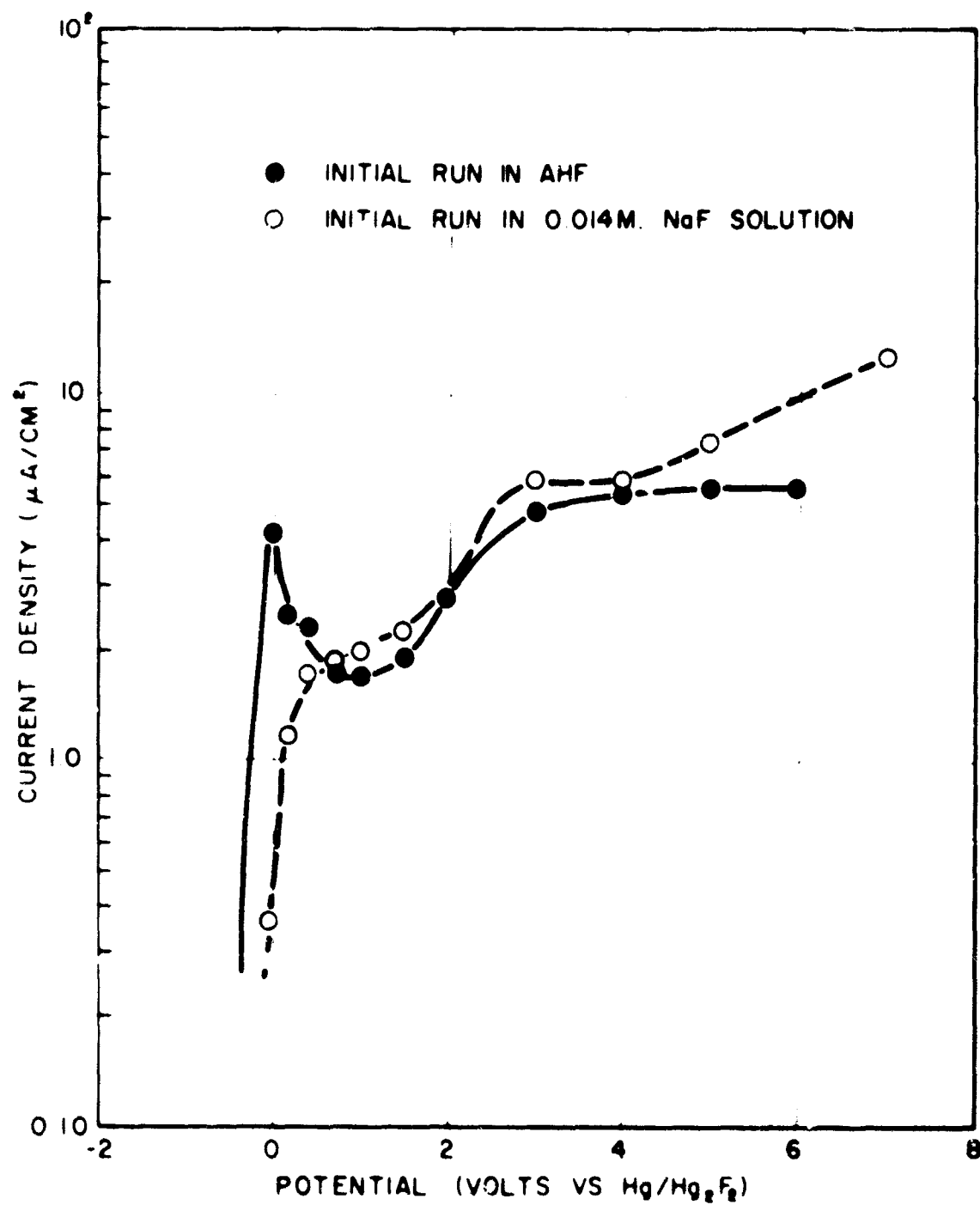 forms a soluble $CrF_3$ film. The behavior of Hastelloy-F, which is 22% chromium (3), is dependent on the $H_2O$ concentration of the HF. For $H_2O$ concentrations greater than 0.05%, no appreciable corrosion was noted; but for lower $H_2O$ concentrations on the order of $10^{-4}$% $H_2O$, corrosion occurred at a high rate. Corrosion current efficiency was found to be nearly 100% assuming an equivalent weight of 28 for Hastelloy-F (3).

The polarization characteristics of Hastelloy-F are also dependent on the $H_2O$ concentration as shown by Figure 33. The electrode used at the lower $H_2O$ concentration was badly corroded and lost 2.28 $mg/cm^2$ during the run, while the electrode used at the higher $H_2O$ concentration showed no visible signs of corrosion and no significant weight change. Evidently this additional amount of $H_2O$ in the HF inhibits corrosion at the higher anodic potentials. This effect has also been observed by Donahue and Nevitt (4).

No significant changes in the polarization characteristics of any of these materials were noted upon the addition of $NH_4F$ to the AHF.

Weight loss data were obtained on all metals in this class at open circuit and/or at anodic bias. Figures 34-44 show weight change as a function of time for aluminum, chromium, Hastelloy-F, and zinc. It is noted that the weight loss reaches a constant
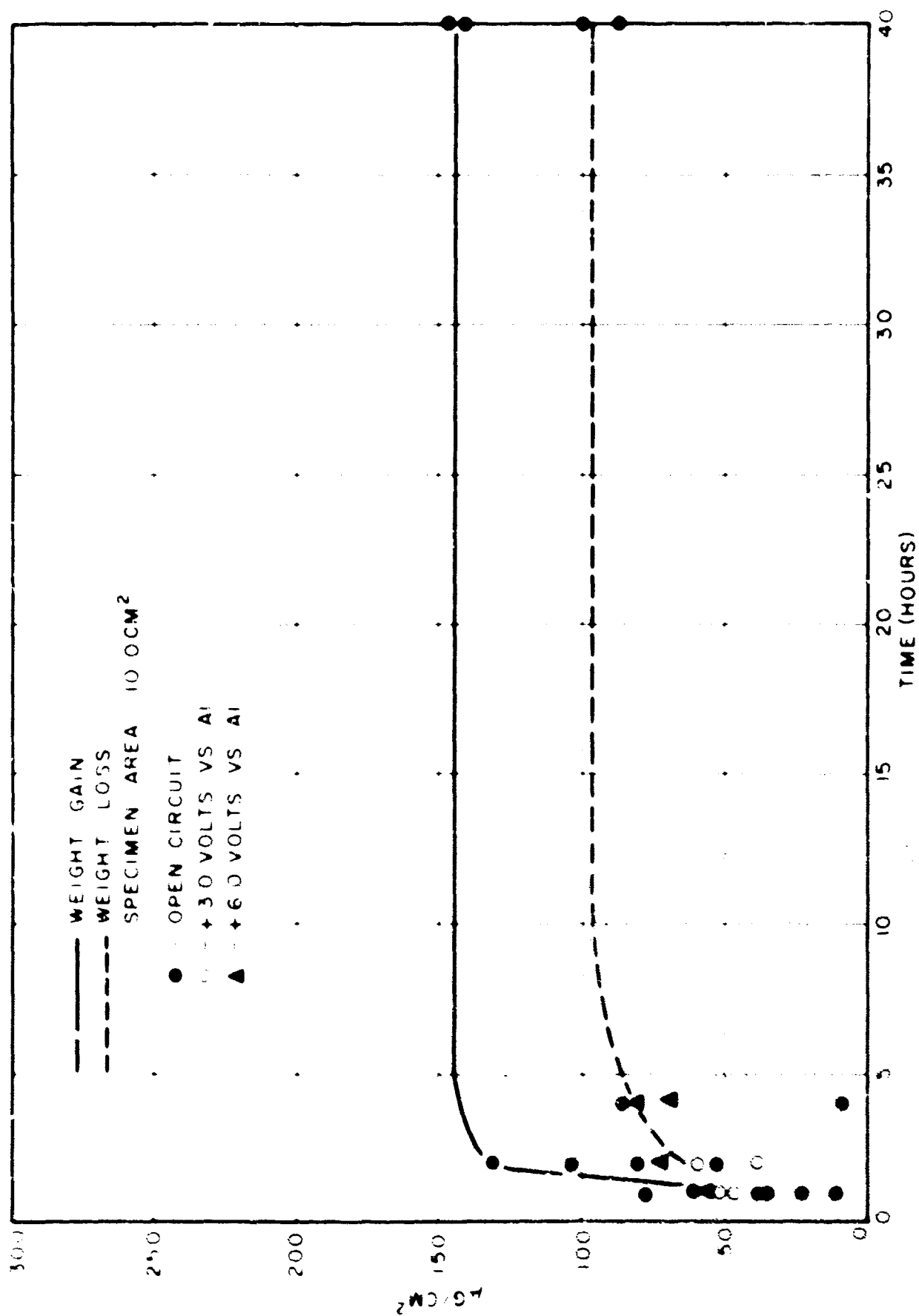
Fig.39- WEIGHT OF FILMED AND DEFILMED ALUMINUM ELECTRODES IN AHF

WEIGHT GAIN
WEIGHT LOSS
SPECIMEN AREA 10 0 CM²

● OPEN CIRCUIT
○ +3 0 VOLTS VS Al
▲ +6 0 VOLTS VS Al

TIME (HOURS)

μG/CM²
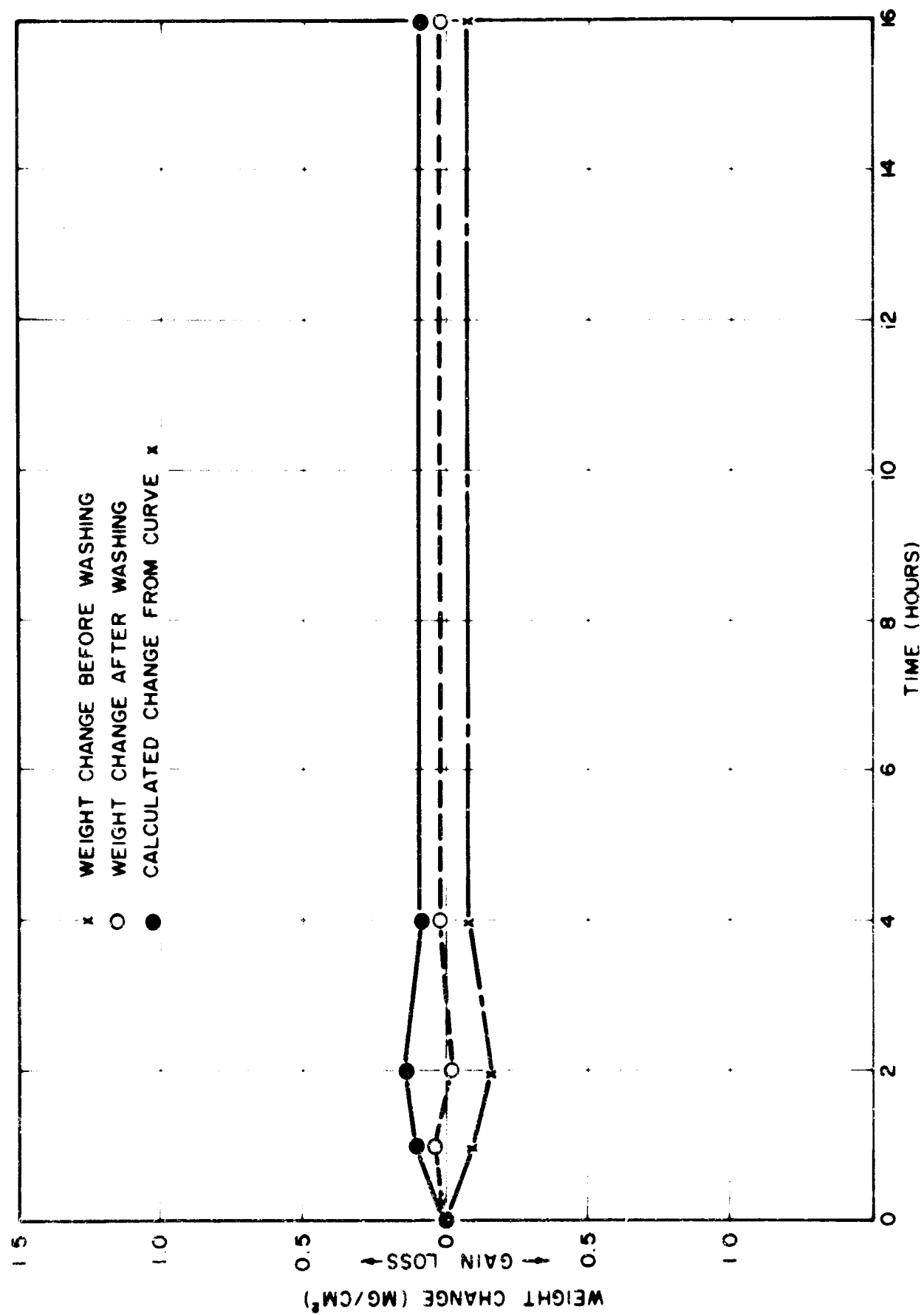
Fig.40-WEIGHT CHANGES OF CHROMIUM IN AHF AT OPEN CIRCUIT

TRACOR, INC   DWG 729-156
AUSTIN, TEXAS   1/3/66   LDF/LBH
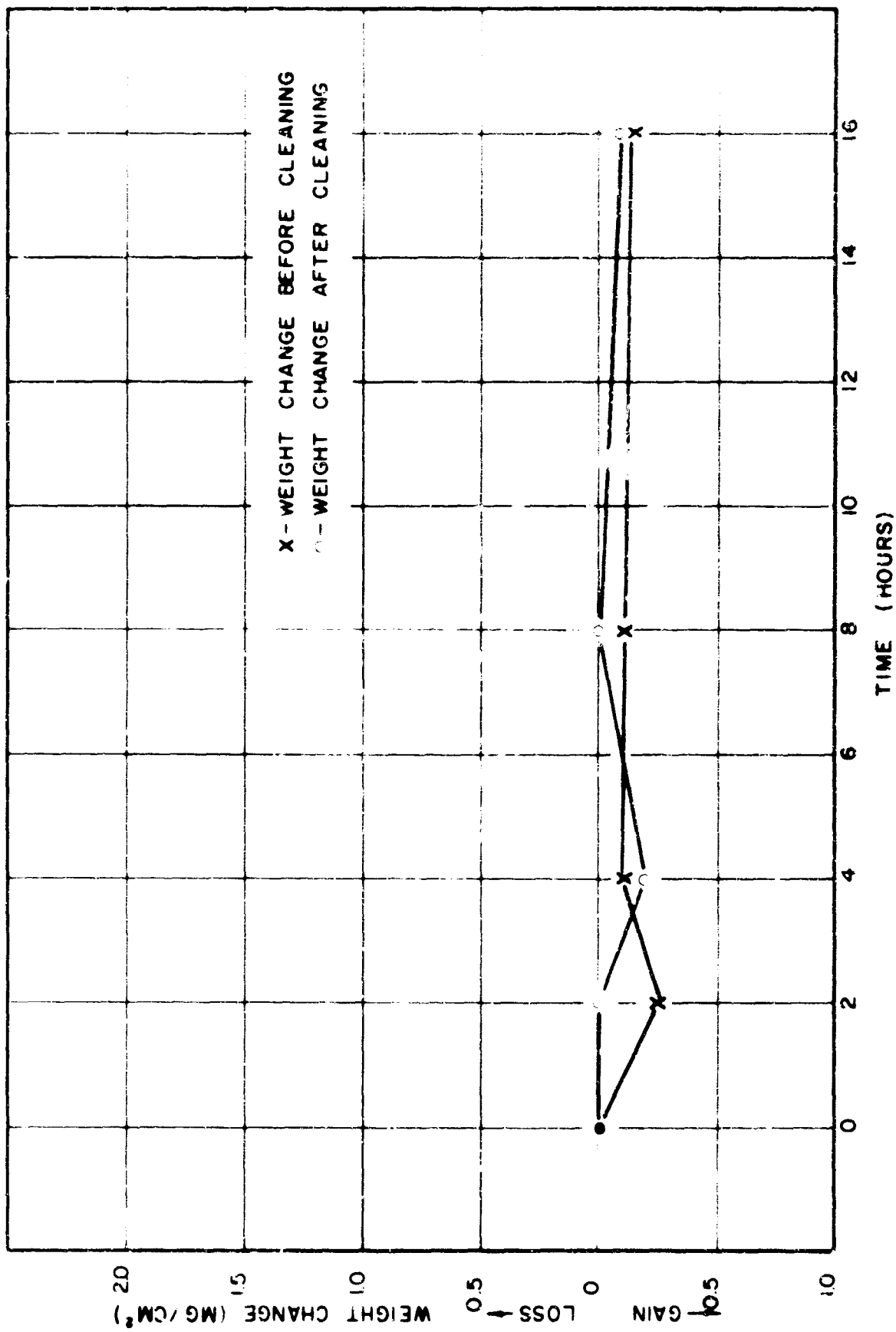
Fig. 41—WEIGHT CHANGES OF HASTELLOY-F IN AHF AT OPEN CIRCUIT
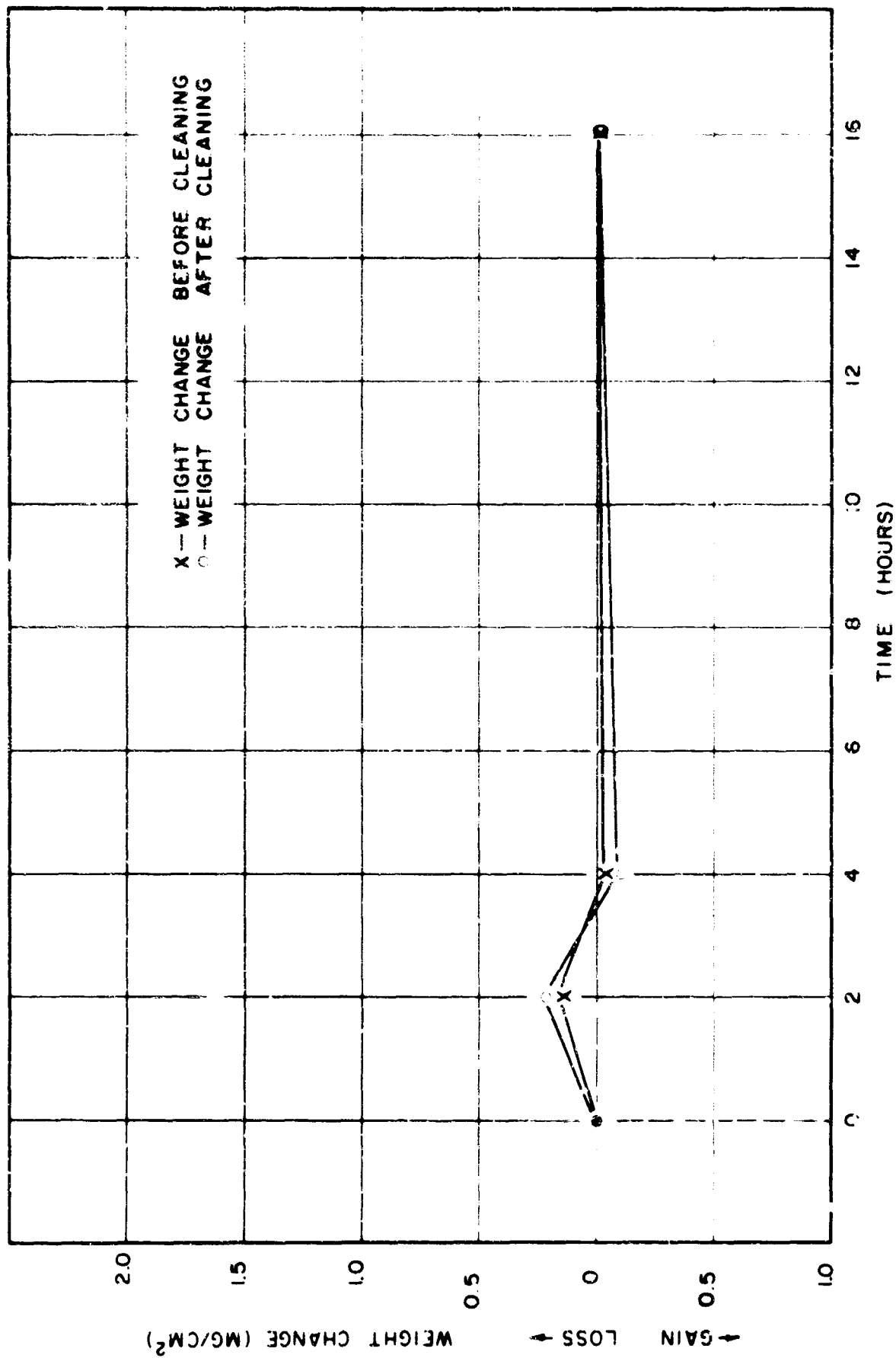
Fig. 42-WEIGHT CHANGES OF HASTELLOY-F IN AHF
AT + 4.0 VOLTS

59
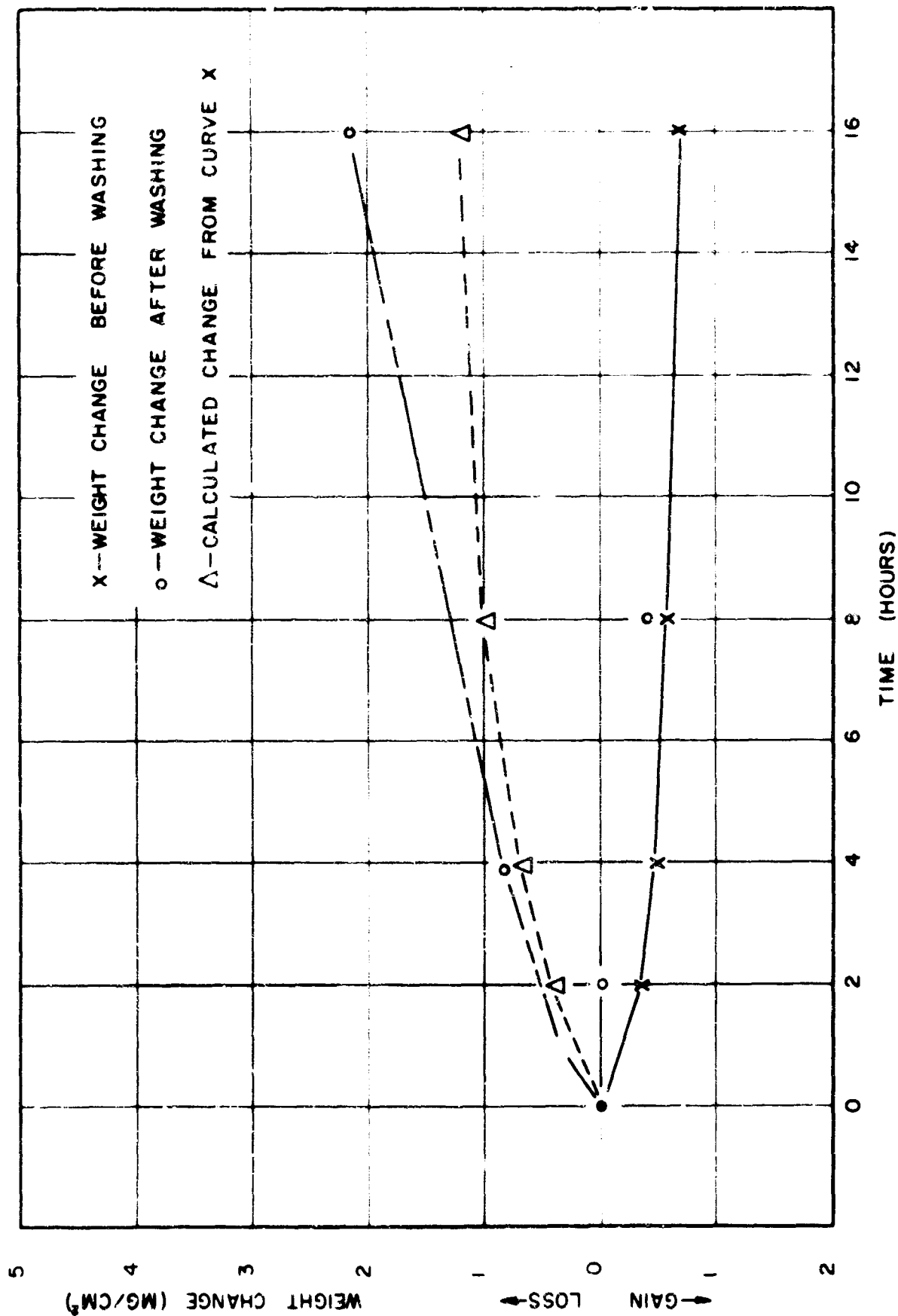
Fig. 43 - WEIGHT CHANGES OF ZINC IN AHF AT OPEN CIRCUIT

68
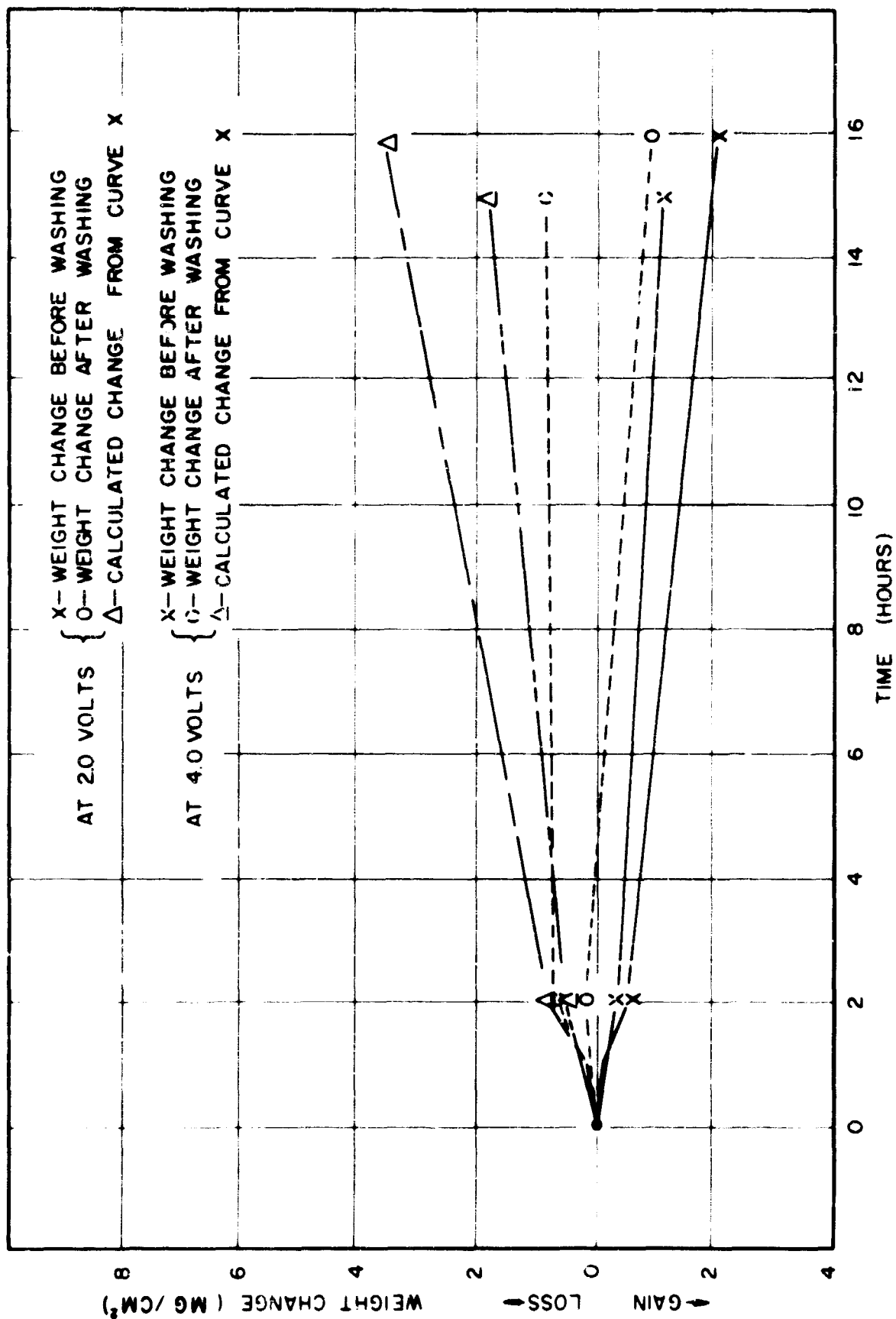
Fig.44-WEIGHT CHANGES OF ZINC IN AHF AT ANODIC BIAS

AT 2.0 VOLTS { X—WEIGHT CHANGE BEFORE WASHING / O—WEIGHT CHANGE AFTER WASHING / Δ—CALCULATED CHANGE FROM CURVE X

AT 4.0 VOLTS { X—WEIGHT CHANGE BEFORE WASHING / O—WEIGHT CHANGE AFTER WASHING / Δ—CALCULATED CHANGE FROM CURVE X

TIME (HOURS)

WEIGHT CHANGE (MG/CM²)

←LOSS      GAIN→

61

TRACOR, INC.    DWG 729-142
AUSTIN, TEXAS

value after several hours for aluminum, chromium, and Hastelloy-F, indicating formation of a passive film. Known solubilities and other weight loss data for these metals are given in Table V. These data, along with the polarization curves, show that a passive or almost passive nonconducting film is formed on each of these metals. No indication of fluorine evolution was noted in any polarization curves.

An interesting observation made during studies on aluminum was the growth of crystals on the aluminum electrode upon removal from the cell after various treatment. For instance, after 20 minutes at the cathodic potential of -3.0 v in a 8% $H_2O$ solution by volume, crystal growth began upon exposure to air. These crystals grew in a planar configuration perpendicular to the electrode, and growth took place at the base rather than at the tip of the crystals. After an initial growth of about 1.5 inches during the first hour, a final length of about 6.0 inches was reached in 24 hours (see Figure 45).

The formation of a nonconducting passive film, and consequently, poor polarization characteristics, render these materials unsuitable for use as anode material for electrochemical studies in AHF.

The Class III materials are Monel and platinum. Both of these materials have low weight loss rates in AHF at open circuit, as shown in Table VI, and allow fluorine evolution upon anodic polarization. Weight loss rates at anodic potentials are higher than at open circuit, particularly on platinum, but still account for only a small fraction of the anodic current up to the highest potentials studied.

## TABLE V

## DATA ON CLASS II MATERIALS

| METAL | METAL FLUORIDE | SOLUBILITY OF METAL FLUORIDE IN AHF[a] (g/100 g AHF) | TEMP. °C | WEIGHT LOSS RATE AT ANODIC BIAS (mg/cm²/hr) | |
|---|---|---|---|---|---|
| | | | | Exptl. | Calc. |
| Al | $AlF_3$ | ≤0.004 | -24.2 | See Figure 39. | |
| Cr | $CrF_2$ | ---- | ---- | See Figure 40. | |
| Cr | $CrF_3$ | ---- | ---- | | |
| Co | $CoF_2$ | 0.040 ± 0.003 | -23.2 | 0.05[b] | 0.015 |
| Co | $CoF_3$ | 0.272 ± 0.016 | -23.8 | | |
| Cu | $CuF_2$ | 0.010 ± 0.004 | -23.1 | 0.133[b] | ---- |
| Hastelloy-F | ---- | ---- | ---- | See Figures 41 & 42. | |
| Fe | $FeF_2$ | 0.005 ± 0.002 | -22.5 | 0.08[c] | 0.07 |
| Fe | $FeF_3$ | ≤0.001 | -25.2 | | |
| Mg | $MgF_2$ | ---- | ---- | 0.04[b] | 0.0024 |
| Ti | $TiF_3$ | ---- | ---- | 0.07[b] | 0.05 |
| Ti | $TiF_4$ | ---- | ---- | | |
| Zn | $ZnF_2$ | 0.016 ± 0.002 | -23.0 | See Figures 43 & 44. | |
| Zr | $ZrF_4$ | 0.023 ± 0.002 | -23.1 | 0.48[d] | 0.20 |

[a] See Reference 2.
[b] During polarization.
[c] 0.3 ma applied current.
[d] 10.0 v vs $Hg/Hg_2F_2$.

63
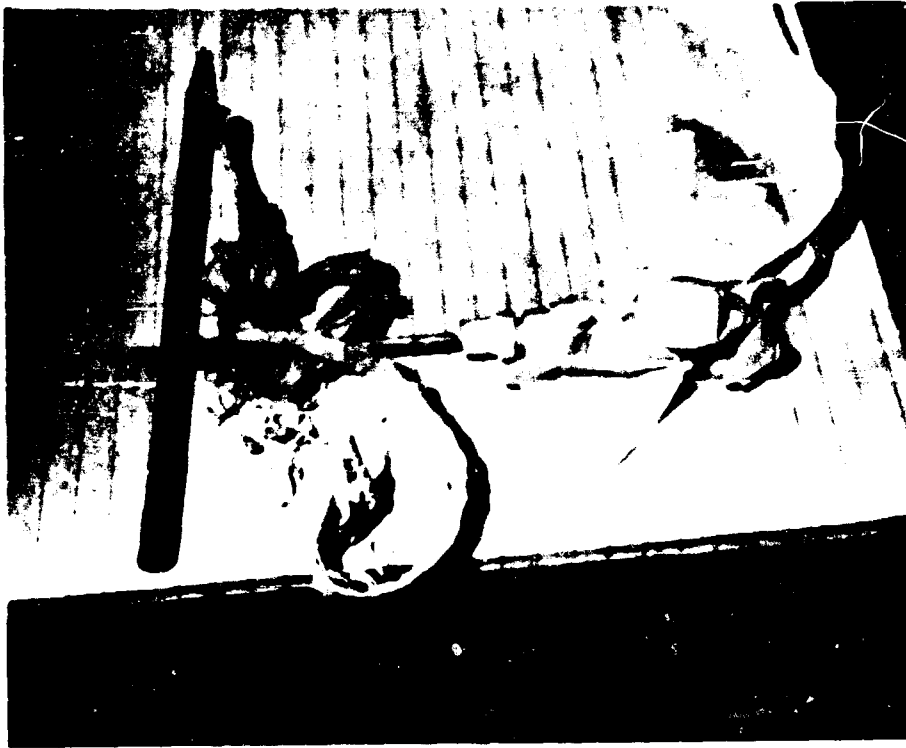
Fig. 45 - CRYSTALLINE GROWTH ON
ALUMINUM ELECTRODE

## TABLE VI

## DATA ON CLASS III MATERIALS

| METAL | POTENTIAL vs $Hg/Hg_2F_2$ | WEIGHT LOSS RATE AT ANODIC BIAS $(mg/cm^2/hr)$ | |
|-------|------------|--------|--------|
| | | Exptl. | Calc. |
| Monel | Open Circuit | -0.154 | ----- |
| Monel | + 8.0 v | +0.054 | +15.4[a] |
| Monel | +12.0 v | +4.4 | + 8.2[a] |
| Pt | Open Circuit | +0.33 | ----- |
| Pt | + 5.0 v | +10.0 | +70.0 |

[a] Assuming formation of $NiF_2$ and $CuF_2$.

The polarization curves obtained on Monel in AHF are
reproducible and stable after the electrode has been in AHF for
several hours. The first polarization curve on a Monel electrode
which has been in AHF for less than one hour has a peak at
about +1.0 v as shown in Figure 46. This peak is probably due to
a film formation and is not observed on successive runs. The
cathodic polarization is completely dominated by the $H_2$ evolution
current as shown in Figure 6.

A typical anodic polarization curve on platinum in AHF is
shown in Figure 47. The high current densities past +2.0 v are
due to fluorine evolution and some metal corrosion as evidenced
by the weight loss rate of platinum at +5.0 v (see Table VI).

Since Monel forms a passive conducting film in AHF and has
the best polarization characteristics of any material tested, it
is being used as the anode for studies of the electrochemical
fluorination of ammonia and hydrazine in AHF.

The Class IV material was pyrolytic carbon. Pyrolytic
carbon disks were sealed in Kel-F so only the surface of the
carbon lamella was exposed to the AHF (see Figure 48). It was
hoped that exposure of only one plane of the pyrolytic layer
structure would prevent the disintegration observed by other
workers. Electrical contact was made by sealing a Teflon-coated
nickel wire to the back side of the carbon electrode.

Anodic polarization caused exfoliation of the layers of
the electrode. An electrode which was immersed in AHF at open
circuit showed no signs of corrosion or exfoliation as seen in
Figure 48. Thus, it was concluded that, although pyrolytic carbon
is resistant to AHF, fluorine penetrates the lattice and causes
disintegration of the structure which makes it unsuitable for use
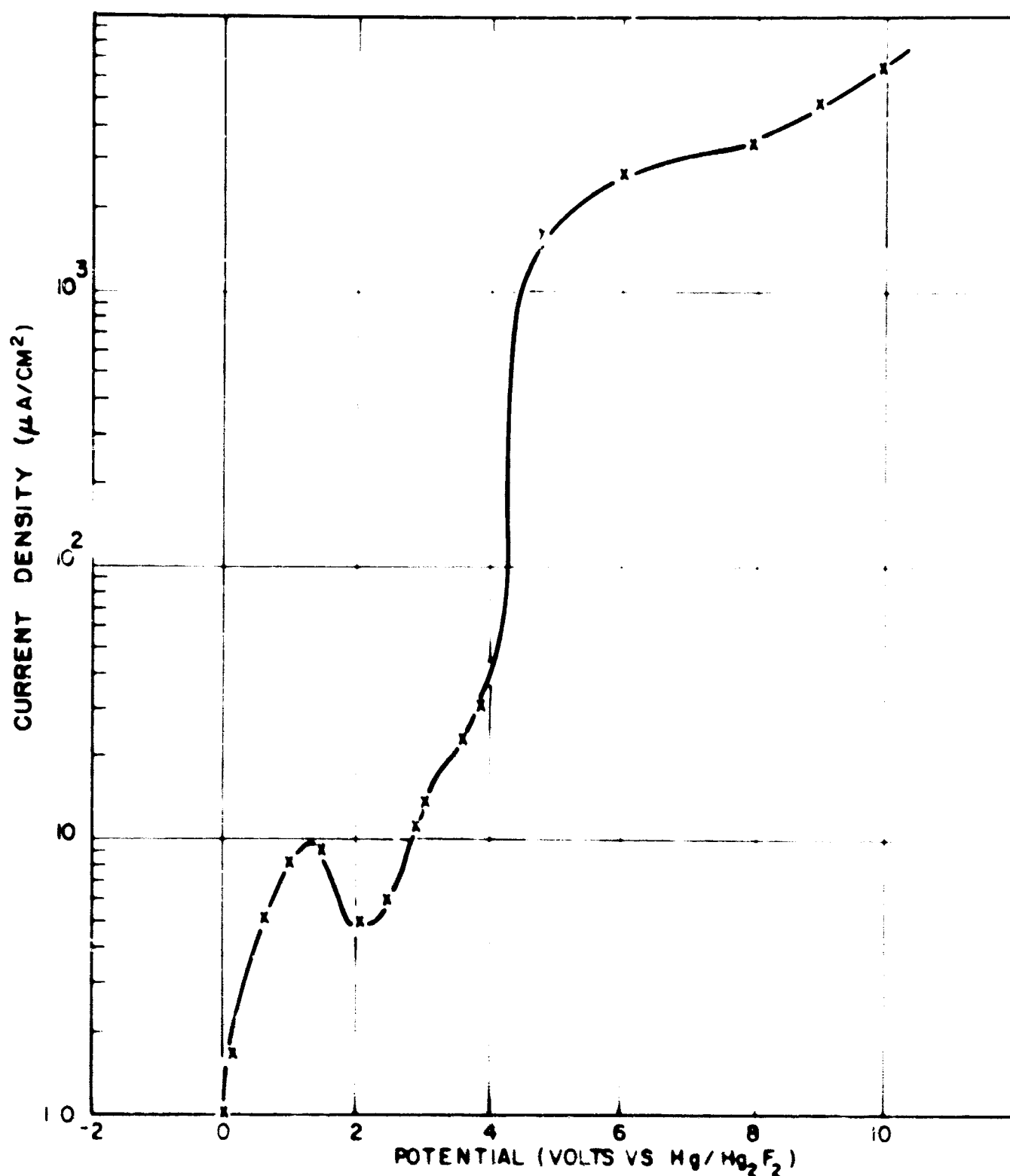as an anode material in AHF.

Fig.46-POLARIZATION CURVE FOR MONEL (IN
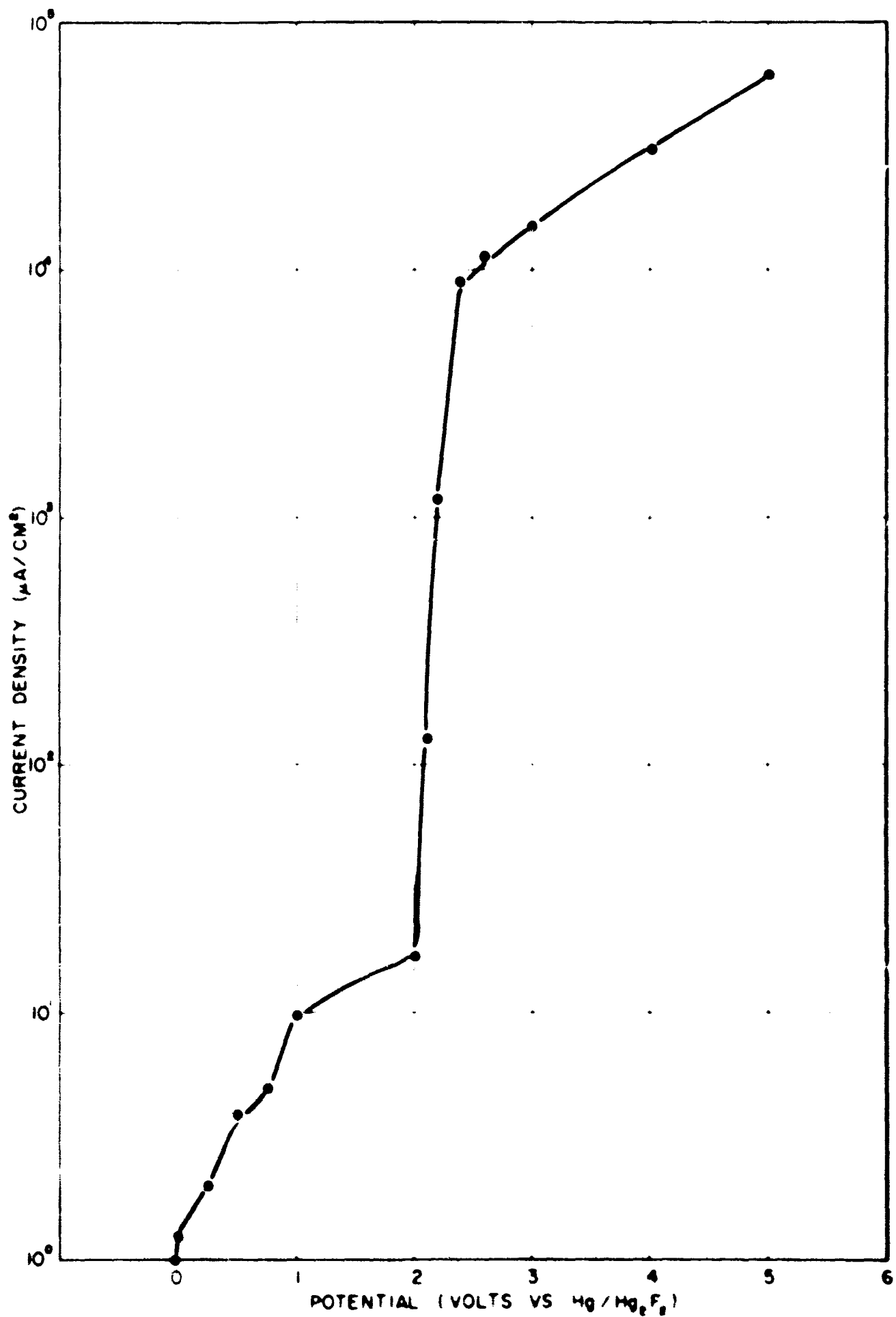AHF FOR 30 MINUTES)
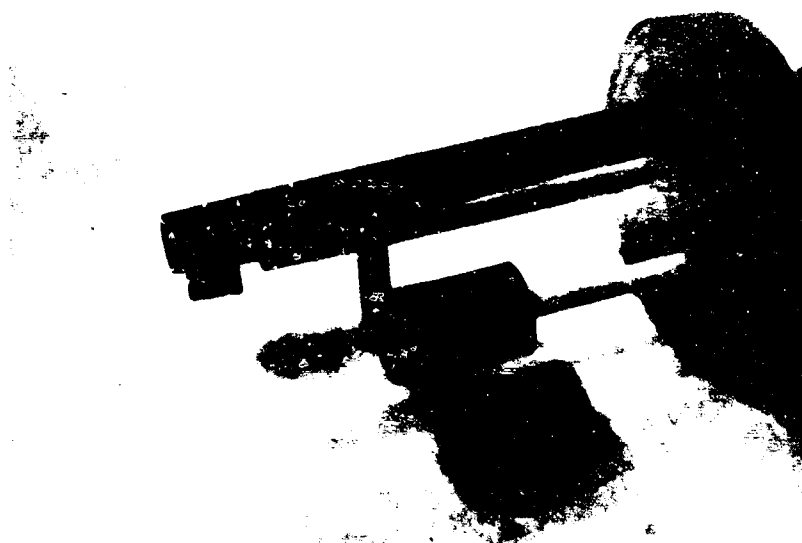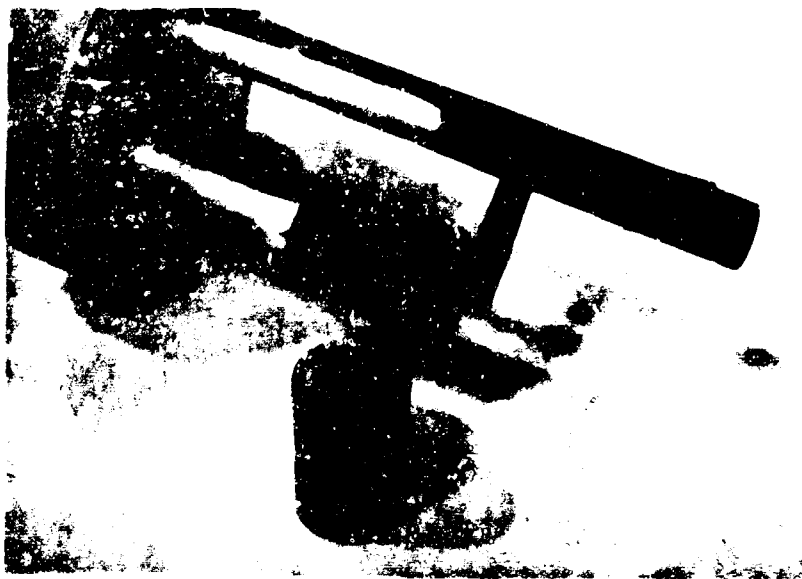
Fig 47 - POLARIZATION CURVE FOR PLATINUM IN AHF

Fig. 48 - PYROLYTIC CARBON ELECTRODES

69

## VIII.  DISCUSSION

The present system of Monel anodes, $Hg/Hg_2F_2$ reference
electrodes, Kel-F conductance and electrolytic cells, and pre-
fluorinated HF handling equipment, have all proved to be satisfactory
and will be used to continue studies of the fluorination of ammonium
and hydrazinium ions.  With this system it is possible to obtain and
maintain HF with a conductivity of $10^{-5} \, \Omega^{-1} \, cm^{-1}$ for use in the
electrolysis studies.

Of the 20 anode materials studied to date, only Monel ful-
fills all of the requirements as a suitable working electrode for
electrochemical fluorination studies in AHF.  It has been determined
that the change in film composition which occurs on Monel electrodes
at potentials of +4.0 v and greater is due to fluorine sorption.
Since a fluoride film of limited thickness and saturated with
fluorine can be obtained, it is still possible to regulate the
amount of fluorine available for the fluorination of $NH_4^+$ or $N_2H_5^+$.

From the results obtained to date, it appears that the
fluorination of ammonium ions proceeds by chemical reaction rather
than by an electrochemical mechanism.  However it should still be
possible to obtain workable concentrations of partially fluorinated
cations by controlling the fluorine evolution rate and diffusion of
$NH_4^+$ ions to the electrode.  In view of the lack of concentration -
dependent waves for the fluorination of ammonium ions, the
electrochemical studies are being supplemented with IR and gas
chromatography analysis.  The data from these analyses will be
compared with data from gas and liquid samples of known composition.
These studies are presently being done with the purpose of identify-
ing the products obtained from constant potential electrolysis of
solutions of $NH_4F$ in AHF.

## IX.    FUTURE WORK

Work now in progress consists of further studies on the electrochemical fluorination of $NH_4F$ at various anodic potentials and identifying any products formed by infrared and gas chromatography analysis. The feasibility of using mass and nuclear magnetic resonance spectra to analyze the electrolysis products will also be considered.

Studies on the behavior of other electrode materials, e.g., nickel and nickel alloys, will also be continued.

# REFERENCES

1.      R. Ukaji and I. Kageyama, Bunseki Kagaku $\underline{9}$, 604 (1960).

2.      Albert W. Jacke and George H. Cady, J. Phys. Chem. $\underline{56}$, 1952.

3.      "Corrosion Resistance of Haynes Alloys," Haynes Stellite
        Company, Division of Union Carbide Corporation, Kokomo,
        Indiana, August 1960.

4.      J. A. Donahue and T. D. Nevitt, ARPA Propellant Contractors'
        Synthesis Conference, Chicago, Illinois, April 13-15,
        1964.

72

## DISTRIBUTION LIST

Advanced Research Projects Agency
Propellant Chemistry
Room 3D165, The Pentagon
Washington 25, D. C.                                    6 copies


Defense Documentation Center (formerly ASTIA)
Arlington Hall Station
Arlington 12, Virginia                                10 copies


Chemical Propulsion Information Agency
    (formerly LPIA and SPIA)
Applied Physics Laboratory
The Johns Hopkins University
Silver Spring, Maryland                                3 copies


Office of Naval Research
Power Branch, Code 429
Navy Department
Washington 25, D. C.                                    2 copies


Commanding Officer
Office of Naval Research Branch Office
86 East Randolph Street
Chicago 1, Illinois                                    1 copy


Department of the Navy
Inspector of Naval Material
708 Jackson Street
Dallas 2, Texas                                        1 copy


NOTE:   Additional copies were distributed according
        to Chemical Propulsion Mailing List following
        CP123, dated June 1963.